Temporal patterns in vegetation in the Mediterranean area

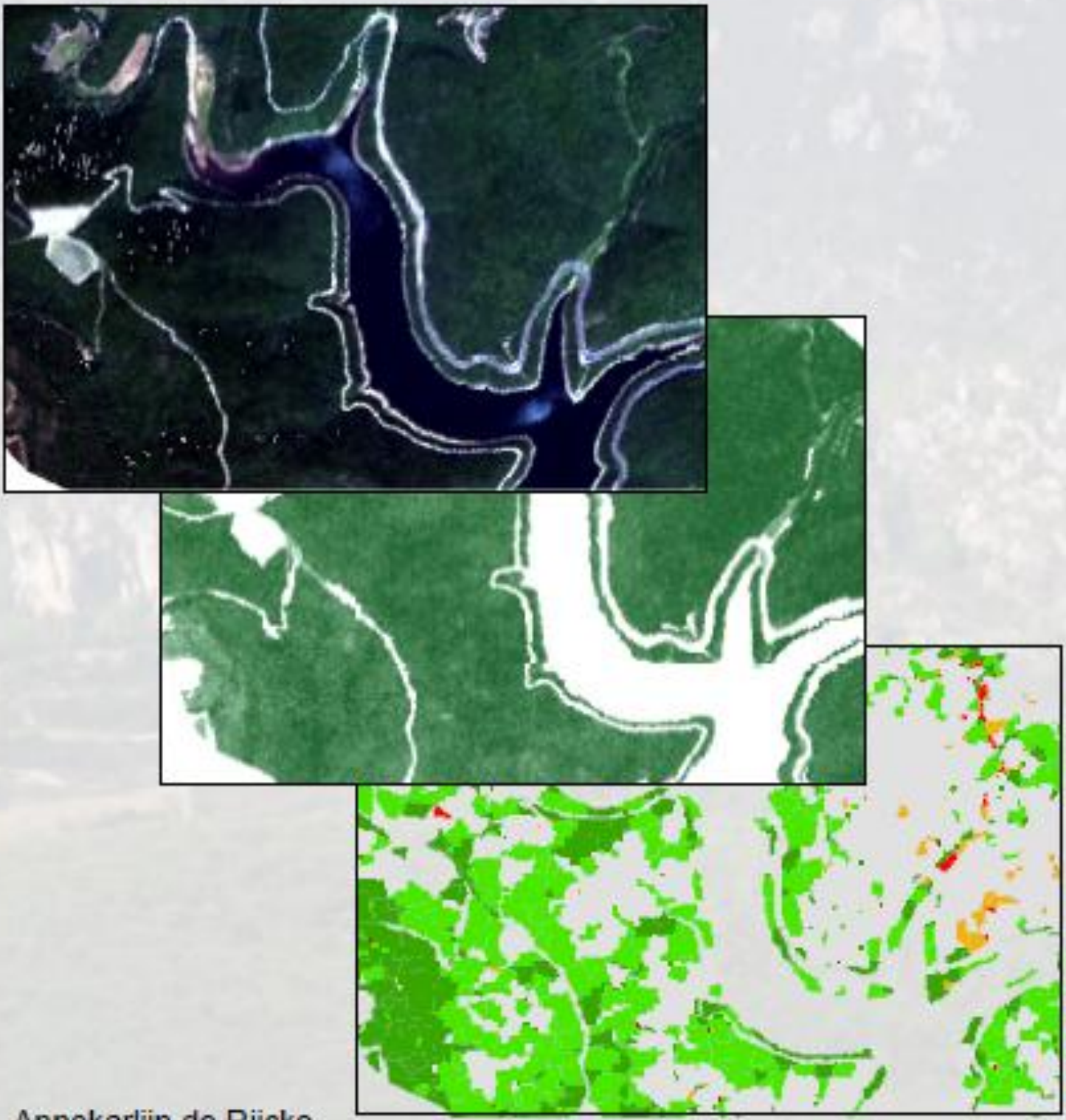

Annekarlijn de Rijcke
Master thesis Physical Geography
Utrecht University
4 February 2011
3279545

Temporal patterns in vegetation in the Mediterranean area

Report

Course:	Msc research
Course code:	GEO4-4407
Part:	Thesis
Date:	4 February 2011
Version:	3
Period:	April 2009 till February 2010
Institution:	Utrecht University
Program:	Physical Geography

Student

Name:	Annekarlijn de Rijcke
Student number:	3279545
Mail address:	A.deRijcke@students.uu.nl

Supervisor

Name:	Elisabeth Addink
Mail address:	E.Addink@geo.uu.nl

Preface

This thesis is written as part of the curriculum of the master Physical Geography at Utrecht University. This study took place between April 2009 and February 2010 and describes the process of the application of object-based change detection to determine temporal patterns in vegetation and to explain these with the use of static environmental factors.

I selected this thesis topic, because it covers my interests in change detection of vegetation. By writing this thesis, I assumed that readers have some knowledge about remote sensing, vegetation and change detection.

The main objective of this study was obtaining temporal patterns in vegetation. Thereby I took the spatial structure and variability in vegetation into account. Besides that I tried to find if environmental factors are responsible for these changes, but this is only done for the main static environmental factors: geology, aspect, slope and elevation. In the study of Simone Hoogeveen more environmental factors are used to describe biomass for 2009.

This thesis was established by a literature study (April till June 2009), fieldwork (September till October 2009), research (November 2009 till February 2010) and writing the thesis (January & February 2010 and November 2010 till January 2011).

Finally, I will thank people who have enabled to perform this thesis:

- Supervisor Elisabeth Addink and Steven de Jong for their guidance and contribution to this thesis and fieldwork.
- Simone Hoogeveen for the collection of field data done in the study area in southern France in September and October 2009.

Contents

Summary

The climate in the Mediterranean area is characterized by hot, dry summers and cool winters. The area has shown climate change in the past (last centuries) and is vulnerable for climate change in the future as result of the location of the area in the climate system. The climate affects the ecosystem and the response of vegetation through time is closely related to this.

Vegetation in the Mediterranean area is subject to changes depending on environmental factors and human influence. The objective is the application of object-based change detection to determine temporal patterns in vegetation and to explain these using static environmental factors. Static environmental factors are factors which do not change over time, such as geological units, aspect, slope and elevation.

Temporal patterns in vegetation are assessed by the variables biomass, Leaf Area Index and cover fraction. These patterns are assessed by the application of regression analyses and image segmentation on hyperspectral images of 2003 and 2008. For the 2003 image field data of 2005 is used (field data of 2003 was not available) and for the 2008 image field data of 2008 and 2009 is used.

Predictive vegetation maps are generated by the application of ridge regression resulting in the following R^2 values: biomass 2003: 0.58 and 2008: 0.55, Leaf Area Index 2003: 0.40 and 2008: 0.44 and cover fraction 2003: 0.35 and 2008: 0.27. Biomass is the best predicted variable followed by LAI and cover fraction. Biomass and LAI can well be estimated by a combination of hyperspectral images and field data. The R^2 values for cover fraction are low compared to the others, meaning that the predictions of this variable are more uncertain.

Object-based image analyses took place by the application of segmentation to obtain the spatial structure and variability present in each variable separately. Segmentation is applied on predictive vegetation variable maps by using three methods and ten different object scales (scale 1 till 10). As expected the highest R^2 is reached by the methods where the predictive vegetation variable maps from both acquisition years are used (R^2 biomass: 0.66, LAI: 0.42 and cover fraction: 0.41).

The optimal segmentation scale varies between the vegetation variables (biomass scale 4, LAI scale 8 and cover fraction scale 3). These differences can be explained by the spatial structure and variability present inside the predictive vegetation variable map (heterogeneity in the data).

Temporal patterns assessed by change detection show that 55% of the natural vegetation areas have an increasing change pattern for biomass. LAI and cover fraction mainly show a decrease (LAI 39% and cover fraction 35% of the natural vegetation areas). This does not immediately mean that these temporal patterns are wrong, because an increase in biomass do not have to result in increasing values for cover fraction and/or LAI.

Temporal patterns in vegetation variables are compared with static environmental factors. There are some patterns visible inside a specific category of an environmental factor (geology and elevation), but it is not certain that this is the case over longer period or that it only dominates in the temporal patterns between 2003 and 2008. To give a more certain conclusion about change patterns on its own and in relation to environmental factors, further investigation over a longer timescale is required.

1. Introduction

The climate in the Mediterranean area is characterized by hot, dry summers and cool winters. The area is located in a transition zone between the arid climate of North Africa and a rainy climate of central Europe and is affected by interactions between mid-latitude and tropical processes.

The Mediterranean area has shown large climate change in the past (last centuries) (Luterbacher et al., 2006) and is one of the most vulnerable locations for climate change in the future (Giorgi, 2006) as result of the location of the area in the climate system. A consequence is an increase in temperature and annual rainfall volumes. Dry summer periods will be longer and precipitation will fall less frequent but probably with higher intensities.

Climate change affects the ecosystem and on longer timescale (thousands of years) are these changes visible in the landscape, such as land degradation, erosion and sedimentation. On a shorter timescale (decades) the effects of climate change are small and not visible. The climate affects the ecosystem and the response of vegetation through time is closely related to this.

Natural vegetation in the Mediterranean area is in a degraded stage of the evergreen forest (Sluiter, 2005). Leaf persistence in evergreen vegetation varies from a few months to several decades. The vegetation is heterogeneous, meaning that a large variety of vegetation types is present. This large variety is a consequence of the large variation at short distances in geology, elevation, climatic factors and human disturbances (Sluiter & de Jong, 2007). The factors mentioned above also affect the water availability of plants. Archibold (1995) concluded that vegetation in the Mediterranean area frequently suffers from water and heat stress, meaning that vegetation productivity in that area is water limited.

The landscape of the Mediterranean area also changes as result of human influence in the past, such as land abandonment, logging and grazing. The general change in landscape is a consequence of land abandonment, the extensification of human land use. In 1850 the area was in use for intensive cultivation, logging and grazing (Sluiter & de Jong, 2007). This has changed as result of crises like flooding, wood scarcity and pests (Mather et al., 1999). Nowadays land abandonment takes place as a result of economical reasons or agricultural areas situated at unfavourable locations. Small parts of the natural vegetation areas are used for logging and grazing of animals.

As mentioned above, vegetation in the Mediterranean area is subject to changes depending on environmental factors and human influence. The subject of interest is finding temporal patterns in vegetation. These can be divided into abrupt and subtle changes. Abrupt changes are the result of logging and forest fires, subtle changes are the result of the growth and development of vegetation, which are influenced by the surrounding ecosystem.

Vegetation in the Mediterranean area can be investigated with remote sensing. Cohen & Goward (2004) and Lu (2006) concluded that remote sensing offers the most suitable tool to obtain spatially continuous data sets of vegetation parameters (Leaf Area Index and biomass). Another interesting point is that hyperspectral sensors are developed to a spatial resolution where it is possible to derive quantitative data on natural vegetation in fragmented and heterogeneous landscapes (Addink et al., 2007b; De Jong et al., 2003). High spatial resolution images allow us to assess the spatial structure and variability of natural vegetation characteristics (Nijland et al., 2008).

Estimation of vegetation parameters with remote sensing can be based on pixels or objects. By pixel estimation are all observation units square pixels of fixed dimensions. These pixels do not accurately represent the true nature of features, which vary in size, shape, colour, texture as well as in degrees of compactness (Ouma et al., 2008).

Disadvantages of per-pixel estimations of vegetation parameters are the spatial mismatch between the image and field observations, and they are limited by neglecting spatial patterns (Addink et al., 2006). Especially in the case of change detection a geometric mismatch component is more vulnerable when pixels are used instead of objects. One of the problems of using objects instead of pixels is that natural vegetation consists of gradual boundaries compared with agricultural fields or urban environments.

Object based image analyses for vegetation has been limited so far, but the main advantages of using objects instead of pixels is that geometric inaccuracies in both field and image data are of lesser importance (Addink et al., 2006), because geometric mismatching is reduced by using objects and besides that take objects the heterogeneity in the data into account. The study of Addink et al. (2006) also shows that segmentation (the creation of objects in an image consisting of pixels) provides better estimates than pixels for the estimation of Leaf Area Index and biomass. The application of object based image analyses for the investigation of temporal patterns in vegetation has not been done before and is investigated in this study.

The aim of this study is to determine temporal patterns in vegetation by use of the application of object-based change detection and to explain these with the use of environmental factors. Specific objectives of this study are:

- Can aboveground biomass, Leaf Area Index and cover fraction be estimated from hyperspectral images?
- Can changes in vegetation parameters be estimated with object-based change detection on hyperspectral images?
- Can changes be explained on basis of environmental factors?

2. Study area

The study area is located in the Southern part of France close to the Mediterranean Sea around 25 km north of the Mediterranean Sea and approximately 60 km west of Montpellier. The area is approximately 33.4 km² and has a length of 16 km and a width of 2 km. The elevation varies from 130m in the south-east to 450m in the north-west part of the study area. The location of the study area in France can be found in figure 1.

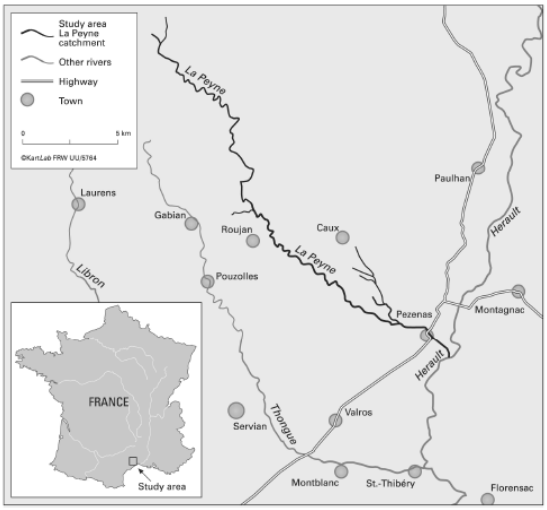

Figure 1: Study area (Source: De Jong et al., 2003)

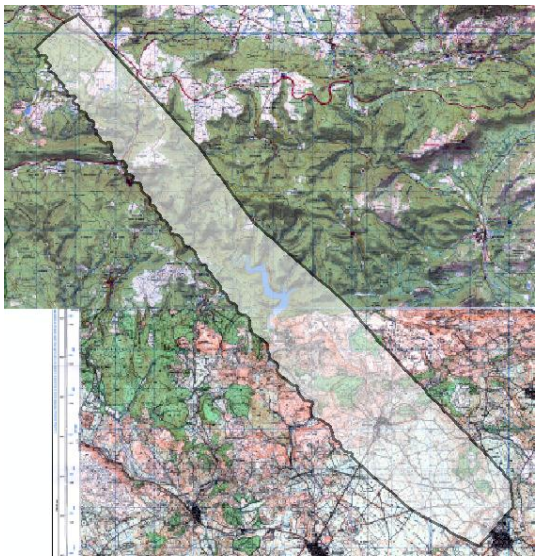

Figure 2: Study area Peyne, France

The area has diverse landscapes with the Mediterranean Sea in the south and mountainous areas in the north. The area is mostly covered by natural vegetation, but near the villages and in the valleys south of Neffiés agricultural land use takes place. Most of these agricultural fields are in use as vineyards.

The study area under consideration is chosen on basis of the part of the area covered by all images (figure 2). In this study only natural vegetation areas are taken into account. Other areas are masked out by use of Normalized Difference Vegetation Index (NDVI) values.

2.1 Climate

The climate in the Mediterranean area is located in a transition zone between the arid climate of North Africa and a rainy climate of central Europe and is affected by interactions between mid-latitude and tropical processes (Giorgi & Lionello, 2008).

The winter Mediterranean climate, and most importantly precipitation, is affected by the North Atlantic Oscillation (NAO) over its western areas (Hurrell 1995), the East Atlantic (EA) and other patterns over its northern and eastern areas (Trigo et al., 2006). The NAO and the EA

are similar to each other in the sense that it are prominent modes of low-frequency variability over the North Atlantic from east to west. The EA is a “southward shifted” NAO pattern, because of south-eastward displaced anomaly centers to the approximate lines of the NAO pattern. The EA patterns are associated with above-average surface temperatures in whole Europe, above-average precipitation over northern Europe and below-average precipitation across southern Europe (NOAA Climate Prediction Centre).

The Mediterranean area is characterized by hot, dry summers with cool winters. Factors that are responsible for these climate characteristics are the latitude position and the Mediterranean Sea. Temperatures lie in winter between 3-11 °C and in summer between 18-30 °C. The temperature in autumn stays relative high as result of the high Mediterranean seawater temperature. Mountains that lie around the Mediterranean protect the area against wind influence.

The summer months are dry and precipitation mainly falls in early spring and autumn (Sluiter, 2005). The average annual precipitation is between 600 and 900mm (Meteo France, 2006). These precipitation characteristics have also consequences for the discharges of the main rivers in this area, the Peyne, Borne and Salagou. They have irregular discharges with monthly and yearly extremes (Sluiter, 2005).

2.2 Geology

The area is situated at the southern end of the Massif Central and the eastern end of the Montagne Noir. It forms a transition zone between the coastal plain of the Mediterranean Sea, the alluvial sediments of the Hérault river (the Peyne river is a sub catchment of this river and is located in the study area) and the metamorphous socle of the Massif Central (Gèze, 1979).

The formation of the Mediterranean area started with the raise of the areas north of the Languedoc area in the Paleozoic period (570-225 million years ago). Incisions in the Massif Central are caused by weathering and erosion and created plains on high elevations surrounded by basins. The basins were covered with ocean water in the Mesozoic period (225-65 million years ago), which resulted in the development of limestone layers. The last million years the landscape has been formed under the current conditions, with fertile soils in lower parts of the region as a result of sedimentation, and incisions in river valleys which lead to the development of gorges (De Graaf, 2006). A gorge is a canyon formed through the incision of a river in a plateau.

Geological substrates in the Peyne area range from sandstone and dolomite formations, limestone plateaus, and volcanic tuffs to volcanic basalt outflows (Sluiter, 2005). An overview of the geological units present in the study area can be found in figure 36. On these geological substrates various lithological substrates can be found, like regosols, lithosols, brown soils and calcareous soils (Sluiter, 2005). The water holding characteristics of soils are important for natural vegetation development, because these determine the amount of water storage in the ground and the accessibility of water for vegetation.

2.3 History

Mediterranean landscapes are disturbed and changed as a result of human influences in the past. During the second half of the nineteenth century large parts of the study area were in use for agriculture (vine and cereals), forest logging and parts with low shrubs for grazing of animals. This has changed as a result of crises like flooding, wood scarcity and pests (Mather et al., 1999).

Changes and disturbances in Mediterranean landscapes are the result of intensification and extensification of human land use. Areas experience increasing pressure due to recreation, urban issues or increasing agricultural activities. The other side is that areas are abandoned where traditional agricultural activities have ceased (Bonet, 2004).

The general changes in landscapes in the Mediterranean area of France are a consequence of land abandonment. Land abandonment can be defined as a change towards a less intensive pattern in land use or as the total termination of the use and managing of the soil: soils are left to their own spontaneous dynamics (Baudry, 1991).

The changes in landscape due to land abandonment are mostly caused by technological, social and economic changes and result in a decrease in biodiversity (traditional patterns of land use disappear), an increase in soil erosion (due to changes in soil properties) and an increase in fire risk (due to homogenization of the landscape in combination with the accumulation of biomass) (Sluiter, 2005).

Characteristics about the history of the area and intensification or extensification patterns of agricultural land use (Sluiter & de Jong, 2007) can be found below:

- 1850 Intensive cultivation, short-time abandonment, woodcutting and grazing;
- Long-time abandonment around 1850, 1900 and 1970;
- Grazing activities were intense before 1950, decreased after it and disappear around 1980. In 1990 these activities are reintroduced;
- Extensively harvesting of forest for fuel wood takes place until 1945;

- Since 1960 replanting of vineyards;
- Around 1980 depopulation stopped in small villages as a result of tourism;

Nowadays land abandonment takes place as a result of economical reasons, but also because of agricultural areas situated on unfavourable locations. Important for vegetation development in abandoned areas are the moment that areas are abandoned and the velocity of recovery of natural vegetation in an abandoned area.

2.4 Vegetation

The large variety of vegetation types in the Mediterranean area are a consequence of the large variation at short distances in geology, soils, elevation, climatic factors and human disturbances, because these are responsible for a wide range of growing conditions (Sluiter & de Jong, 2007).

This study considers only natural vegetation and this is in a degraded stage of the evergreen forest. It consists of shrubby formations, also referred to as matorral (Tomaselli, 1981). Matorral is defined as a formation of woody plants, whose aerial parts are not differentiated into trunks and leaves, because they are much ramified from the base, and are of shrubby habit (Tomaselli, 1981). These matorral / shrubby formations can be divided into three categories based on height, density and species composition (Tomaselli, 1981; Sluiter, 2005):

- Maquis: Is the tallest (2-5m) and most dense type. It consists of dense and impenetrable thickets of tall shrubs. This category may be considered as a regional climax. Dominant tree species are the Holly oak (*Quercus ilex*) and the Strawberry tree (*Arbutus unedo*) (figure 3). Undergrowth of herbaceous species is usually absent, because of the little light that can penetrate through the dense shrubs.
- Garrigue: Ranges in height from 0.6m to 2m and consists mostly of low scattered bushes interspersed with bare patches of rock, sand or stony ground. Undergrowth of herbaceous species is possible when the density of shrubs is not too high.
- Les landes: also called short matorral, consists of vegetation under 0.6m. Besides by low shrubs les landes areas are dominated by herbaceous species.

Figure 3: Strawberry tree (Arbutus unedo) and Holly oak (Quercus Ilex) (Source: Sluiter, sluitertijd.org).

The development of vegetation takes place in different phases: from les landes, to garrigue, maquis and finally a climax forest. If agricultural land is abandoned the soil and vegetation development are left to their own spontaneous dynamics. The development takes place across the matorral types present in the area (Tomaselli, 1981; Sluiter, 2005):

- First les landes vegetation with some small shrubs, but mostly herbaceous species.
- Secondly garrigue vegetation. First this type has a low cover fraction, which makes the undergrowth of herbaceous species possible. When taller become denser the undergrowth of herbaceous species will be less (closed garrigue vegetation).
- Thirdly the maquis matorral type. Also in the beginning open, but when dominant species are well developed the vegetation is called closed maquis vegetation.

If the forest is full-grown given limitations of water, nutrients and radiance the climate forest is reached, meaning that the ecosystem is complete and that all functions in the forest are present and energy- and material losses are minimal (Van der Windt, 1995). To reach this phase forests must be in a condition of relative stability. This means that the composition and structure of the forest will not change much over long periods of time. This type of forest is seen as an endpoint of the successional sequence (Snyder, 2006).

This phase is difficult to reach in the study area, because of the unique combination of climate, relief, soil and human use of the landscape, which results in a forest that is not and will not reach a condition of relative stability.

3. Data and Methods

Different data and methods are used in this study to determine temporal patterns in vegetation. Data used in this study can be divided in three categories: remote sensing images, field data and maps. The most important data sets are the remote sensing images and field data, because these yield predictive models for vegetation variables. Besides that maps are used which describe the geology, slope, aspect and elevation in the area.

Topics discussed in this chapter are: remote sensing images, methods for the aggregation of field information, the determination of natural vegetation areas, the application of regression analyses, image segmentation and finally change detection. Figure 4 shows an overview of the research steps.

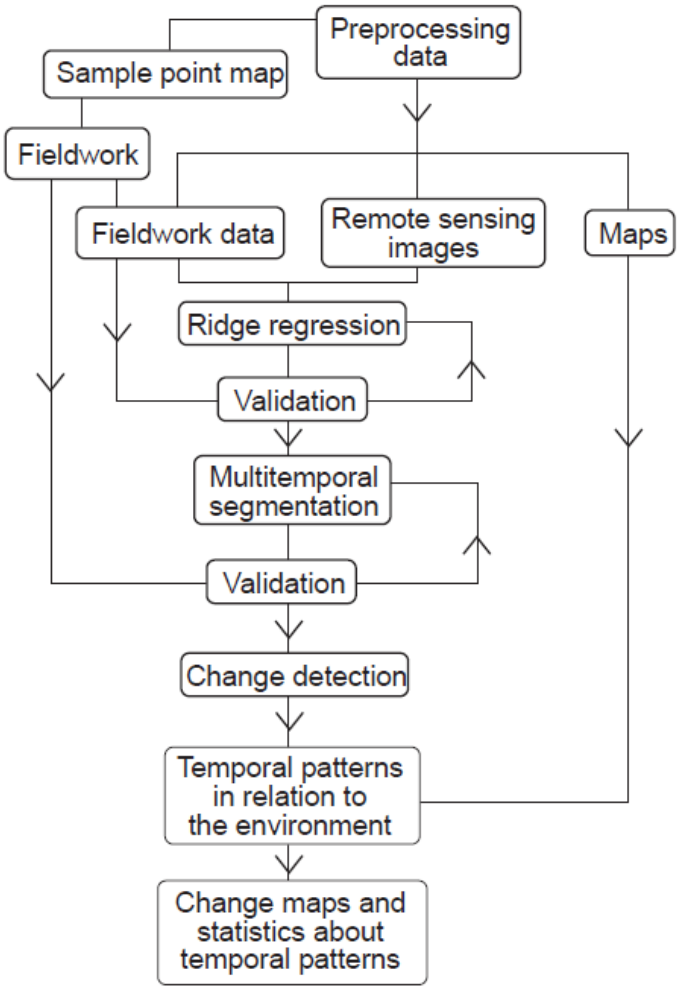

Figure 4: Flow diagram with research steps

3.1 Imagery

Remote sensing images have different characteristics based on the sensor used to acquire the image. Differences between sensors are:

- Spectral characteristics (amount of bands available, the position of bands in the electromagnetic spectrum and the width of bands);
- Spatial resolution (the size of pixels);
- Type of acquisition (Aerial or satellite images);

Images used for this study are hyperspectral images. Hyperspectral sensors obtain images in many narrow spectral bands. The electromagnetic spectrum covered by a sensor depends mostly on sensor characteristics, but mainly cover the range of 400-2500nm in the visible-, near- and shortwave infrared part.

The acquisitions in many narrow spectral bands make it possible to do environmental monitoring of vegetation, mineral mapping, etc. These hyperspectral systems can distinguish earth surface features on basis of their absorption feature position, depth and asymmetry and the reflection characteristics in narrow band intervals (Lillesand et al., 2004).

Images used in this study are obtained in 1997, 2003 and 2008 and have a ground resolution of 5m. These fine resolution images make it possible to identify individual tree crowns depending on their size and spacing. A high spatial resolution image allows assessing the spatial structure and variability of natural vegetation characteristics (Nijland et al., 2009) and to apply change detection to determine temporal patterns in vegetation through time.

Processing of data after fieldwork revealed that field data of 1997 cannot be used, because of wrong coordinates for field plots; some plots were located in the lake, because of a translation error in the coordinate system used. The original field locations of 1997 cannot be acquired and a consequence of this is that in the resulting part of this study only imagery of 2003 and 2008 is used.

Before the imagery was used the quality of individual image bands was observed. Most of these bands are from good quality, but band 1 and 126 of the Hymap images of 2003 and 2008 contain noise and are not used in the rest of this study.

3.1.1 Sensors

Hyperspectral images available for this study are the Digital Airborne Imaging Spectrometer (DAIS) 7915 in 1997 and HyMap in 2003 and 2008.

DAIS 7915 stands for Digital Airborne Imaging Spectrometer and is developed in Germany. The spectral range of this sensor includes the Visible-, Near-, Shortwave- and Thermal infrared part of the electromagnetic spectrum and consists of 79 channels (German Aerospace Center, DAIS).

HyMap is an airborne hyperspectral imaging spectrometer built and maintained by the HyVista cooperation in Australia and is operated in Europe by DLR in Germany. It covers the electromagnetic spectrum between 400nm and 2500nm with 126 spectral bands with a band width of approximately 16nm (German Aerospace Center, HyMap).

3.1.2 Orthorectification

Geometric distortions in images are caused by the movements of an aircraft (pitch, roll, heading, flight elevation and sideways through wind), distortions in the sensor and topographic relief. The result of orthorectification is an image mapped to a known location on earth, by referencing it to a map projection.

Distortions in images become relevant if pixel accuracy is acquired (Schläpfer & Richter, 2002). This pixel accuracy is necessary, because of the calculation of vegetation variable information on basis of field data. Small deviations in the position of an image with respect to the field location introduce uncertainties in the final result. Good orthorectification is especially necessary by change detection, because images and their results are sensitive to misregistration.

Approaches to solve the distortions in images are: the polynomial rubber sheet method, correlation matching algorithms and the parametric approach. The polynomial rubber sheet method requires a large number of ground control points to correct for the movements of the sensor. Correlation matching algorithms deliver accurate orthorectification results if an image is structured, because the image is automatically fit to orthophoto imagery. The parametric approach do not require referenced image data sources, correction takes place on basis of sensor models (Schläpfer & Richter, 2002).

The accuracy of orthorectification depends on a geometric sensor model and the uncertainty in the position of the aircraft and movements of the aircraft itself. Critical details of individual parameters are that if only a non-differential GPS (Global Positioning System) is used (instead of differential GPS) the elevation becomes inaccurate to several tens of meters and also drift of the aircraft in horizontal position must be taken into account. Also measurements of roll, pitch and heading are important, but the accuracy of these measurements depends on the system used. An example of a distortion in an image as a result of aircraft movements

during image acquisition is presented in figure 5. Finally the sensor model itself is an error source, because the exact knowledge of the lines of sight to every across-track pixel is crucial in the solution of orthorectification.

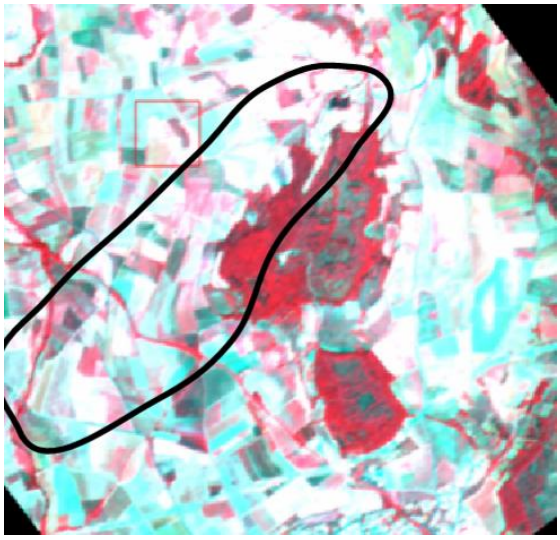

Figure 5: The shape of agricultural fields distorted by aircraft movements (DAIS 1997). The distortion is located inside the area marked with black line.

HyMap images are automatically orthorectified on basis of Differential Global Positioning Systems (position of the aircraft in x-, y- and z-direction) and an Inertial Navigation System (movements of the aircraft itself (roll, pitch and heading)) that describe the movements of the aircraft during image acquisition.

For the DAIS 7915 image is this not available and orthorectification takes place with Ground Control Points (GCP) between the DAIS and HyMap images. GCP's are used to establish the exact spatial position of a point in an image. Ground control refers to physical points on the ground whose ground position is known with respect to a coordinate system.

The HyMap images of 2003 and 2008 are used to orthorectify the DAIS 1997 image. The location of GCP's in both images are based on clearly identifiable locations (Lillesand et al., 2004), as roads, building areas, lakes and corners of agricultural fields. The polynomial rubber sheet method approach is used to correct the image for aircraft movements.

GCP's in the images are related to each other with geographic points on the earth. Envi uses two kinds of images for orthorectification with GCP's. The base image is the image which is already orthorectified and has a known map projection (HyMap 2003 or 2008). The warp image is the one which is not orthorectified (DAIS 1997) and has geometric distortions. Geocoding of the warp image took place on basis of the known coordinate system in the base image.

3.2 Field data

Data in the field was collected to obtain information about vegetation variables. Field data was already available for certain years in the past (2003 and 2008) and more vegetation variable information is collected in the field in September and October 2009.

For the HyMap 2003 image field data from 2005 (collected by Wiebe Nijland) was used. Field data of 2003 was not available. In the resulting part of this study must be remembered that 2005 data is used to determine patterns in vegetation for the Hymap 2003 image. Also if there is referred to 2003, 2005 field data was mentioned. For the HyMap 2008 image field data from 2008 (collected by Erik Baptist and Rik van Pruissen) and 2009 was used.

Information collected during the fieldwork is used for the calibration and validation of model predictions for vegetation variables. This part of the report describes the methods used to determine sample point locations and the collection of field data for the determination of Leaf Area Index, cover fraction and aboveground biomass.

3.2.1 Field plot locations

The locations of sample points are based on the main geological units. These main units mainly control the amount of water and nutrient availability for vegetation which are important for the growth and development of vegetation.

The locations inside a geological entity are based on change/no-change areas of vegetation and are obtained by the use of change patterns in Normalized Difference Vegetation Index values.

The Normalized Difference Vegetation Index (NDVI) reflects the vegetation cover in images in a way that the target being observed contains live green vegetation or not. It is a ratio which uses a red and near infrared band of a remote sensing image to emphasize vegetation. Healthy vegetation has a strong reflection in the Near-Infrared part and absorbs radiation in the visible red part of the spectrum, because of active radiation of photosynthesis.

Values of NDVI are varying between -1 and +1 (equation 1). Strong negative values correspond to bare areas, values around zero to water, low positive values represents shrubs and grassland and higher values can be reached by forests (Lillesand et al., 2004).

NDVI= (NIR-Red) / (NIR+Red) *eq.1*

Red= 0.65 nm

NIR=0.86 nm

Equation 1: Calculation of the Normalized Difference Vegetation Index

The imagery used to obtain this change/no-change patterns are HyMap 2003 and 2008. The DAIS 1997 image is not used, because there was a certain offset between NDVI values of this image and the HyMap 2003 and 2008 image. The change/no-change areas are obtained by subtracting the NDVI-values from the 2008 image from the 2003 image.

The locations of sample points are randomly distributed over the main geological units. Inside a geological unit, the location depend on change/no-change areas in NDVI, because of the collection of ground truth data at locations where changes in NDVI in the last five year have or have not taken place, but the distribution is a clumped random distribution. This clumped distribution is based on the fact that more points can be visited during the fieldwork if points are located closer to each other, so that more information can be collected in the field.

Also plot locations were visited which are defined in other studies in this area. These points, also called Q-plots, are visited one or more times every year, to collect Leaf Area Index values at certain locations on a longer timescale.

The field plots have a size of 5 by 5m and this corresponds with the size of a pixel in the imagery used. The main vegetation variable information collected in the field are biomass in ton/ha, LAI (Leaf Area Index) and cover fraction (these variables are explained in the next paragraphs). Other information collected at a plot location are location coordinates, slope, aspect and descriptions about the accessibility of the plot, vegetation species and weather.

3.2.2 Leaf Area Index

Leaf Area Index (LAI) is an important variable for determining temporal patterns in vegetation. It is defined as the projected (one-sided) total green leaf area per unit ground surface area (Ross, 1981). This is a uniform definition, but there are a lot of methods to measure this variable, which result in significant differences between calculated LAI values (Jonckheere et al., 2004).

LAI is an important variable in processes, such as canopy photosynthesis and evapotranspiration. It is a biophysical parameter which is directly related to the exchange of

energy and mass between vegetation canopies and the atmosphere, because it determines the size of the plant-atmosphere interface (Weiss et al., 2004).

LAI values in the Mediterranean area range from 0 for land with no vegetation to 6 with dense vegetation. This variability depends on the composition of species, the development of vegetation, the environmental conditions on the location where vegetation stands, seasonality and human influence. It is a dynamic parameter and changes from day to day, and, driven by forest dynamics, from year to year (Welles, 1990).

In the study area LAI is largely determined by the yearly situation (large parts of the vegetation under consideration consists of trees that contain leaves in the winter period): in the case of evergreens the situation of the previous two to four years is dominant (Addink et al., 2007 a).

3.2.2.1 Field estimation

Estimation of LAI in the field takes place with an indirect non-contact determination method. It is an optical method based on the measurement of transmission of light through vegetation canopies. The amount of radiation intercepted through the canopy depends on several factors, as the structure of the canopy, incident irradiance and optical properties (Jonckheere et al., 2004).

During fieldwork hemispherical canopy photography is used to study vegetation canopies. Hemispherical pictures provide an extreme angle of view, generally 180 degrees (fisheye lens). The pictures provide valuable information about position, size, density and distribution of vegetation canopy gaps. These pictures make it possible to do spatial discrimination in vegetation canopies and have the greatest potential when hyperspectral remote sensing images of the study area are available (Jonckheere et al., 2004).

The plots in the field have a size of 5 by 5m and 5 pictures were taken for the determination of LAI: one in the centre and the other four one meter from the corner (figure 6). Pictures of the vegetation canopy are taken from the ground in upwards direction and produce an image with the projection of a hemisphere on a plane.

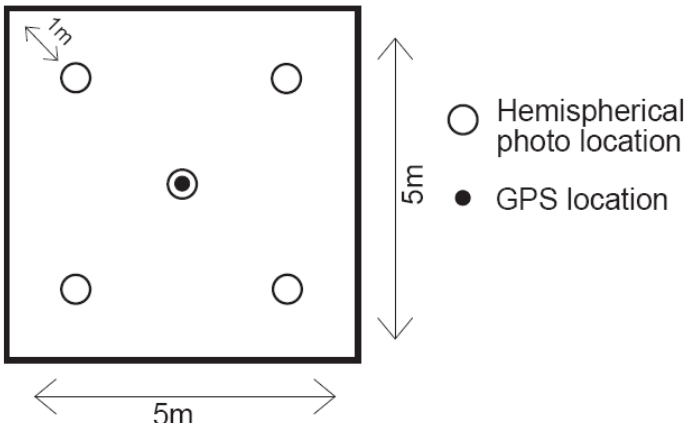

Figure 6: Locations of hemispherical photos in a field plot

3.2.2.2 Can-Eye

The application CAN_EYE (INRA 2004) is used for processing hemispherical pictures and delivers information about the true and effective Leaf Area Index and cover fraction. Estimation of LAI from hemispherical canopy photography is based on the measurement of gap fraction, which means the transmittance of light through the vegetation canopy considering vegetation elements as opaque (INRA 2004). Gap fraction refers to the integrated values of gap frequency over a given domain, especially using hemispherical images.

Processing of hemispherical pictures in CAN-EYE delivers information about LAI, faPAR and cover fraction. Besides LAI also cover fraction is used as a vegetation variable to assess temporal patterns in vegetation. Cover fraction is defined as the ground fraction covered by vegetation projected at the ground surface (Liu et al, 1995).

CAN-EYE can be divided in a number of processes, such as setting up processing, selecting images, pre-processing of images, classification and generation of outputs.

Setting up processing consists of setting up the calibration parameters of the camera used to collect hemispherical pictures. The pre-processing of images makes it possible to mask parts in images that are undesirable (like bright sun spots and the surrounding sun, haze, people, etc.) and change image characteristics for better visual discrimination.

The most important part is image classification. Classes are defined to separate vegetation elements from sky or soil. The classification is partly automated by the program itself (selecting colours belonging to sky or soil), but manual changes can be made to make the classification more accurate: especially in areas where sunspots influence the colours in surrounding areas. This results in branches and twigs that are classified as sky, but are

vegetation elements. Also edges of leaves deserve in most cases manual changes. Classification takes place with interactive colour classes where colours of each class depend on illumination conditions and objects in an image. After allocation of colours to classes, images are transformed into classified images (figure 7).

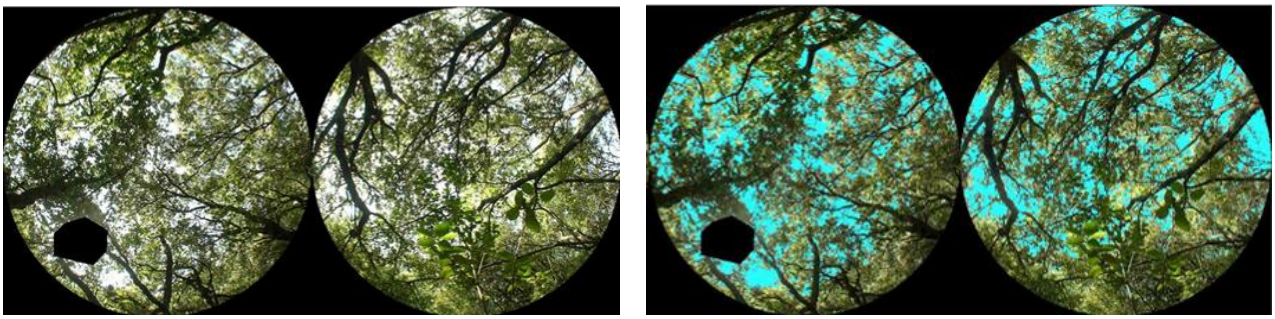

Figure 7: Hemispherical pictures in Can-Eye. Left: Original pictures with mask. Right: Classified pictures where blue represents sky.

Outputs of CAN-EYE are generated automatically. The calculation of variables includes the computation of gap fraction images, distribution and matrices and the clumping factor. The clumping factor is an important variable for the calculation of trueLAI and depends both on plant-, and canopy structure, also shape and size of leaves play a role.

The clumping factor λo in combination with effective LAI results in true LAI values. The true LAI is related to the effective LAI (equation 2). The computation of the clumping index is based on the assumption that vegetation elements are locally assumed randomly distributed, where each zenithal ring is divided into groups of individual pixels. The clumping factor is calculated for each zenithal ring (equation 3), which result in a trueLAI for every plot location where hemispherical pictures are processed in CAN-EYE.

$$LAI^{eff} = \lambda_0 \, LAI \qquad \textit{eq. 2}$$

LAI^{eff}= effective Leaf Area Index
λ_0 = clumping index
LAI = true Leaf Area Index

Equation 2: Relation between effective and true LAI, with λo as clumping index (CAN-EYE output variable description).

$$\lambda^0 (\theta, ALA^{eff}) = (\text{mean}[\log(P_0^{Cell}(\theta))]) \,/\, (\log[\text{mean}(P_0^{Cell}(\theta))]) \qquad \textit{eq. 3}$$

$\lambda^0 (\theta, ALA^{eff})$= clumping parameter for each zenithal ring
$P_0^{Cell}(\theta)$ = gap fraction of a pixel (cell)

Equation 3: Clumping parameter for each zenithal ring (The ratio in the equation provides the clumping parameter λo for each zenithal ring) (CAN-EYE output variable description).

3.2.3 Biomass

Biomass can be divided in above- and belowground biomass. Together are these defined as the amount of living matters (leaves, twigs, stems and woods) of vegetation. In this study only aboveground biomass is considered, because with remote sensing images only aboveground biomass information can be assessed and the collection of belowground samples is difficult.

In the rest of the study biomass is meant as aboveground biomass and is defined as the total amount of aboveground living organic matter (leaves, twigs and stems) (De Jong et al, 2003) in tons per hectare and is determined as the accumulation of yearly net growth.

Temporal monitoring of aboveground biomass reflects the degradational status of areas on basis of increasing or decreasing values. This temporal monitoring is necessary, because the mass of this vegetation components change with time as a result of natural (amount of water and nutrient availability for vegetation) and human influences (logging, reforestation). These changes in aboveground biomass are low between different years, but are useful by the determination of increasing or decreasing patterns in vegetation development as a result of land degradation or climate influences. In this study the influence of climate can be neglected, because the time scale wherein vegetation changes are observed is too short.

3.2.3.1 Field estimation

In the field aboveground biomass is estimated by an indirect method. This involves the establishment of relationship(s), through regression analysis, between biomass and measurable tree parameters, such as diameter at 50cm or at breast height, total height, crown diameter, etc. (Araujo, 1999).

Measurements in the field differ for trees or shrubs. Shrub measurements include the height and maximal projected diameter of shrubs. For trees are there measurements for trunk diameter and height. The height of trees and shrubs is visibly estimated without instruments.

The maximum projected area of shrubs and the circumference of trees are measured with a measure tape. The circumference of trees is measured at 50cm above the ground (figure 8).

Figure 8: Circumference measurement in the field

The classification of a vegetation element in a tree or shrubs depends on its shape and not on the height. A vegetation element is considered as shrub if it is a low woody vegetation element with sufficient development in up and sideways direction.

3.2.3.2 Allometric relations

The allometric relation (table 1) used to calculate the aboveground biomass of a tree is a function of vegetation species (Ogaya et al, 2003). There are two allometric tree relations based on the Strawberry tree (*Arbutus unedo*) or the Evergreen oak (*Quercus ilex*). Other tree species measured were divided in two groups on basis of morphological similarity to the Strawberry tree (*Arbutus unedo*) or the Evergreen oak (*Quercus ilex*).

Shrubs use another allometric formula which is based on the height and the maximum projected area of a shrub (Pereira et al, 1994). The vegetation species by shrub measurements is not considered.

Equation	Species	Source
ln AB = 3.830 + 2.563 * ln D50	Strawberry tree (*Arbutus unedo*)	Ogaya et al, 2003
ln AB = 4 .900 + 2 .277 * ln D50	Evergreen oak (*Quercus ilex*)	Ogaya et al, 2003
AB = 0.642 * H^0.0075 * Dmax^2.4901	shrubs	Pereira et al, 1994

AB is the aboveground biomass in kg
D50 is the tree diameter in cm, measured at a height of 50cm
Dmax is maximal projected diameter of shrubs in m
H is the height in m

Table 1: Allometric relations for the calculation of aboveground biomass

The aboveground biomass within a plot is calculated by summing the aboveground biomass results of trees and/or shrubs for a plot divided by the area of the plot. The units of aboveground biomass are tons per hectare.

3.2.4 Field data for regression analyses

Later in this study a regression analysis is used to create a relation between the spectral signatures of pixels in images with respect to field estimates. Not all observations contain reliable data as result of disturbances, such as areas with low shrubs and locations that lay near a road. These disturbances result in significant differences between observations in the field and predictions through the application of regression on images. These disturbed observations are reduced to a minimum to make the prediction model more accurate.

Rules are applied on data to remove unreliable/suspicious observations. An observation is supposed as unreliable when values are located in a range where observations of this variable are difficult. LAI and cover fraction together are used to detect unreliable observations, because these variables are generated with the same technique (hemispherical photos).

In this study observations for LAI and cover fraction are unreliable if values for LAI are lower than 0.5 and/or cover fraction is lower than 10%. These values are based on underestimation of LAI and cover fraction with hemispherical photos. This underestimation is the result of:

- Areas with low vegetation heights (les landes). Hemispherical photos do not cover low vegetated areas completely. The fisheye lens takes photos from 30cm above the ground and misses the part with vegetation located below this lens. The resulting photos contain sky in particular.
- High vegetation with a low cover fraction (as example: *Spartium junceum* and *Ulex parviflorus*) and dense grasses on the ground. Estimations are based on high vegetation with a low cover fraction and do not take into account the dense grasses on the ground. This results in observations where the estimation of cover fraction in the field is low, but in reality and in an image is high.

For biomass, observation values located below 2 ton/ha are supposed to be unreliable, because of:

- Field locations with a high number (above 50) of shrubs. The number of shrubs is difficult to estimate. Small deviations in the prediction of the number of shrubs result in significant differences in biomass value estimations.

- Field locations with a few shrubs and dense grasses below it. Grasses are not taken into account by biomass estimations. Estimations in the field are low, but in reality and in an image are higher.

Observations are removed from the data set by the application of the rules mentioned above. For the HyMap 2003 image field data from 2005 was used with 202 observations for biomass, LAI and cover fraction. For the 2008 image field data of 2008 and 2009 was used with 433 observations for biomass and 438 for LAI and cover fraction.

Note: in the resulting part of this study must be remembered that 2005 data is used to determine patterns in vegetation for the Hymap 2003 image. Also if there is referred to 2003, 2005 field data was mentioned.

3.3 Natural vegetation areas

In this study, vegetation under consideration is natural vegetation. Temporal patterns in vegetation are the result of the influence of environmental factors. Vegetation growth and development in natural vegetation areas takes place as a result of natural circumstances, concerning the climate, water and nutrient availability, etc.

The study area under consideration is chosen on basis of the part of the area covered by all images (figure 2). In this study only natural vegetation areas are taken into account. Other areas are masked out by use of Normalized Difference Vegetation Index (NDVI) values.

As is mentioned in the study area, areas with another cover than natural vegetation are masked out of the area of interest for the study of temporal patterns in vegetation. This is done by of vegetation indices values. These emphasize vegetation in images in a way that it possible to observe variations in vegetation indices values in time.

Normalized Difference Vegetation Index (NDVI) values are calculated for the imagery of 1997, 2003 and 2008. The information about change/no-change areas forms an additional component to distinguish natural vegetation areas from other areas. The combined NDVI image is segmentated to create objects.

An object that is formed represents a group of pixels with similar spectral properties and is created on basis of the properties of each cell and the cells surrounding that cell. An object contains besides spectral information, also information about shape, texture and morphology (Ouma et al., 2008).

Objects are used to assess natural vegetation areas, because objects divide the image in homogeneous patches. Spectral and shape information of the objects are used to classify the objects in vegetation, agricultural fields, roads and other. For each class certain rules are formed when an object belongs to that class or not.

This was also difficult, because some objects have similar properties for more than one class: as example agricultural fields and areas consisting of natural vegetation. Both have high NDVI values, so separation has to take place on basis of other information, like differences in NDVI between years or the shape of objects. The shape of agricultural field objects resembles a more square shape than the shape of natural vegetation areas. In table 2 rules are defined to distinguish classes from each other.

Object class	Rules
Natural vegetation	-NDVI values above approximately 0.3 -Differences between years ≤ 0.1
Agricultural fields	-NDVI values above approximately 0.3 -Differences between years ≥0.15 -Mostly rectangular shaped as a result of the shape of the agricultural field plot
Other	-NDVI values under approximately 0.3
Roads	-High length/width values -Mostly low NDVI values, but average NDVI values of roads are influenced by surrounding vegetation.

Table 2: Rules to divide objects in classes. For the difference between years the value was obtained by subtracting the 2008 image from the 2003 image.

After automatic classifying objects, some manual changes are done in ArcGIS to finally end with only areas consisting of natural vegetation. Examples of areas where manual changes took place are:

- Areas with large differences in NDVI values between years classified as agricultural areas, but are natural vegetation, because of vegetation growth and development (reforestation and/or recovery of vegetation after logging).
- Les landes vegetation areas have low NDVI values and are classified in the category other areas, but are natural vegetation areas consisting of herbaceous species.
- Areas classified as natural vegetation, but in reality agricultural areas where the difference in NDVI values between years is small.

The areas classified as natural vegetation areas cover 19.9 km² of the study area (approximately 59%). Temporal patterns in vegetation are only assessed for these natural vegetation areas. An overview of these natural vegetation areas can be found in figure 9.

Natural vegetation areas

Figure 9

Natural vegetation

N

Created by: Annekarlijn de Rijcke
Project: Temporal patterns in vegetation in the Mediterranean area
Date: 17-12-2010

1:50.000

0 500 1.000 2.000 3.000 4.000 5.000 Meters

3.4 Regression analyses

Vegetation variables for the whole study area are mapped by a combination of field estimates and information present in images (spectral signature of pixels) with regression analysis. These analysis of data aims at discovering how one or more variables (called independent variables, predictor variables or regressors) affect other variables (called dependent variables or response variables) (Sen & Srivastava, 1990). Regression creates a relation between the spectral signatures of pixels in images with respect to field estimates.

In this study, hyperspectral images are used. These images contain information in many narrow bands over the visible-, near- and shortwave infrared part of the electromagnetic spectrum. Image reflectance values are related to field estimates and used to compute a regression function. This function is applied to images to predict vegetation variables at new-visited locations.

3.4.1 Regression analyses principles

Regression is used for predictive modelling on the basis of statistical relations. The relation implies that the value of a variable depends on one or more other variables. In a simple linear model the variations in the dependent variable are attributed to changes in only a single independent variable (Schroeder et al., 1986).

In this study there are more independent variables. The dependent variable is the vegetation variable (biomass, Leaf Area Index or cover fraction) and depends on other independent variables, which are the reflectance values of pixels (pixel signatures) corresponding to field plots. Several factors simultaneously affect the dependent variable; this is also called multiple linear regression analysis.

A problem by fitting a regression model to hyperspectral images is the large correlation between spectral bands (multi-collinearity). When two or more regressors (variables) are closely related, it is hard to untangle their separate effects on the predicted value Y. When one regressor increases, the other increases at the same time (Wonnacott & Wonnacott, 1990)

Multi-collinearity in the application of multiple linear regression analyses results in model parameters that become unstable. The multi-collinearity manifests itself in large variances (uncertainty) in the model parameters and these cannot be used for interpretation, because it makes the predictions unreliable.

A solution for this is ridge regression, because it takes this multi-collinearity into account. Ridge regression is based on proportional shrinkage of coefficients. This is done by imposing a penalty on the size of the regression coefficients (Hastie et al., 2009). The general ridge regression equation is described below:

$$RSS(\lambda) = \sum_{i=1}^{n} (y_i - \hat{y}_i)^2 + \lambda \cdot \sum_{j=1}^{p} \beta_j^{\,2}$$

eq. 4

RSS (λ) will be minimized
n is the number of observations
ŷ is the predicted value
j is the predictor
ß is the regression coefficient
i is the observation
y is the observed value
λ is the ridge parameter
p is the number of predictors

Equation 4: General equation for ridge regression

Λ controls the amount of shrinkage of regression coefficients. A larger value of λ means a greater amount of shrinkage (Hastie et al., 2009). The optimal value for λ is obtained by the use of Generalized Cross-Validation and is the λ value where the Generalized Cross-Validation is the lowest. The Generalized Cross-Validation is equal to the total variance of the residuals.

Cross-validation is a simple and widely used method for the estimation of the prediction error. In the ideal situation (where the amount of observations is much larger than the amount of the independent variables plus one), a validation data set can be used to assess the performance of the prediction model.

3.4.2 Processing of data for ridge regression

Data collected in the field is processed with ridge regression to calibrate and validate the vegetation variable information. Data needed for ridge regression consists of vegetation variable information (Leaf Area Index, Biomass and cover fraction) and their belonging pixel signatures from remote sensing images.

In the regression model the explanatory variables are the vegetation variables and their belonging band information. The outputs of the model are the response variables. The explanatory variables are independent of the response variable and the dependency between these variables is determined by the regression model.

Images consist of pixels of 5 by 5m and have a similar size as the field plots. Coordinates of sample point location in the field are obtained with a GPS-device (Global Positioning System). Although coordinates will match, field observations are not necessarily linked to the correct pixel (geometrical mismatching). To reduce this problem field observations are linked to windows consisting of 3 by 3 pixels. The window is created on basis of a buffer around the centre point of a pixel wherein the plot location is found (figure 10).

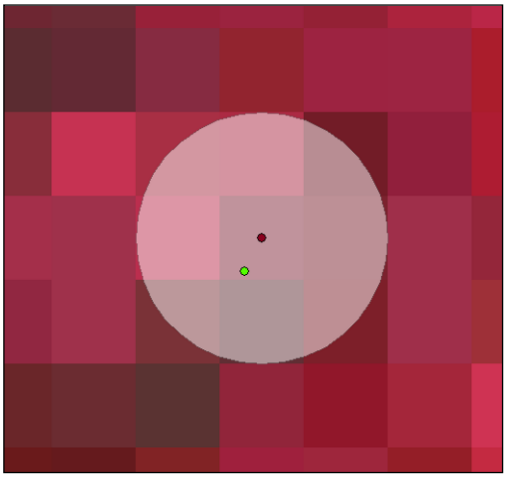

Figure 10: Original sample point location (green), the center location of the pixel (dark red) which corresponds to this plot and the created buffer window (white haze).

Buffer windows (consisting of 3 by 3 pixels) created in ArcGIS are imported in ENVI and represent the green dots in figure 11. Statistical information is obtained of pixels covered with a green dot. The average pixel value for a green dot (3x3 window) is obtained of spectral information present in hyperspectral images. Spectral information for each green dot is plotted (figure 12) and processed to numeric values. The numeric output values represent information for every band available in an image. The band information is added to the belonging plot numbers and vegetation variable information.

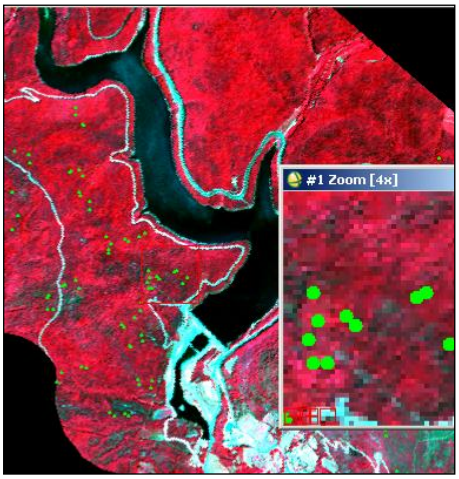

Figure 11: Buffer windows in an image

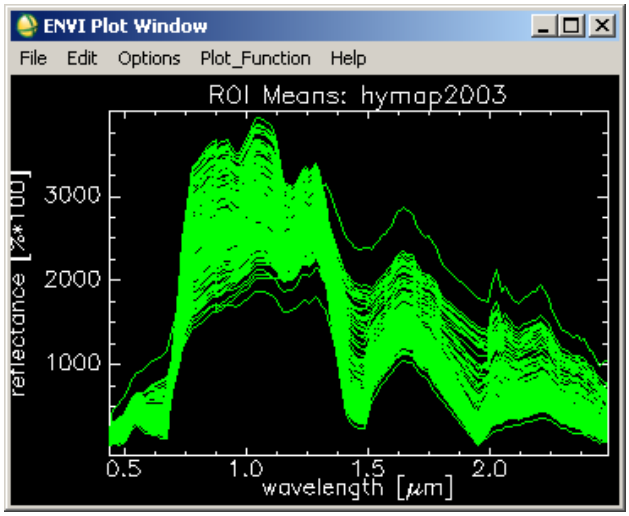

Figure 12: Spectral information about 2003 plot locations

Finally a matrix arises where the first column defines the plot number, the second the value of the vegetation variable under consideration and the other columns the band numbers of the remote sensing images. Every row in the matrix represents another sample point location and their belonging field and image values.

Ridge regression is performed with in a program called R and is a language and environment for statistical computing and graphics (GNU project). It provides a wide variety of statistical and graphical techniques and is highly extensible (R project).

Ridge regression took place with a function called lm.ridge. An overview of the script used for the application of ridge regression can be found in appendix 3. This script invokes the matrix with vegetation variable information and their belonging band information. Besides that is indicated that the vegetation variable is the dependent variable and the columns with band information are the independent variables.

Important output information for ridge regression is the Generalized Cross Validation, the associated value of λ and the effective degrees of freedom. λ Values (normally a vector) are defined at the beginning of the script and can be adapted on basis of the results. Every λ value has a solution and controls the size of the coefficients. The optimal value for λ is where the Generalized Cross-Validation is the lowest (Hastie et al., 2009). To interpret the impact of the penalty that is applied on the size of coefficients, effective degrees of freedom are used. These measure the flexibility in the fit of the model. The model prediction consists of an intercept and coefficients (equation 5) that can be applied on band information present in remote sensing images.

$$y = a + b1*x1 + b2*x2 + \ldots + b_n * x_n \quad \text{eq.5}$$

y is the resultant model, in this case vegetation variable information
a is the intercept of the formula
b1, b2, …, b_n are the regression coefficients based on band number of an image
x1, x2, …, x_n are the reflectance values from an image based on band number

Equation 5: Model which describes the spatial variability of the dependant variable

3.4.3 Calibration of regression data

As mentioned in paragraph 3.1 and 3.2 this study only considers 2003 and 2008 imagery and field data from 2005 for the 2003 image and from 2008 and 2009 for the 2008 image. Information used for ridge regression consists of two parts: the part with field estimates and the part with data of remote sensing images. Both parts should include reliable data without disturbances. Data is controlled to remove unreliable/suspicious information out of data used to apply ridge regression on.

For the HyMap 2003 image field data from 2005 was used. This dataset contains, after removing unreliable data, 202 observations for biomass, LAI and cover fraction. For the HyMap 2008 image the dataset contains 433 observations for biomass and 438 for LAI and cover fraction.

A regression analysis for aboveground biomass was performed by the logarithm of the value. The original values measured in the field are not normally distributed. Figure 13 contains histograms of the biomass data used for the 2003 and 2008 image. For the 2003 image field data of 2005 is used. For the 2008 image field data of 2008 and 2009 is used.

The histograms of biomass show that most field observations are located below 250 ton/ha with a long tail with low frequencies to 400 ton/ha for 2003 and 700 ton/ha for 2008. By taking the logarithm of biomass observations, the right side of the distribution lay closer to other observations with lower biomass values and the set of observations becomes more normal distributed. For both years the typical bell-shaped distribution is situated between a log-biomass of 1.5 till 3, but now there is a long tail with low frequencies to the left. Still log-biomass is used, because the histogram is close to a normal distribution.

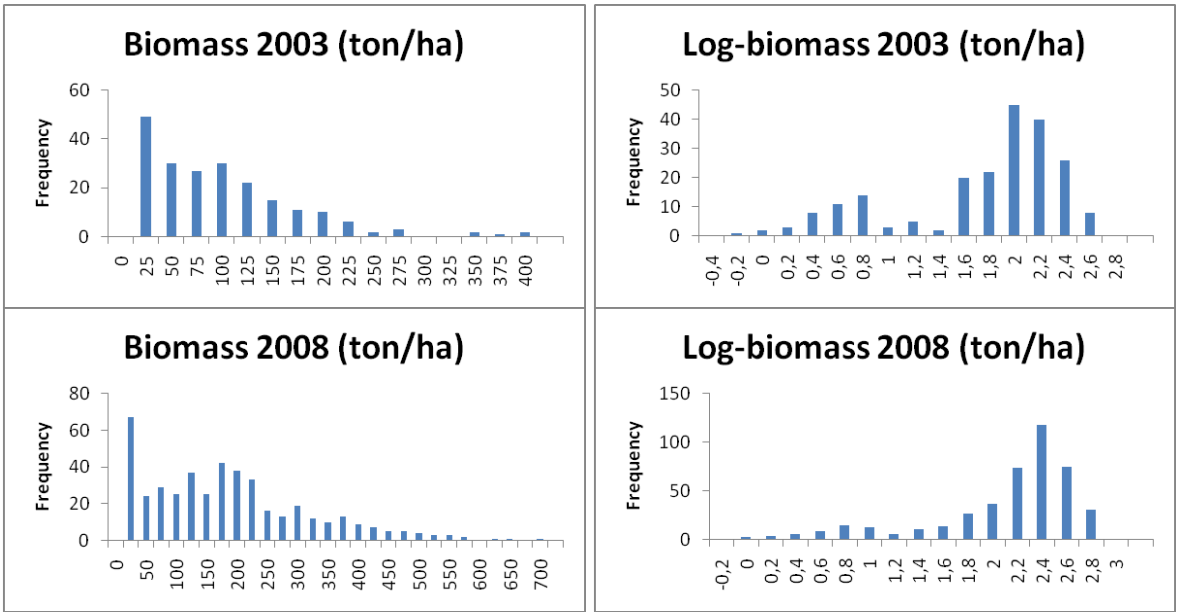

Figure 13: Histograms of biomass and log-biomass data for the 2003 (field data 2005) and 2008 image

Ridge regression is not applied on the entire dataset, because a part of the dataset is needed for estimating the accuracy. This is the reason that the dataset is divided in a part for calibration and validation. Regression analyses are applied on calibration data and the result are model predictions. The validation part is used to control the accuracy of model predictions.

2/3 of the observations are used for calibration and 1/3 for validation. The distribution of data for calibration and validation cannot take place randomly, because a good model prediction and assessing the accuracy of this prediction needs estimates over the entire range of values. To distribute the observations over the calibration and validation part well, the observation values are sorted from small to large and get additional numbers from 1 to 3 in sequences. Inside a sequence the first and third value are used for calibration and the second for validation. The advantage of this distribution of data over both categories is that both data sets contain values over the entire range of observation.

A disadvantage from distributing these values over both categories is that the amount of field observations for the 2003 image and the amount of bands used lay close together. This means that the number of degrees of freedom is low. The degrees of freedom for multiple regression are estimated by the number of observations and the number of variables (equation 6) (Wonnacott & Wonnacott, 1990).

$$df = N - k - 1 \qquad \text{eq.6}$$

df=degrees of freedom
N=number of data points
k=number of regressors (variables)
Equation 6: Degrees of freedom for multiple regression

If more regressors are used, the degrees of freedom are lower and this result in a smaller ability to test the model. More degrees of freedom are obtained by reducing the number of regressors. For the 2003 image 135 field observations and 124 bands are available to apply ridge regression on. The degrees of freedom are then 10. To increase the number of degrees of freedom fewer bands from the image are used. There is chosen to use only half of the available bands, so instead of 124 regressors, 62 are used. These are alternately chosen is such a way that the entire electromagnetic spectrum of hyperspectral images is covered.

3.5 Image segmentation

Images that are created with the predictive models of regression analyses consist of pixels. Pixels do not accurately represent the true nature of features. These features vary in size, shape, colour, texture as well as in degrees of compactness (Ouma et al., 2008).

Image segmentation is a technique to convert an image (consisting of pixels) into homogeneous patches. Objects aggregate pixels into homogeneous segments on basis of adjacent pixels that share similar spatial or spectral properties.

The aim in this study is to assess temporal patterns in vegetation by using change detection. Advantages and disadvantages of using pixels or objects by change detection (the process of identifying differences between images acquired at different times) are:

Advantages of pixel-based change detection are:

- It uses true pixel values, which come from image spectral bands or vegetation indices.

Disadvantages of pixel-based change detection are:

- Different land cover classes can have similar spectral properties, like degraded land with a bit of vegetation on it in comparison to harvested cropland (Gao, 2008).
- Pixels do not accurately represent the nature of features on the Earth surface. Features are varied in size, shape, colour, etc. (Ouma et al., 2008).
- It is sensitive to misregistration and the existence of mixed pixels (Lunetta & Elvidge, 1998).
- The resulting map consists of a “salt and pepper” effect, as result of sensor variations and characteristics of land covers (Desclee et al., 2005).
- It is more difficult to apply on hyperspectral images, because the pixel size is small and contain detailed information.

Advantages of object based change detection are:

- Besides spectral information, contain objects also information about shape, texture and morphology which can be used in image analysis (Navulur, 2007).
- Objects of no interest on larger scale can be masked out, so the focus lay on the extraction of features of interest to the end user (Navulur, 2007).
- Objects can be created at different levels, which can improve/enhance the feature extraction process in change detection (Navulur, 2007).
- The image consists of a group of homogeneous objects and these are more intelligent than pixels in the sense of knowing their neighbours and their spectral and spatial relations within and among them (Ouma et al., 2008).

Disadvantages of object based change detection are:

- Natural vegetation consists of gradual boundaries and not of straight lines, and vegetation in an object is mostly a mixture of different vegetation species.
- The application of object-based change detection depends on the properties of land covers. Important by this are their spatial scale and spectral distinctiveness (Gao, 2008). The properties of land covers influence the application of object-based change detection, as mentioned above natural vegetation is mostly a mixture of different vegetation species and it is more difficult to distinguish objects from each other than in comparison with agricultural fields.

There are three ways to create objects: segmentation, stratification and a combination of these two. By segmentation objects are created on basis of neighbouring pixels with similar

spectral properties. For stratification pixels are grouped on basis of an external variable, such as soil or land cover classes.

In this study segmentation is used to create objects, because the patterns in vegetation variables depend on static (for example geology or soil) and dynamic environmental factors. There is not one clear factor that describes the temporal patterns in vegetation, because a lot of factors together influence the ecosystem wherein vegetation is growing.

3.5.1 Object based image analyses

An object can be defined as a group of pixels with similar spectral properties. They are created on basis of the properties of each pixel and the pixels surrounding that pixel. Each object can contain spectral, spatial, morphological, contextual and temporal information (Navulur, 2007). In this study objects are created on basis of vegetation variable (biomass, LAI and cover fraction) maps produced with predictive models of regression analyses.

Image segmentation is done with Definiens developer (eCognition). Objects in this application are created by combining the four criteria of scale, colour, smoothness and compactness. The scale parameter determines the maximum allowed heterogeneity for the resulting image objects. For heterogeneous data, the resulting objects for a given scale are smaller than in more homogeneous data (Definiens eCognition Developer, 2009).

The object homogeneity to which the scale parameter refers is defined by the three criteria of colour, smoothness and compactness. The colour criterion is the most important one of this three for the creation of meaningful objects. However, a certain degree of shape homogeneity often improves the quality of object extraction, because the compactness of spatial objects is associated with the concept of image shape (Definiens eCognition Developer, 2009). By adjusting the parameters of colour, smoothness and compactness the quality of object extraction can be improved.

Different scale levels are used to determine the optimal scale for image segmentation. Default values are used for the criteria of colour, smoothness and compactness. The end product of image segmentation is a file consisting of objects (polygons) instead of pixels, where objects contain attribute information about the vegetation variable under consideration of the acquisition years used.

3.5.2 Methods of image segmentation for change detection

Patterns in vegetation are assessed by object based change detection. These patterns are observed in the time span 2003 to 2008. The vegetation variables are segmented separately from each other, because all have their own characteristics (spatial and spectral variability) and these are in most cases not similar to the characteristics of another vegetation variable.

Three segmentation methods are developed to determine the optimal way of image segmentation. The inputs for segmentation are the predictive vegetation variable maps for 2003 and 2008. The patterns for a certain or both years are used to create objects from.

The image segmentation methods applied on each vegetation variable are:

Method 1:

Vegetation variable maps of 2003 and 2008 are used to create objects simultaneously (figure14). Both maps are aggregated in one image consisting of two layers. Image segmentation takes place on this image, resulting in objects formed on basis of characteristic patterns present in 2003 and 2008 at the same moment. Object attribute information depends on the pixel values present in the predictive vegetation variable maps.

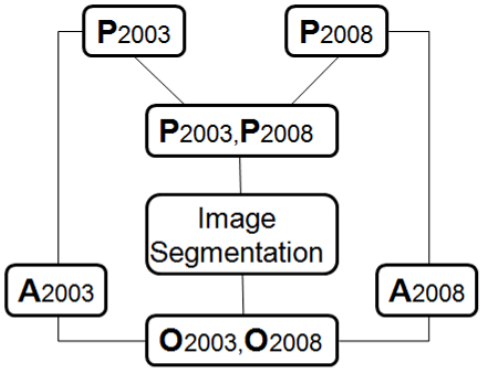

P = Predictive vegetation variable map
O= Image consisting of objects
A=Attributes from objects

Figure 14: Image segmentation method 1

Method 2:

Vegetation variable maps from 2003 and 2008 are segmentated separately from each other (figure 15). The final object boundary locations are defined by merging the boundaries (overlay of two layers) of the objects formed for 2003 and 2008.

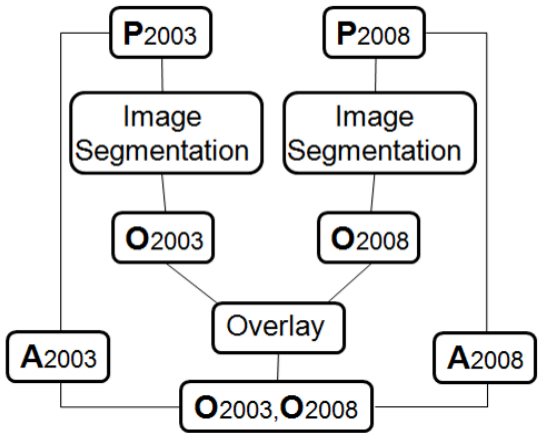

Figure 15: Image segmentation method 2

Method 3:

Object boundaries are defined by segmentation of the vegetation variable 2003 map on its own (figure 16). Object are created on basis of vegetation patterns present in 2003. Objects for 2008 are based on the location of objects in the 2003 image. Changes can be determined through the comparison of object attributes values for 2003 and 2008.

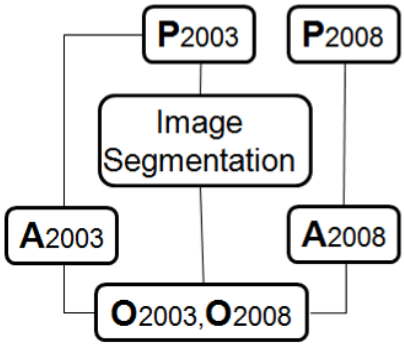

Figure 16: Image segmentation method 3

3.5.3 Validation of image segmentation

Image segmentation accuracy assessment takes place to identify the best method and scale to determine temporal patterns in vegetation. The outcome of image segmentation is a file consisting of objects (polygons) for each segmentation method and scale. The value of an object represents the average value of pixels located inside an object.

The validation of image segmentation is performed by using the validation part of field observations, earlier defined in paragraph: 3.4.3 calibration of regression data. This means that 1/3 of the dataset with field data is used to estimate the prediction accuracy. It should be noted that for the 2003 image field data of 2005 and for the 2008 image field data of 2008 and 2009 were used.

For the validation of image segmentation the value of a field observation is compared with the value of the object wherein the field observation is located (figure 17). The object value is based on the segmentation applied on the predicted vegetation variables maps. Object values are joined to validation points, resulting in object information added to the attribute table of the point. The point file contains information about the measured value of a point in the field and the value of the object.

The accuracy for each segmentation method and scale is assessed by calculating RMSE and R^2 values on basis of the attribute information assessed by joining attribute information of objects to the validation points.

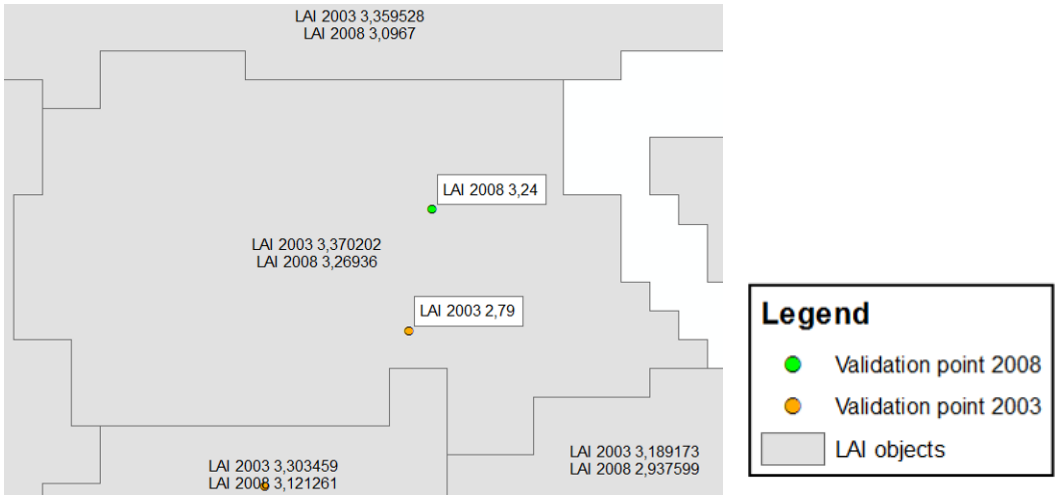

Figure 17: Validation points and objects for image segmentation. It should be noted that 2005 field data is used to assess the accuracy of the 2003 prediction.

3.6 Change detection

Change detection is defined as the process of identifying differences in the state of an object or phenomenon by observing it at different times (Singh, 1989). In this study change detection takes place on objects generated with image segmentation. The changes of interest are increasing or decreasing patterns in the vegetation variables under consideration.

The observed changes can be divided into two categories: relevant and irrelevant changes. Relevant changes are the ones where the observer is interested in. In this study are these temporal patterns in vegetation variables between 2003 and 2008. Irrelevant changes are modifications of single objects and do not contain conversions from one object into another. These changes can be caused by differences in illumination conditions and geometric mismatches (Addink et al., 2006).

Change detection approaches are divided in post-classification and pre-classification. By post-classification are changes analysed between two independent classification products. The advantage is that data normalization is not necessary, because two or more images are classified separately from each other. By a pre-classification approach are images compared with each other, without doing a classification. Data normalization (if images with spectral information are used) is than necessary to correct for variations in solar illumination and atmospheric conditions, but also for differences between sensor systems used (Lillesand et al., 2004).

For this study the pre-classification approach is chosen, because the images are compared with each other in terms of absolute values and not in terms of classified products. Inside the pre-classification approach image differencing is used, because it is a simple, robust and easy to interpret method to derive changes.

By image differencing images from different acquisition years are subtracted from each other and the change is present in the residual image. The advantage is that besides the determination of vegetation patterns also the size of the change can be assessed. A disadvantage is the interpretation of the residual image, because different input values can have the same result after subtraction of the images and the original object value is not retained (Singh, 1989). For this study is this disadvantage not a problem, because the aim is to assess increasing or decreasing patterns in vegetation.

For the determination of change areas a threshold for the change magnitude is used. This “change no-change” threshold is obtained by using the image segmentation validation file.

This file contains information about the measured value of a point in the field and the value of the object, as earlier explained in paragraph: 3.5.3 Validation of image segmentation. Regression analyses are used to obtain residual information. The average absolute residual value is used as threshold to define change areas.

An area is detected as changed area if the change is higher than the threshold value. Changes are mapped as follow: increase, decrease or no-change. The increase and decrease category are further subdivided in a low or high change. Areas are regarded as high change areas if changes are bigger than two times the threshold.

The distribution of temporal patterns in vegetation is further analysed with maps, graphs and tables on basis of increasing, decreasing or no-change areas. Also change patterns between the vegetation variables are mutually compared.

Besides that the effect of environmental factors on change patterns of vegetation variables are analysed on basis of change percentages present in different categories of an environmental factor. Static environmental factors are factors which do not change through time, such as the geological unit, slope, aspect and elevation. On the other hand dynamic factors will change through time, like water availability, radiation and nutrients. These factors together influence the ecosystem. An ecosystem consists of biotic and abiotic components (Jordan, 1981) that influence the growth and development of vegetation. Static environmental factors analysed are geology, elevation, slope and aspect.

4. Temporal patterns in vegetation

Different methods are used to map the spatial distribution of vegetation variables. These different methods together contribute to the final result of this study; Temporal patterns in vegetation in the Mediterranean area.

In this chapter the results of the different methods used to assess temporal patterns are described. These topics are fieldwork data analyses with the observation locations and analyses on basis of vegetation variable information. Regression analyses and the optimal prediction model which is applied on remote sensing images to obtain vegetation variable information. Image segmentation methods and the accuracy by different object scales and finally change detection.

4.1 Fieldwork data analyses

Fieldwork took place in September and October 2009. The purpose of the fieldwork was to collect samples of vegetation variables used to map vegetation variable information for the whole study area.

4.1.1 Sample point locations

The total number of visited sample point locations is 201 and an overview of these locations is shown in appendix 1. As mentioned earlier the sample point locations inside a geological unit are based on the locations of change/no-change areas in NDVI. In reality the exact sample point locations are in most cases not visited, because of inaccessible locations (steep slopes, very dense plots, private properties, etc) and that more sample points can be visited if sample points lay closer together, so that more information can be collected in the field.

Besides the sample point locations that where defined with the method mentioned above also called Q-plots were visited as earlier mentioned in paragraph 3.2.1 (Field plot locations). From the 201 plots visited, 30 plots were Q-plots.

During the fieldwork the aim was to equally distribute the number of sample points over the main geological units. The main geological units (1 till 9) are visited 19-25 times (figure 18). An explanation of the geological units and their facies can be found in table 3.

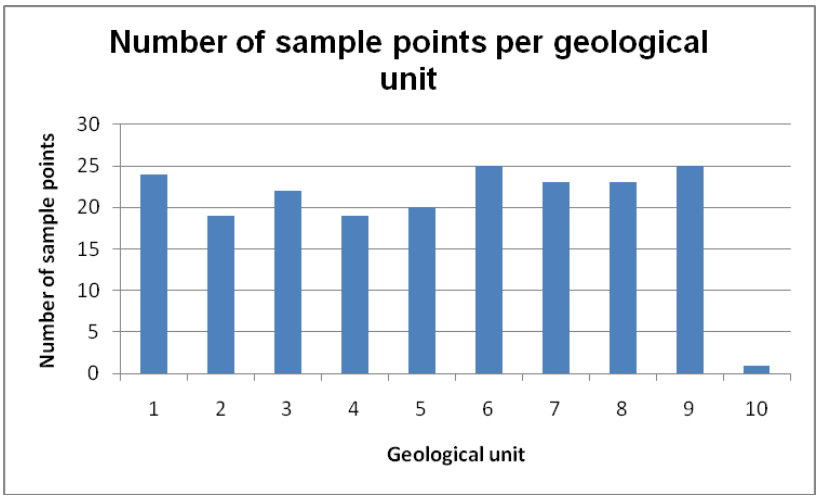

Figure 18: Number of visited sample points per geological unit in 2009, geological units are presented in table 3 on the following page.

Unit	Facies
1	Dolomite
2	Meltflows, basaltes, tuffs
3	Flysch with conglomerates, with limestone products, with olistholites
4	Schistes and quartzite
5	Sandy shale, schistes, coals and limestone
6	Argilites, red slate/mudstone with some conglomerates
7	Sandstone, sandy limestone
8	Limestone, Limestones with chert (limestone with silicified corals)
9	White limestone, sandstone, marls
10	Fluvial sediments

Table 3: Geological units in the study area

Geological unit 10 is visited only once, because this unit does not belong to the main geological units with natural vegetation. The reason that this unit is visited is, because it was located just a few tens of meters outside one of the main geological units and the sample points that has to be visited over there where more or less located on the border of the main geological unit.

On average the main geological units (1 till 9) are visited 22 times, but still there are deviations between the units. Minimal 19 visits in unit 2 and 4 and maximum 25 in unit 6 and 9. In the fieldwork is tried to visit all units equally, but this is not always possible, because of the locations of sample points and time limitations.

4.1.2 Descriptive statistics

Vegetation variable information collected in the field in 2009 is biomass, Leaf Area Index (LAI) and cover fraction. Descriptive statistics of these variables can be found in the tables 4, 5 and 6 and figure 19, 20 and 21.

Biomass (ton/ha) 2009	
Average	249.95
Standard deviation	136.80
Skewness	0.54
Minimum	1.92
Maximum	680.76

Table 4: Descriptive statistics of biomass field data 2009

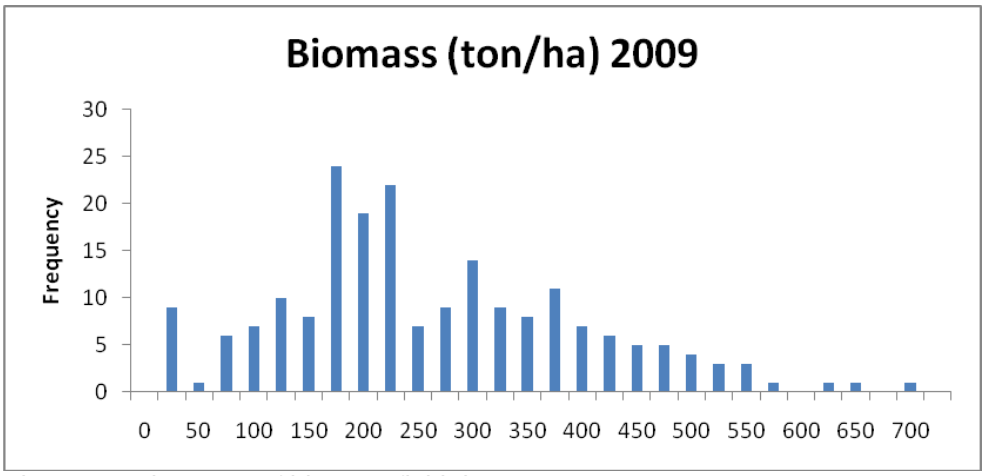

Figure 19: Histogram of biomass field data 2009

The descriptive statistics of biomass (table 4) show that the data is nearly normal distributed (skewness is 0.54). A large part of the estimations have been done in plots with low biomass values (between 0-25 ton/ha) and the highest frequencies are reached around 200 ton/ha (figure 19). Biomass values are distributed over a long range and this result in a long tail with observations at the right side of the histogram. The shape of the histogram does not look like a normal distribution, but the skewness value is good. A reason for this can be that the high biomass values compensate for the high frequencies in the first part of the histogram.

For regression analyses log-biomass values are used, because by taking the logarithm the observations at the right side of the distribution lay closer to the other observations with lower biomass values. Biomass data from other years were not normally distributed and by taking the logarithm the set of observations becomes more normal distributed.

Leaf Area Index (-) 2009	
Average	3.26
Standard deviation	0.77
Skewness	-0.42
Minimum	0.78
Maximum	5.50

Table 5: Descriptive statistics of Leaf Area Index field data 2009

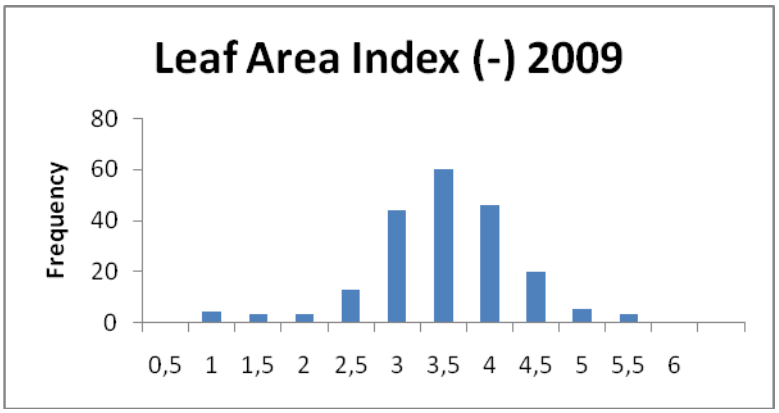

Figure 20: Histogram of Leaf Area Index field data 2009

The skewness value of LAI is -0.42 which means that observations are located at the right tail of the histogram. Also the shape of the histogram shows a normal distribution between an LAI of 2 till 5 (figure 20). The observation frequencies are low in the outer left en right part of the histogram, because most observations are done in plots consisting of forest resulting in LAI values around 2 till 5. LAI values obtained in areas with low shrubs (les landes vegetation) are excluded in further analysis, because it was difficult to obtain good hemispherical photographs.

Cover fraction (-) 2009	
Average	0.69
Standard deviation	0.16
Skewness	-1.72
Minimum	0.06
Maximum	0.95

Table 6: Descriptive statistics of cover fraction field data 2009

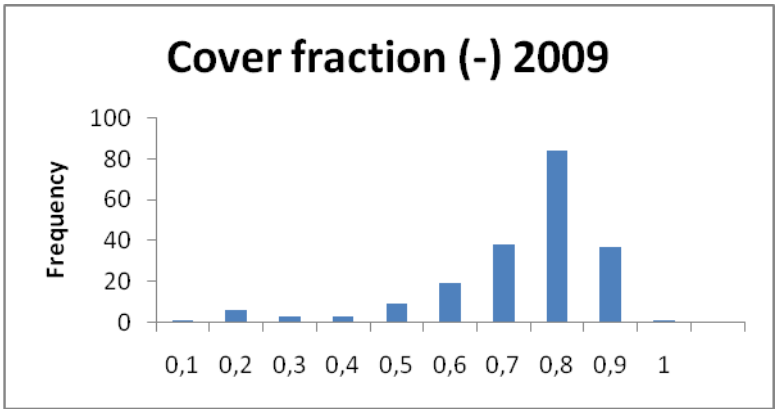

Figure 21: Histogram of cover fraction field data 2009

Cover fraction has a skewness value of -1.72 meaning that the data is largely located at the right tail of the histogram with a long tail to the left. The histogram of cover fraction is more or less similar to LAI (figure 21); because of low frequency values for low cover fraction and LAI

values. The low observation frequency is a consequence of observations that mostly took place in forested areas, which have a cover fraction above 50%.

Vegetation variables under consideration are biomass, LAI and cover fraction. An increase or decrease in one of the vegetation variables does not immediately mean an increase or decrease in one of the other variables. All have their own characteristic values in the development and growth of vegetation (figure 22 and table 7).

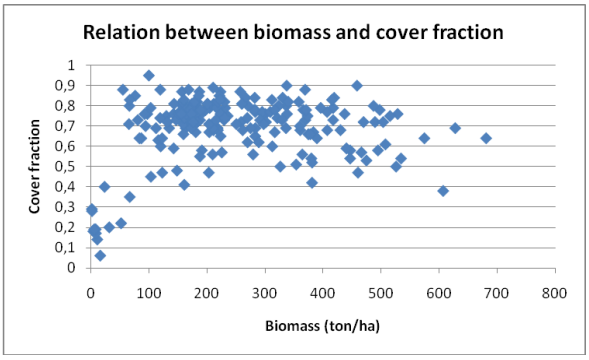

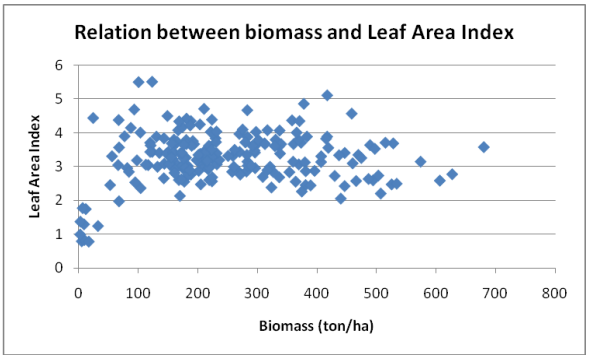

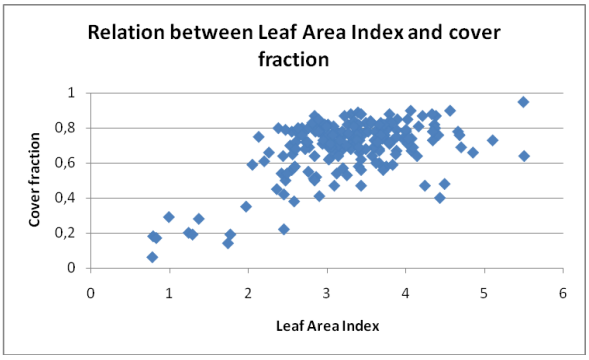

Vegetation variables	Biomass	LAI	Cover fraction
Biomass	1.00	0.11	0.17
LAI	0.11	1.00	0.56
Cover fraction	0.17	0.56	1.00

Figure 22: Scatter plots with the relation between vegetation variables for field data of 2009
Table 7: Correlation between vegetation variables for field data of 2009

The correlation values in table 7 show the degree to which two variables are linearly related. The relation between LAI and biomass and cover fraction and biomass is low, because biomass depends on the weight of the tree or shrub, cover fraction depends on the amount of coverage and LAI on the surface area of leaves.

Figure 22 of biomass against LAI and against cover fraction shows that low biomass values result in low values for LAI and cover fraction. Possibly these observations are obtained in plots with only low shrubs. The determination of LAI and cover fraction inside these plots is difficult, because hemispherical pictures are taken around 30cm above the ground. The biomass values for observations above an LAI of 2 and a cover fraction of 0.35 are distributed over the entire range of values. Between biomass and LAI and biomass and cover fraction no general trend is present in the data, which is confirmed by the correlation values.

The plot of LAI against cover fraction shows a general trend in the data (figure 23). This is proved with the correlation values between these variables. In most cases an increase in LAI results in an increase of cover fraction.

4.1.3 Vegetation species

As earlier mentioned there is a large variety of vegetation types in the Mediterranean area. This is a consequence of the large variation at short distances in geology, soils, elevation, climatic factors and human disturbances. Each geological unit has its own vegetation characteristics. An overview of the distribution of the number and kinds of species present in the 9 main geological units can be found in table 8 for shrubs and table 9 for trees. Geological unit 10 is not described, because this unit is only visited once and does not belong to the main geological units visited during the fieldwork.

In the table, the values below a geological unit represent the relative amount that a vegetation specie is present inside one plot location. Empty boxes below a geological unit mean that the vegetation specie under consideration was not present inside one of these plots. The last row in the table shows the average number of trees / shrubs present inside one plot location. A list of common vegetation names and their Latin names used in the tables below can be found in appendix 2. The geological units and their belonging geological facies are described in table 3.

General characteristics in table 8 about the relative amount of shrub species in a plot sorted per geological unit are:

- During the fieldwork two locations inside geological unit 1 (dolomite) were completely covered with *Quercus coccifera* shrubs. The other visited locations inside this unit do not contain *Quercus coccifera* shrubs. To get a good representation of the vegetation species present in a plot with geological unit 1 (dolomite) the number of *Quercus coccifera* shrubs present in the two locations that where completely covered with it are not taken into account.
- The relative amount of shrubs shows the chance that a certain vegetation specie is present in a plot. To convert this to numbers of a vegetation specie the average number of shrubs per plot has to be taken into account;
- Geological units with high relative amounts of shrubs are: unit 3 (flysch) with 82% *Erica arborea*, unit 6 (argillites) with 82% *Prunus padus*, unit 7 (sandstone) with 60% *Quercus coccifera* and unit 9 (white limestone, sandstone, marls) with 65% *Buxus sempervirens*;
- A lot of different shrub species are present in geological unit 5 (sandy shale). This is possibly the result of the geological unit under consideration: sandy shale, schistes, coals and limestone. This probably creates circumstances where a lot of species can growth and develop and maybe is this the reason that the highest number of shrubs is reached in this geological unit;
- Entity 7 (sandstone) has a low average number of shrubs inside a plot, because this area is in use as an reforestation area and mainly consists of large *Pinus sylvestris* trees with sometimes one or two shrubs inside the plot location.

Shrubs	**Geological unit**								
Vegetation species	**1**	**2**	**3**	**4**	**5**	**6**	**7**	**8**	**9**
Arbutus unedo			4%		3%			2%	2%
Buxus sempervirens	45%	55%	2%	18%	4%			29%	65%
Castanea sativa								1%	
Erica arborea			82%	23%	7%	2%	30%		
Jasminum fruticans			2%						
Juniperus communis					8%				
Ligustrum vulgare	3%								
Pistacia lentiscus					3%				
Prunus padus	7%	4%	4%	7%	23%	82%	10%	1%	3%
Quercus coccifera					1%	2%	60%		
Quercus ilex	45%	33%	6%	46%	9%	12%		12%	5%
Quercus pubescens		8%		5%		2%			1%
Ruscus aculeatus								55%	25%
Spartium junceum					24%				
Ulex parviflorus					18%				
Average number of shrubs species per plot	**1.21**	**2.58**	**2.23**	**2.95**	**5.60**	**2.28**	**0.43**	**4.13**	**4.40**

Table 8: Distribution of shrub species within plots sorted by geological unit. Geological units are presented in table 3 on page 41

Trees	**Geological unit**								
Vegetation species	**1**	**2**	**3**	**4**	**5**	**6**	**7**	**8**	**9**
Acer monspessulanum	3%			1%				3%	
Arbutus unedo	19%		39%	4%	31%	5%		3%	12%
Buxus sempervirens	4%	5%	1%	2%				4%	2%
Castanea sativa				1%				2%	
Colutea arborescens	1%	1%				1%			
Erica arborea	3%		10%	15%	15%				
Jasminum fruticans			1%						
Juniperus communis			2%	1%	1%				
Ligustrum vulgare	1%								
Prunus padus			3%	4%	11%	8%		10%	1%
Pinus sylvestris	10%						100%		
Quercus ilex	49%	89%	45%	61%	41%	80%		74%	81%
Quercus pubescens	10%	5%		11%	1%	7%		3%	3%
Average number of tree species per plot	**12.58**	**14.68**	**18.00**	**14.05**	**16.65**	**14.84**	**6.00**	**13.39**	**18.12**

Table 9: Distribution of tree species within plots sorted by geological unit. Geological units are presented in table 3 on page 41

General characteristics in table 9 about the relative amount of tree species in a plot sorted per geological unit are:

- The most common species is *Quercus ilex*. In 201 plot locations 1772 Q*uercus ilex* trees were present. The relative amount of this specie lay between 41-89% for all units except unit 7 (sandstone);
- Unit 7 (sandstone) consists of a reforestation area and vegetation inside this unit is planted by humans and the distance between the trees is large. The average number of trees per plot is 6. This is very low compared with the average number of other units (12-19 trees per plot);
- Unit 2 (meltflows), 6 (argillites) and 9 (white limestone, sandstone, marls) have high relative amounts of *Quercus ilex*;
- *Arbutus unedo* trees are most common in geological unit 3 (flysch) and 5 (sandy shale). In 201 plot locations 410 A*rbutus unedo* trees were present.

4.2 Validation of regression

Ridge regression is used to create a relation between the spectral signatures of pixels with respect to field estimates. The dependant variable is the vegetation variable under consideration and depends on the independent variables with pixel signatures corresponding to field plots. 62 independent variables (band numbers) are used to create a model prediction function.

The number of observations for the dependent variables depends on the observations available for a certain image year and the rules that are applied on data to remove unreliable values. The rules used to remove unreliable values are mentioned in paragraph 3.4.3 (calibration of regression data). The resultant number of available observations is for the 2003 image field data of 2005 with 202 observations for biomass, LAI and cover fraction and for the 2008 image field data of 2008 and 2009 with 433 observations for biomass and 438 for LAI and cover fraction.

The observations and corresponding pixel signatures of field plots are divided in a calibration and validation part as described in paragraph 3.4.3 (calibration of regression data). The regression analysis is applied on calibration data and the accuracy of the model predictions is assessed by the validation part.

Different lambda (λ) values are used to create model predictions. Every λ has a solution for the Generalized Cross Validation (GCV) and degrees of freedom, and controls the size of the coefficients. The optimal model prediction is reached by the lowest GCV, because the GCV is equal to the total variance of residuals. The lowest GCV has a certain effective degrees of freedom. The coefficients corresponding to these effective degrees of freedom are used for the predictive model. Plots of degrees of freedom against the GCV for vegetation variables are shown in figure 23.

	Optimal prediction values		
Variables	**GCV**	**Effective degrees of freedom**	**Lambda**
LAI 2003	0.5638	7.12	6.01540e+00
LAI 2008	0.6911	20.85	4.62969e-01
Biomass 2003	0.3779	12.59	1.06354e+00
Biomass 2008	0.3417	45.13	1.55108e-02
Cover fraction 2003	0.1131	32.67	2.04662e-02
Cover fraction 2008	0.1237	16.46	1.06354e+00

Table 10: Optimal prediction values for ridge regression

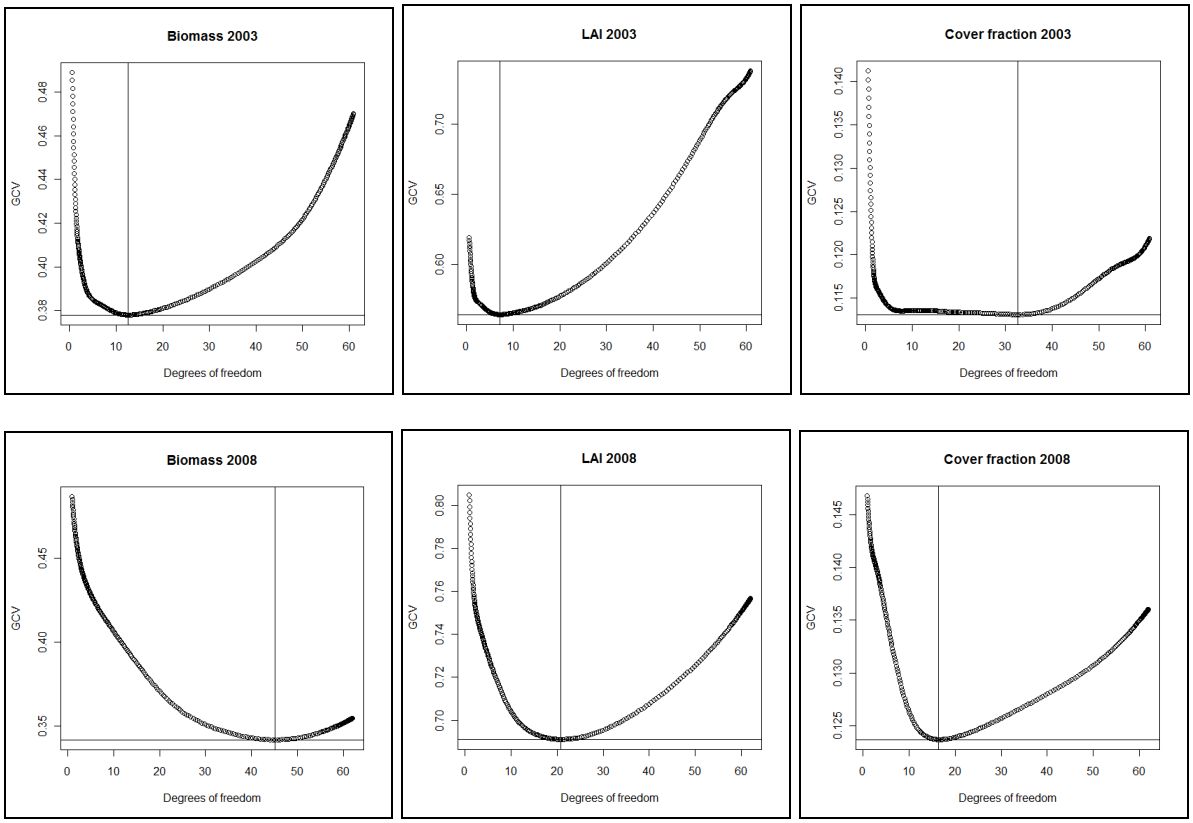

Figure 23: Degrees of freedom against Generalized Cross Validation after the application of ridge regression for vegetation variables of 2003 and 2008.

The optimal model prediction (point with the lowest GCV) for biomass and Leaf Area Index (LAI) is clearly identifiable in figure 23. For cover fraction of 2003 this is not the case, because the optimal model prediction is not situated at a particular point (like in other graphs), but is found over a range of 8 till 40 degrees of freedom. The degrees of freedom for a certain λ value represent the effective number of degrees of freedom used and this indicates the effective number of independent variables used to describe the value of the dependent variable. Table 10 shows that the effective degrees of freedom for biomass 2008 are the highest and for LAI 2003 the lowest.

The optimal value for λ is used to generate a predictive model. This model consists of an equation with an intercept and coefficients as earlier mentioned in paragraph 3.4.2 (processing of data for ridge regression). For biomass 2003 the following predictive model is generated (equation 7).

biomass 2003=(2.95068925068672) + b2*float(-0.00596342340313544) + b4*float(0.002952550711811)
+b6*float(0.00140995495396534)+b8*float(-0.00090553352811284) + b10*float(-0.00188517993604260)
+ b12*float(-0.00170103976400236) + b14*float(-0.00149721537573547) +b16*float(-0.000294620258523946)
+b18*float(0.00222341242075259)+ b20*float(0.000280533007056993) + b22*float(5.37906163283353e-05)
+ b24*float(1.19428672257231e-05)+b26*float(-3.02714830727246e-05)+b28*float(-7.80165988104192e-05)
+ b30*float(-5.50179429638469e-05)+b32*float(-6.38622182004785e-05)+b34*float(-5.29324989220346e-05)
+ b36*float(8.56505356731027e-06)+b38*float(4.63307476091344e-05)+b40*float(-7.02034552274082e-05)
+ b42*float(-0.000371074056195999) + b44*float(-0.000141476004558516) + b46*float(-0.000125619186707591)
+b48*float(-1.98346006160676e-05) + b50*float(0.000179922334924728) +b52*float(0.000302619467446933)
+b54*float(0.000252976566295748) +b56*float(0.000172525735434636)+b58*float(-0.000115697740219612)
+b60*float(-0.000179179773532144)+b62*float(-0.000655120930908515)+ b64*float(-0.000231038982641447)
+b66*float(-8.81067126109879e-05)+b68*float(5.49261792192903e-05)+b70*float(-6.05647887215058e-06)
+b72*float(-0.000289093752380596)+b74*float(-0.000404217757800240)+b76*float(-0.000478985452734562)
+b78*float(-0.000272147908321149)+b80*float(0.000327599543641784)+b82*float(0.000618994050129143)
+b84*float(0.000543997434108433)+b86*float(0.000542301320710534)+b88*float(0.000726567118531107)
+b90*float(0.000438839880356478)+b92*float(0.00046204166614966)+b94*float(0.000477553310308092)
+b96*float(0.000651660828115314)+b98*float(-0.0001477179600732)+b100*float(-0.000330514940161092)
+b102*float(-0.00108377457944429)+b104*float(-0.00107829203298774)+b106*float(-0.00108471042014730)
+b108*float(-0.000772569978126291)+b110*float(-0.000501000530749255)+b112*float(-0.000492567406769459)
+b114*float(1.87923993209947e-05)+b116*float(0.000219457040371807)+b118*float(0.00108491433259059)
+b120*float(0.00109024294261197)+b122*float(0.000746384364178907)+b124*float(0.000459365815376402)

Equation 7: Predictive model biomass 2003 with field data of 2005

The other predictive models for biomass, LAI and cover fraction of 2003 and 2008 can be found in appendix 4. Equation 7 is applied on the validation part of the data set and on the hyperspectral aerial photograph of 2003. The b's in the equation refer to the band number in the image and the values behind the numbers represent coefficients.

The accuracy of the predictive model is assessed by the validation part of the data set. The relation between field observations and model predictions is obtained by information about R^2 and the Root Mean Squared Error (RMSE). R^2 is the square of sample correlation coefficients between field observations and model predictions and is the proportion of variability in a data set. The RMSE (equation 8) is a measure of precision and represents the size of the error in a model between two variables. It gives a relative high weight to large errors since errors are squared before they are averaged. The error values can range from 0 till infinity, with 0 corresponding to the ideal situation.

$$Ei=\sqrt{(1/n \sum (Xi - Yi)^2)} \qquad \text{eq.8}$$

Ei = RMSE
n= amount of observations
Xi=observed values
Yi=predicted values

Equation 8: Formula of Root Mean Squared Error

The predictive model mentioned in equation 7 is applied on the validation data set of biomass 2003 and results in a graph of observed and predicted values (figure 25). The optimal prediction in the scatter plot is reached when x=y (field observations are equal to model predictions). In figure 24 a linear regression line is fitted trough the biomass points to visualize the relation between observed and predicted values. Low observed biomass values (0.3 – 0.6) are difficult to predict. They are distributed over a predicted log-biomass range of 0.2 till 1.8. The observed biomass values above 0.6 are closer located around the linear

regression line. Probably is this the result that most field observations for the biomass 2003 image are located in a range between 1.6 and 2.6.

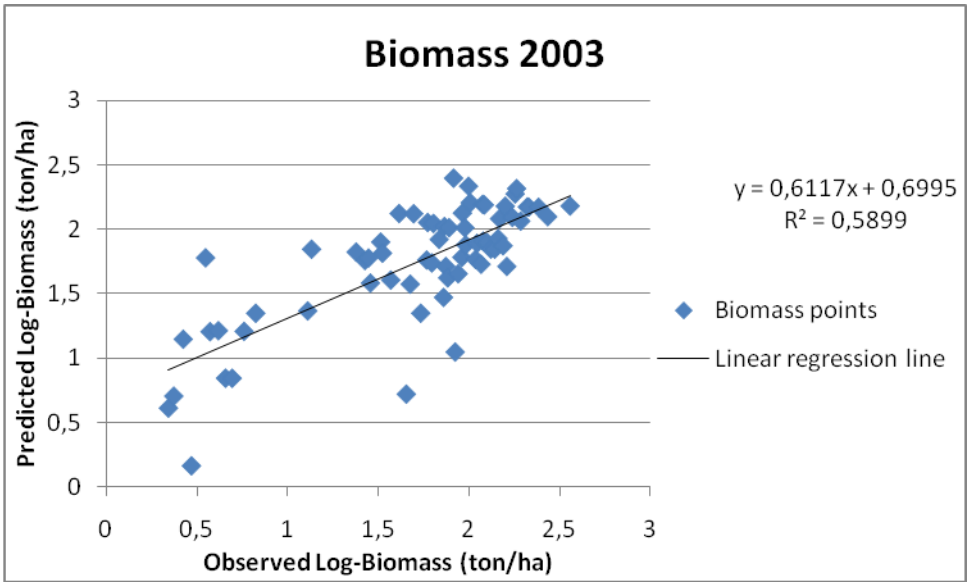

Figure 24: Relation between observed (field data 2005) and predicted values for biomass in 2003

The accuracy of predictive models with the validation parts of the data sets are described in table 11. The variability in the data set is small for biomass (higher prediction accuracy) and high for cover fraction (smaller prediction accuracy) as can be seen by the R^2 values. The RMSE of vegetation variables cannot be compared with each other, because the units of the variables under consideration are different. As earlier mentioned the values of RMSE can range from 0 to infinity and in the table below the values are closely located to the ideal situation where the RMSE is zero. Later in this study R^2 and RMSE information is used to assess the accuracy of image segmentation methods.

Vegetation variable	Equation	R^2	RMSE	n
LAI 2003	y=0.3463x+2.1999	0.40	0.51	66
LAI 2008	y=0.4488x+1.671	0.44	0.66	136
Biomass 2003	y=0.6117x+0.6995	0.58	0.37	66
Biomass 2008	y=0.6141x+0.8184	0.55	0.36	138
Cover fraction 2003	y=0.5024x+0.3294	0.35	0.14	66
Cover fraction 2008	y=0.3355x+0.4553	0.27	0.13	133

Table 11: Accuracy of vegetation variable information after regression analyses. It should be noted that 2005 field data is used to assess the prediction accuracy of the 2003 image.

The predictive model equations (described in appendix 4) of vegetation variables are applied on hyperspectral aerial photographs. The resultant vegetation variable maps (Biomass, LAI and cover fraction) for the corresponding years can be found in figures 25, 26 and 27.

Predictive maps Biomass

Figure 25

Biomass 2003

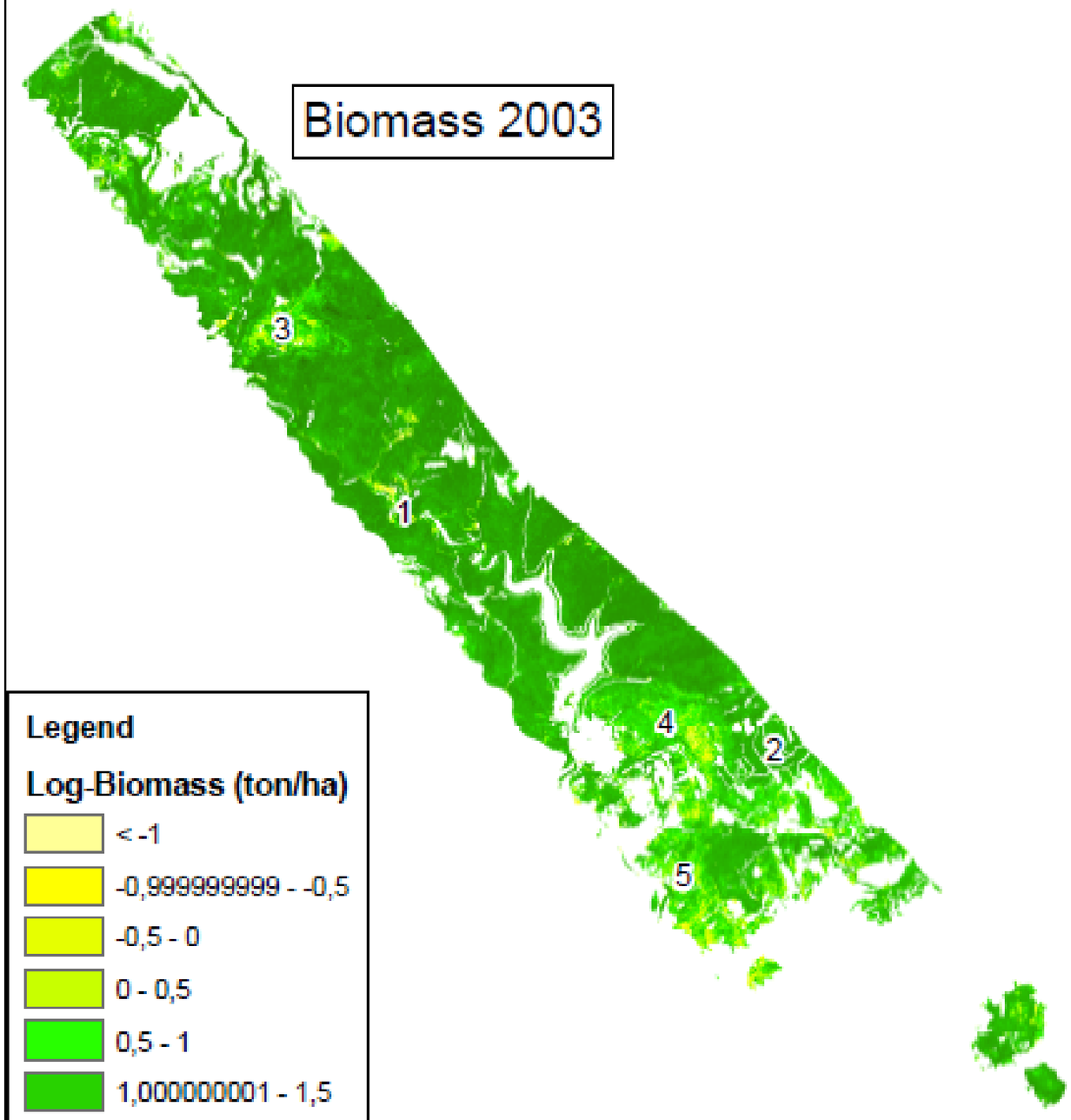

Biomass 2008

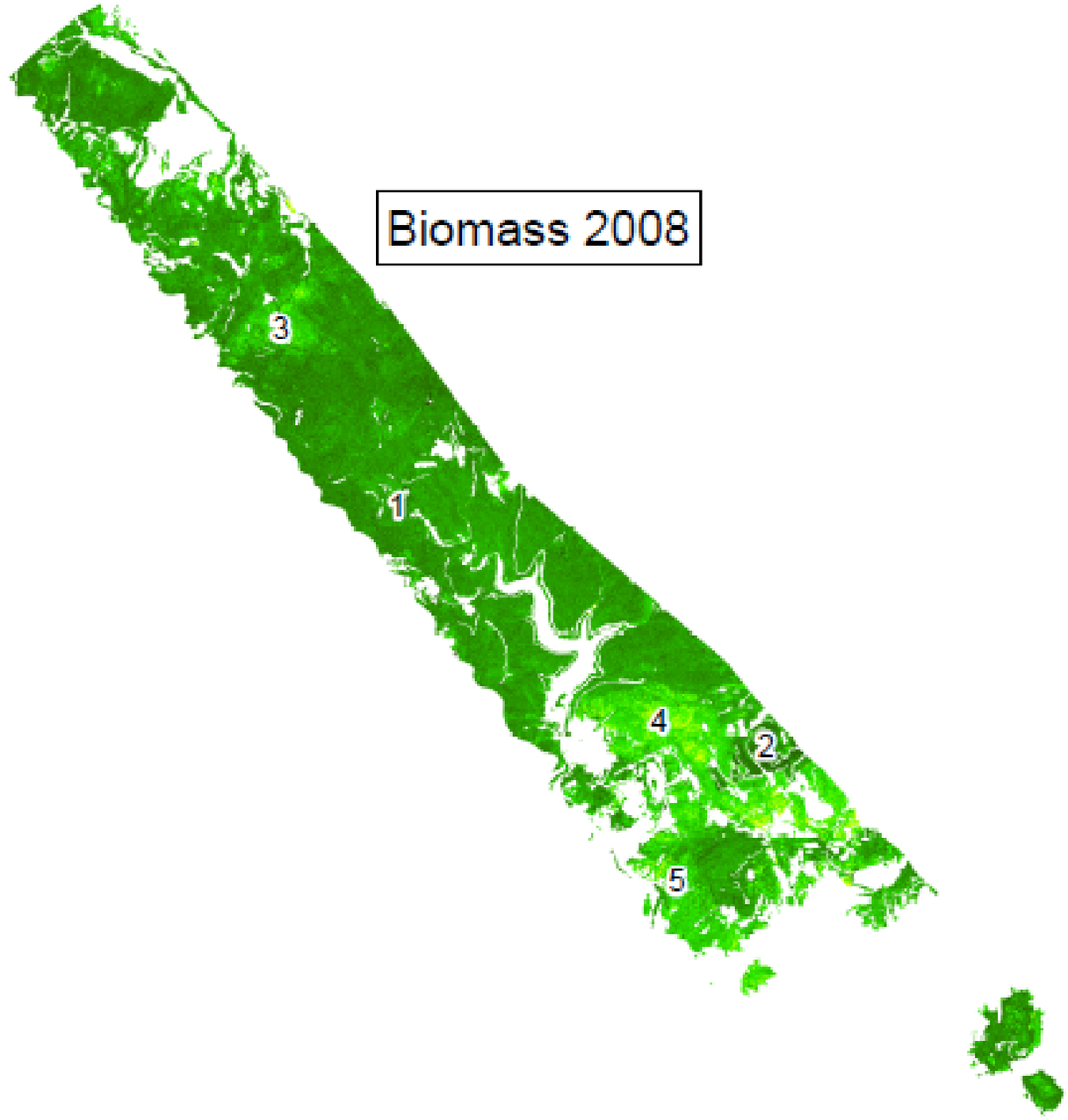

Legend

Log-Biomass (ton/ha)

- < -1
- -0,999999999 - -0,5
- -0,5 - 0
- 0 - 0,5
- 0,5 - 1
- 1,000000001 - 1,5
- 1,500000001 - 2
- 2,000000001 - 2,5
- 2,500000001 - 3
- > 3

Explanation

The predictive maps of biomass are expressed in log-biomass in ton/ha. In general there is an increase in biomass values from 2003 to 2008. Especially in reforestation areas marked with the numbers 1 and 2 and in les landes vegetation areas marked with the numbers 3, 4 and 5.

N

1:60.000

Created by: Annekarlijn de Rijcke
Project: Temporal patterns in vegetation In the Mediterranean area
Date: 2-2-2011

0 750 1.500 3.000 4.500 6.000 Meters

Predictive maps Leaf Area Index

Figure 26

LAI 2003

LAI 2008

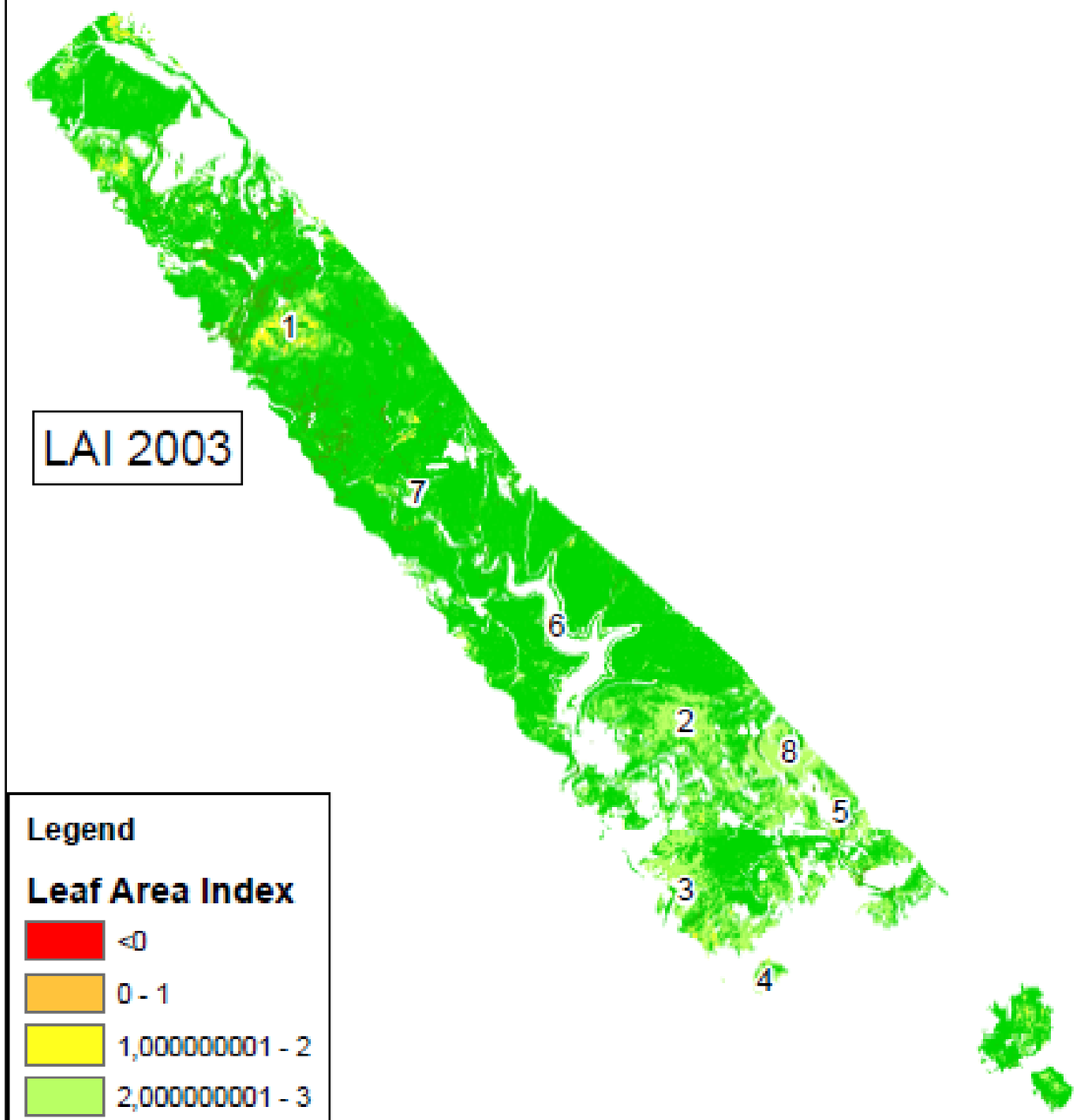

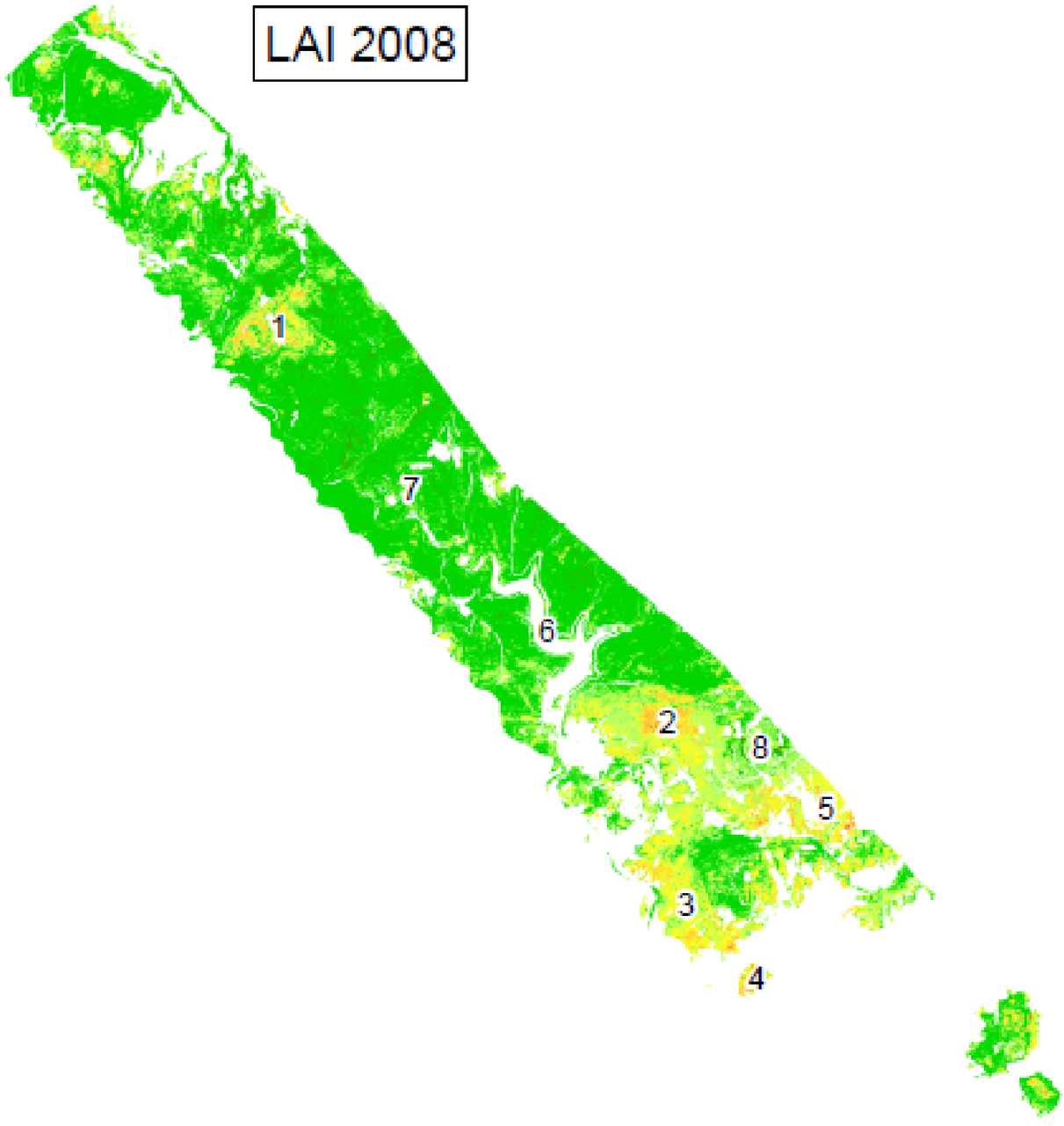

Legend

Leaf Area Index

- <0
- 0 - 1
- 1,000000001 - 2
- 2,000000001 - 3
- 3,000000001 - 4
- 4,000000001 - 5
- 5,000000001 - 6
- >6

Explanation

For LAI is not a general trend from 2003 to 2008 present. The decrease of LAI in les landes vegetation areas (numbers 1 till 5) is relative large compared to the rest of the area. Around the lake (number 6) and in the reforestation areas (number 7 and 8) there is a little increase.

N

Created by: Annekarijn de Rijcke
Project: Temporal patterns in vegetation in the Mediterranean area
Date: 2-2-2011

1:60.000

0 750 1.500 3.000 4.500 6.000 Meters

Figure 27

Predictive maps Cover fraction

Cover fraction 2003

Cover fraction 2008

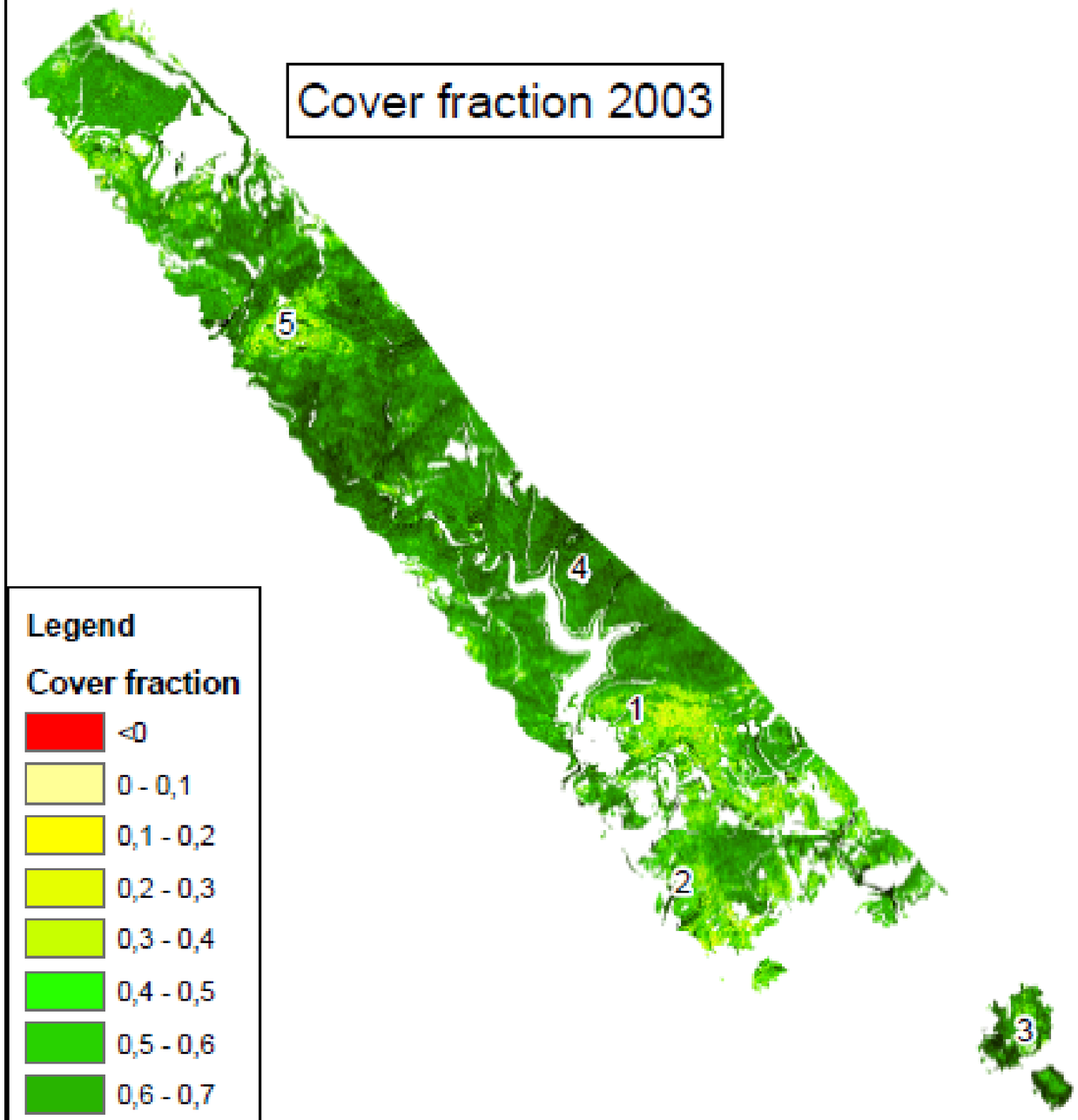

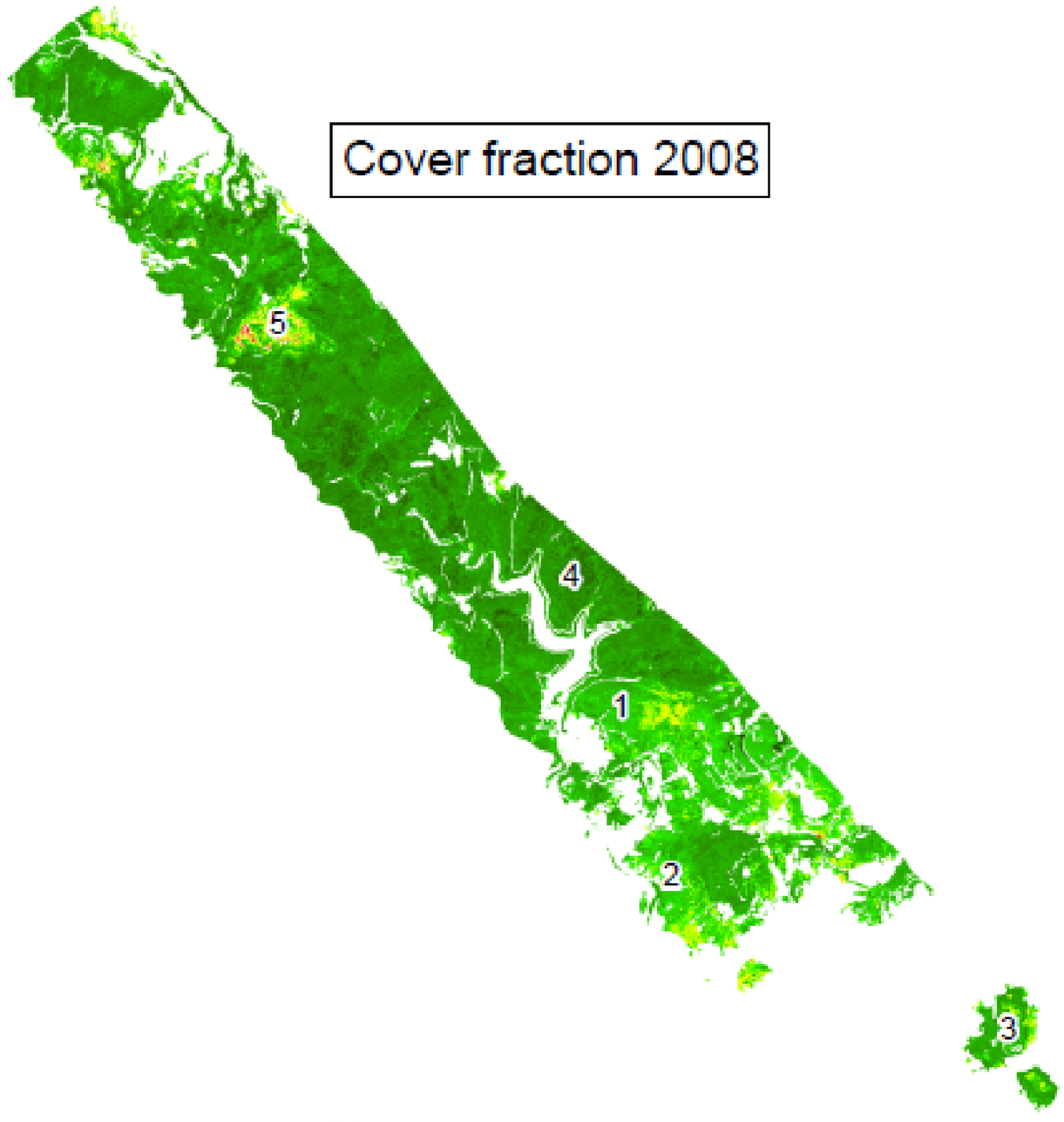

Legend

Cover fraction

- <0
- 0 - 0,1
- 0,1 - 0,2
- 0,2 - 0,3
- 0,3 - 0,4
- 0,4 - 0,5
- 0,5 - 0,6
- 0,6 - 0,7
- 0,7 - 0,8
- 0,8 - 0,9
- 0,9 - 1
- >1

Explanation

Values for cover fraction are slightly increasing from 2003 to 2008 (les landes vegetation areas, numbers 1 and 2) or decreasing (for forested areas, numbers 3 and 4). A striking characteristic are the cover fraction values below zero for 2008 (number 5).

N

Created by: Annekarlijn de Rijcke
Project: Temporal patterns in vegetation in the Mediterranean area
Date: 2-2-2011

1:60.000

0 750 1.500 3.000 4.500 6.000 Meters

Later in this study, temporal patterns in vegetation are discussed with object based change detection, but some general characteristics of figure 25, 26 and 27 are described below. It should be mentioned that predictive maps are only generated for areas consisting of natural vegetation. The classification of areas consisting of natural vegetation is earlier explained in paragraph 3.3 (Natural vegetation areas) and an overview of these areas can be found in figure 9.

The predictive maps of biomass (figure 25) are expressed in log-biomass in ton/ha. In general there is an increase in biomass values from 2003 to 2008. Especially in reforestation areas marked with the numbers 1 and 2 (in figure 25) and in les landes vegetation areas marked with 3, 4 and 5.

For LAI (figure 26) there is not a general trend from 2003 to 2008 present. The decrease of LAI in les landes vegetation areas (marked with numbers 1 till 5) is relative large compared to the rest of the area. Around the lake (marked with number 6) and in the reforestation areas (number 7 and 8) there is a little increase.

Values for cover fraction (figure 27) are slightly increasing (les landes vegetation areas, marked with 1 and 2) or decreasing (for forested areas, marked with 3 and 4). A striking characteristic are the cover fraction values below zero for 2008 (marked with 5).

4.3 Image segmentation

For 2003 and 2008 predictive vegetation variables maps are segmentated on basis of different methods and scales. These different methods and scales are used to determine the best method for change detection of vegetation variables.

Accuracy assessment of image segmentation is performed by using the validation part of field observations. The object values are joined to the attribute values of field observations as explained in paragraph: 3.5.3 Validation of image segmentation. The relation between the measured values of points in the field and the corresponding values of objects are obtained by information about R^2 and the Root Mean Squared Error (RMSE). The best image segmentation method and scale for biomass, LAI and cover fraction is the one having the smallest uncertainty (RMSE) and the largest R^2.

The methods applied on the predictive vegetation variable maps are earlier explained in paragraph: 3.4.3 Image segmentation methods, and are in this chapter mentioned as m1 for method 1 (figure 14), m2 for method 2 (figure 15), and m3 for method 3 (figure 16). The scale determines the maximum allowed heterogeneity for the resulting image objects and the scales used vary from 1 till 10. Scales above 10 are not used, because dry runs show a fast decreasing accuracy by increasing scale levels.

The image segmentation accuracy for each vegetation variable is summarized in table 12, 13 and 14, with information about the RMSE, R^2 and the number of objects generated. The best object scale for each segmentation method is marked with a grey colour. The optimal method and scale for RMSE and R^2 are underlined, bold and grey marked. This optimal method is used for the application of change detection. Besides the information in tables, R^2 is also plotted in graphs (figure 28, 29 and 30).

Scale	RMSE m1	RMSE m2	RMSE m3	R^2 m1	R^2 m2	R^2 m3	objects m1	objects m2	objects m3
1	0.3530	0.4122	0.3576	0.6218	0.5144	0.6115	85240	272380	78511
2	0.3422	0.3492	0.3614	0.6507	0.6273	0.6009	18363	75767	20419
3	0.3525	0.3384	0.3597	0.6219	0.6488	0.6084	8552	36298	9622
4	0.3584	**0.3380**	0.3650	0.6106	**0.6602**	0.5996	5165	**22209**	5880
5	0.3660	0.3565	0.3690	0.5906	0.6148	0.5900	3587	15178	4000
6	0.3724	0.3528	0.3707	0.5763	0.6244	0.5859	2685	11299	2945
7	0.3794	0.3622	0.3798	0.5607	0.6057	0.5644	2115	8735	2282
8	0.3885	0.3610	0.3837	0.5366	0.6076	0.5537	1736	7052	1856
9	0.3920	0.3646	0.3873	0.5272	0.5994	0.5449	1478	5874	1577
10	0.3913	0.3645	0.3832	0.5304	0.5996	0.5534	1228	5084	1350

Table 12: Image segmentation accuracy of biomass

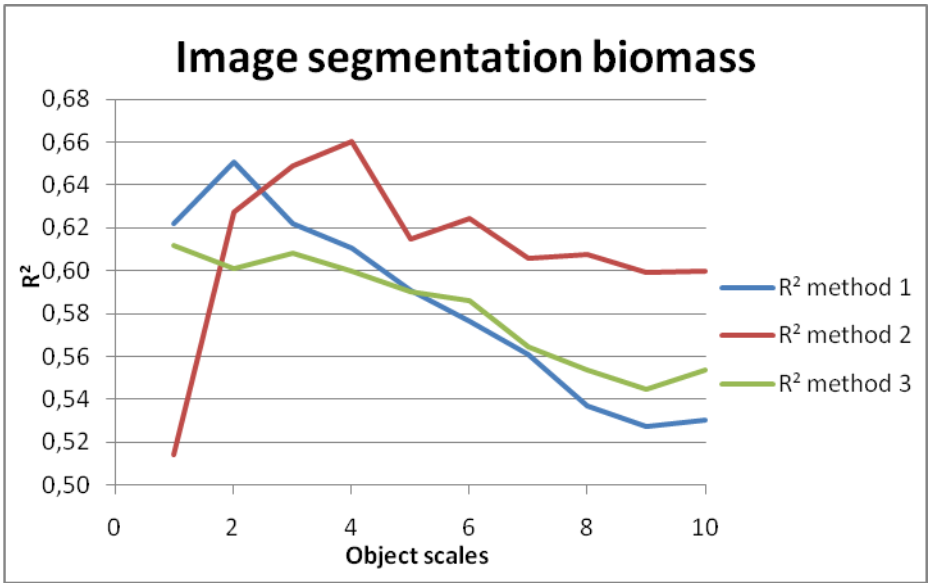

Figure 28: R² for image segmentation of biomass

Table 12 shows the image segmentation accuracy for biomass. Values for RMSE vary between the different object scales and methods used. The range of these values is located between 0.3380 and 0.4122 and these values are used to express the uncertainty that is present in the data. The best method is the one with the lowest uncertainty / RMSE.

The values for R^2 strongly depend on methods and scales used. This can be explained by the fact that the accuracy of image segmentation methods is checked by a set of validation points (earlier explained in paragraph: 3.4.3 Calibration of regression data). The value of an object underlying a validation point can have great differences in the way that image segmentation takes place, because by image segmentation play the heterogeneity in the data and thus in the predictive maps of vegetation variables a large role.

These great differences result in a large variability in R^2 values in figure 28 (jumpy shapes of the curves in the graph). In the graphs of LAI (figure 29) and cover fraction (figure 30) is this jumpy shape more evident than for biomass. Probably is this the result of the fact that the R^2 value obtained by ridge regression for LAI and cover fraction do not come close to the R^2 value of biomass, and thus have a larger uncertainty.

The best prediction for each segmentation method is located below object scale five. Probably is this the result of the biomass pattern in the predictive map (figure 25) which varies over short distances. As consequence a higher segmentation accuracy is reached by a lower object scale. This large variation at short distances can also be declared by the high number of objects (22209) by the optimal segmentation method 2 and object scale 4.

Scale	RMSE m1	RMSE m2	RMSE m3	R^2 m1	R^2 m2	R^2 m3	objects m1	objects m2	objects m3
1	0.6495	0.6497	0.6191	0.3422	0.3442	0.3979	84015	245128	78284
2	0.6258	0.6327	0.6356	0.3848	0.3725	0.3658	20308	84088	22455
3	0.6407	0.6374	0.6370	0.3563	0.3650	0.3632	9419	42213	10297
4	0.6312	0.6460	0.6331	0.3741	0.3490	0.3704	5631	25799	5960
5	0.6394	0.6269	0.6410	0.3572	0.3828	0.3663	3811	17542	3957
6	0.6552	0.6351	0.6375	0.3252	0.3659	0.3626	2845	13034	2886
7	0.6536	0.6129	0.6317	0.3289	0.4138	0.3754	2166	10033	2204
8	0.6514	**0.6106**	0.6394	0.3332	**0.4206**	0.3602	1793	**7918**	1760
9	0.6449	0.6173	0.6376	0.3475	0.4067	0.3644	1500	6579	1467
10	0.6376	0.6469	0.6513	0.3626	0.3430	0.3348	1279	5778	1285

Table 13: Image segmentation accuracy of LAI

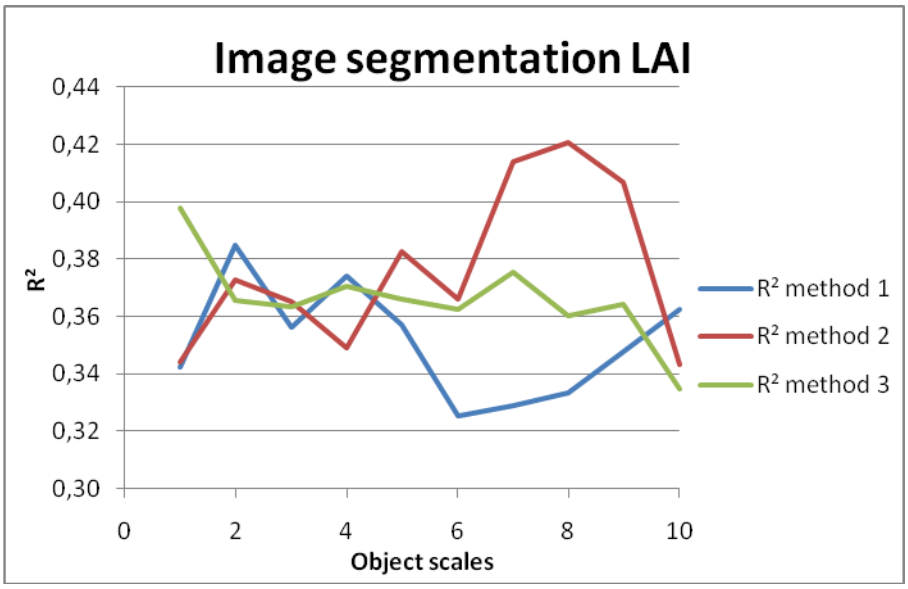

Figure 29: R^2 for image segmentation of LAI

The RMSE value for LAI strongly depends on the segmentation method and object scale used. Table 13 shows that the best RMSE for method 1 is reached by scale 2, for method 2 by scale 8 and for method 3 by scale 1, so there is a large optimal object scale difference between method 2 in comparison with method 1 and 3. It is probable that this is the result of the way how image segmentation took place for the different methods. The higher optimal object scale for method 2 is reasonable, because the final objects are the result of an aggregation of objects that are separately segmentated for the years 2003 and 2008. This is also shown in the number of objects generated for each method and scale, because in all cases the number of objects for method 2 is much higher than for method 1 or 3.

Figure 29 shows that the R^2 values for LAI lay close together for the first five object scales. For a certain object scale the methods alternate each other concerning the optimal segmentation method. A striking characteristic is the high accuracy peak for method 2 in comparison with the location of the accuracy curves of method 1 and 3, which stays among

the several object scales more or less the same. The optimal prediction for change detection with LAI is reached with method 2 and object scale 8. The total number of objects is 7918.

Scale	RMSE m1	RMSE m2	RMSE m3	R^2 m1	R^2 m2	R^2 m3	objects m1	objects m2	objects m3
1	0.1277	0.1260	0.1237	0.3122	0.3438	0.3499	44164	142768	49846
2	0.1184	0.1188	0.1185	0.3933	0.3979	0.3910	13056	47004	13551
3	**0.1166**	0.1211	0.1204	**0.4113**	0.3702	0.3711	**6585**	24495	6696
4	0.1186	0.1199	0.1221	0.3906	0.3785	0.3536	4205	15549	4297
5	0.1232	0.1181	0.1195	0.3420	0.3960	0.3820	3002	10826	2943
6	0.1252	0.1225	0.1214	0.3216	0.3493	0.3614	2302	8062	2203
7	0.1228	0.1220	0.1211	0.3482	0.3547	0.3655	1802	6475	1797
8	0.1220	0.1222	0.1215	0.3582	0.3522	0.3609	1482	5343	1524
9	0.1230	0.1218	0.1210	0.3464	0.3568	0.3671	1276	44570	1283
10	0.1270	0.1204	0.1242	0.3005	0.3734	0.3314	1107	3952	1125

Table 14: Image segmentation accuracy of cover fraction

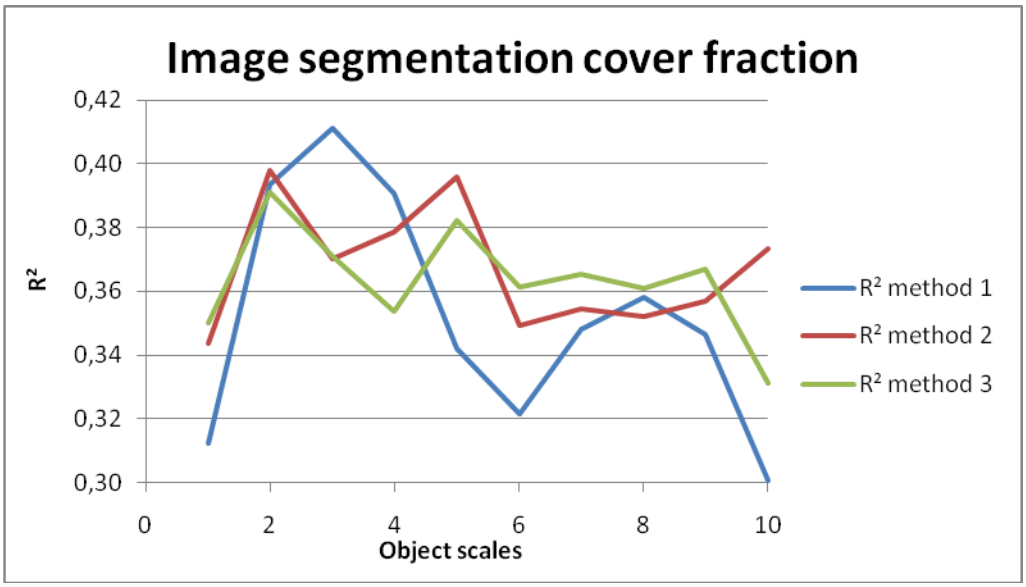

Figure 30: R^2 for image segmentation of cover fraction

The RMSE variation for cover fraction among the methods and object scales is very small. The range of RMSE values is located between 0.1166 and 0.1270 as shown in table 14. This is not the case for R^2, where the optimal prediction method and scale can better be identified, because the larger differences among the methods and the object scales used. The small variation in RMSE is probable the result of the cover fraction unit located between 0 (no coverage) and 1 (completely covered). The RMSE values for LAI and biomass show a larger range as result of the range of the unit under consideration.

R^2 in figure 30 shows the relation between the values of validation points and the corresponding object values. The shape of the curves in the graph is jumpy, as earlier explained is this probably the result of how image segmentation takes place and the

heterogeneity present in the predictive vegetation variable maps. In the case of cover fraction method 1 with object scale 3 shows the best result with an R^2 of 0.41 and a total number of 6585 objects.

Each variable (biomass, LAI and cover fraction) has its own characteristic pattern which results in different optimal segmentation methods and scales used for change detection as can be seen in table 15. As example the pattern of increasing or decreasing biomass values is not similar to increasing or decreasing patterns for LAI or cover fraction, so the shape and total number of objects depend on the vegetation variable under consideration.

If the R^2 values of table 15 are compared with the R^2 values of table 11 (accuracy of vegetation variables after regression analyses) can be concluded that there is an increase for biomass (R^2 2003: 0.58 and 2008: 0.55) and cover fraction (R^2 2003: 0.35 and 2008: 0.27). The R^2 for LAI (R^2 2003: 0.40 and 2008: 0.44) are in both cases relative the same.

This is probably the result of that objects represent homogeneous segments in data. The object wherein a validation point is located include pixels that have similar spatial and spectral properties. This means that the value of an object probably more corresponds to the value of a validation point than the 3x3 window used in paragraph 3.4.2 (Processing of data for ridge regression) to obtain the accuracy of regression analyses.

Vegetation variable	Optimal method	Optimal scale	R^2	Number of objects
Leaf Area Index	2	8	0,4206	7918
Biomass	2	4	0,6602	22209
Cover fraction	1	3	0,4113	6585

Table 15: Optimal image segmentation methods and object scales for vegetation variables

4.4 Change patterns

Temporal patterns in vegetation are investigated with change detection. Images used to apply change detection on are obtained by the application of image segmentation on the predictive vegetation maps. The optimal image segmentation for the vegetation variables under consideration are used for change detection.

Change areas are determined with image differencing where the image of 2003 is subtracted from 2008. The resulting image shows the differences. Changes of interest are increasing or decreasing patterns in vegetation. These are observed with the variables biomass, Leaf Area Index and cover fraction.

An area is detected as change area if the change is higher than a certain threshold. This threshold value is the absolute average residual, as earlier explained in paragraph: 3.6 Change detection. Changes are mapped as follow: increase, decrease or no-change. The increase and decrease category are further subdivided in a low or high change. Areas are regarded as high change areas if changes are bigger than two times the threshold.

The thresholds used for change detection are summarized in table 16. The threshold value depends on the residuals present in the validation data set of image segmentation and the unit of the vegetation variable under consideration. The resulting change maps for vegetation variables are shown in figure 31, 32 and 33.

	Vegetation variable thresholds		
Change categories	**Biomass log(ton/ha)**	**LAI (-)**	**Cover fraction (-)**
High increase	> 0.372018	> 0.522772	> 0.10498
Low increase	0.186009 - 0.372018	0.261386 - 0.522772	0.05249 - 0.10498
no-change	-0.186009 - 0.186009	-0.261386 - 0.261386	-0.05249 - 0.05249
Low decrease	-0.186009 - 0.372018	-0.261386 - 0.522772	-0.05249 - 0.10498
High decrease	< -0.372018	< -0.522772	< -0.10498

Table 16: Vegetation variable thresholds for the temporal patterns 2003-2008

Change map Biomass

Figure 31

Biomass change

- High decrease
- Low decrease
- No-change
- Low increase
- High increase

Explanation

A general increasing trend (55%) is present for biomass. Change areas with a high increase are located just north from Neffiés (number 1), in the reforestation area consisting of pine trees (number 2), the small forested areas between the vineyards (number 3) and along the west side of the natural vegetation areas under consideration. The relative decreasing amount in biomass is low. A decrease in biomass is the result of dying vegetation (les landes vegetation areas, number 4) or deforestation (number 5) by human influence.

N

1:45.000

Created by: Annekarlijn de Rijcke
Project: Temporal patterns in vegetation in a Mediterranean area
Date: 2-2-2011

0 625 1.250 2.500 3.750 5.000 Meters

Change map Leaf Area Index

Figure 32

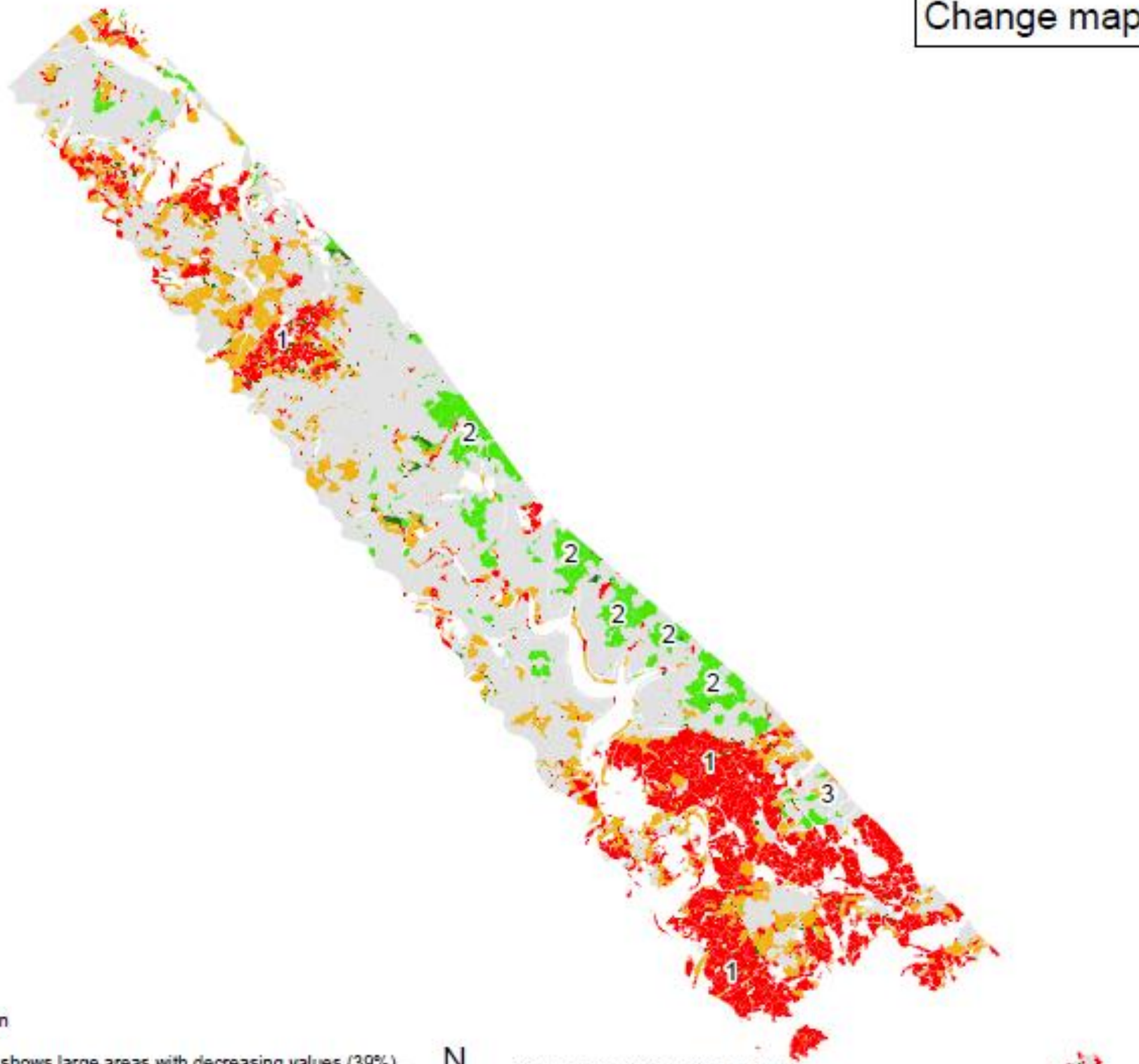

Leaf Area Index
change

- High decrease
- Low decrease
- No-change
- Low increase
- High increase

Explanation

The figure shows large areas with decreasing values (39%). These are mostly located in les landes vegetation areas (number 1). The relative increasing LAI amount is low (8%) and these are located along the east side of the natural vegetation area (number 2). A striking characteristic is that Leaf Area Index does not change for the reforestation area (number 3).

N

1:45.000

Created by: Annekarlijn de Rijcke
Project: Temporal patterns in vegetation in a Mediterranean area
Date: 2-2-2011

0 625 1.250 2.500 3.750 5.000 Meters

Change map Cover fraction

Figure 33

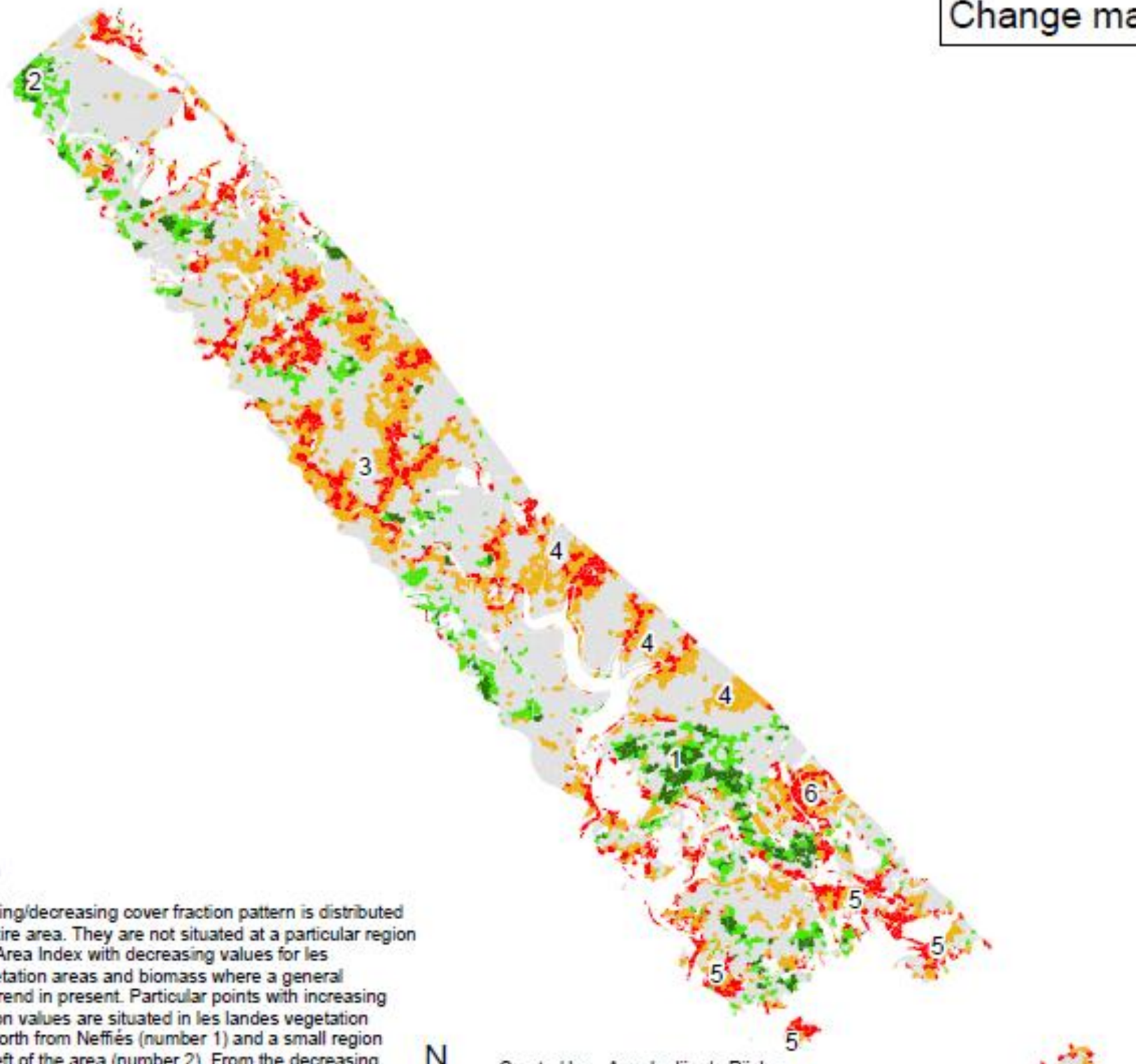

Cover fraction change

- High decrease
- Low decrease
- No-change
- Low increase
- High increase

Explanation

The increasing/decreasing cover fraction pattern is distributed over the entire area. They are not situated at a particular region as for Leaf Area Index with decreasing values for les landes vegetation areas and biomass where a general increasing trend in present. Particular points with increasing cover fraction values are situated in les landes vegetation areas just north from Neffiés (number 1) and a small region in the top left of the area (number 2). From the decreasing part (35%) most areas are low decreasing (20%) and are distributed north west (number 3) and north east (number 4) of the lake. Particular high decreasing cover fraction areas (15%) are situated in the small forested areas along and between the vineyards (number 5). A decreasing trend is present in the reforestation area (number 6).

N

1:45.000

Created by: Annekarlijn de Rijcke
Project: Temporal patterns in vegetation in a Mediterranean area
Date: 2-2-2011

0 625 1.250 2.500 3.750 5.000 Meters

The change patterns for biomass, Leaf Area Index and cover fraction have their own characteristics, in terms of change patterns, size of objects, etc, as is shown in figures 31, 32 and 33.

A general increasing trend is present for biomass (figure 31). These are distributed over the entire natural vegetation area (figure 9). The biomass pie chart in figure 34 shows that 55% of the area has an increase in biomass. The areas in figure 31 with a high increase (18%) are located just north from Neffiés (marked with number 1 in figure 31), in the reforestation area consisting of pine trees (number 2), the small forested areas between the vineyards (number 3) and along the west side of the natural vegetation areas under consideration.

The relative decreasing amount in biomass is low. This is probable, because biomass represents the accumulation of the yearly net growth. A decrease in biomass is the result of dying vegetation (les landes vegetation areas, number 4) or deforestation (number 5) by human influence.

Figure 32 with Leaf Area Index shows large areas with decreasing values (39%). These are mostly located in les landes vegetation areas (marked with number 1 in figure 32). These are areas consisting of small shrubs and herbaceous vegetation species. 16% of the decreasing areas show a high decrease (figure 34). It is probable that environmental factors during the last years negatively affect vegetation resulting in decreasing LAI values, because the Leaf Area Index value depends on the environmental situation of the previous two to four years.

The relative increasing LAI amount is low (8%) and these are located along the east side of the natural vegetation area (marked with number 2). A striking characteristic is that Leaf Area Index does not change for the reforestation area (number 3). An increase was expected as result of the growth of Pine trees, but this not the case, because the change does not exceed the threshold. A reason for this is that Pine trees do not have leaves, but consists of needles and that Leaf Area Index than mostly depends on the stem of the tree present in hemispherical photos. Probably there is an increase in LAI, but this change is not large enough to exceed the thresholds and is than not determined as a change, but as an area with no-change.

The cover fraction pattern (figure 33) is less detailed compared to biomass and Leaf Area Index. The amount of detail and size of objects depend on the segmentation method used. In the case of cover fraction the predictive maps are segmentated with method 1, which means that objects are generated for both years at the same time. For biomass and LAI method 2 is used, resulting in smaller objects depending on the heterogeneity in the predictive maps.

The increasing/decreasing cover fraction pattern is distributed over the entire area. They are not situated at a particular region as for Leaf Area Index with decreasing values for

les landes vegetation areas and biomass where a general increasing trend in present. Particular points with increasing cover fraction values are situated in les landes vegetation areas just north from Neffiés (marked with number 1 in figure 33) and a small region in the top left of the area (number 2). From the decreasing part (35%) most areas are low decreasing (20%) and are distributed north west (number 3) and north east (number 4) of the lake. Particular high decreasing cover fraction areas (15%) are situated in the small forested areas along and between the vineyards (number 5). A decreasing trend is present in the reforestation area (number 6). This is probably the result of that cover fraction decreases when Pine trees are growing. The needle density in Pine trees is getting lower for larger trees and the biomass values for this region show that these trees grow during the last years.

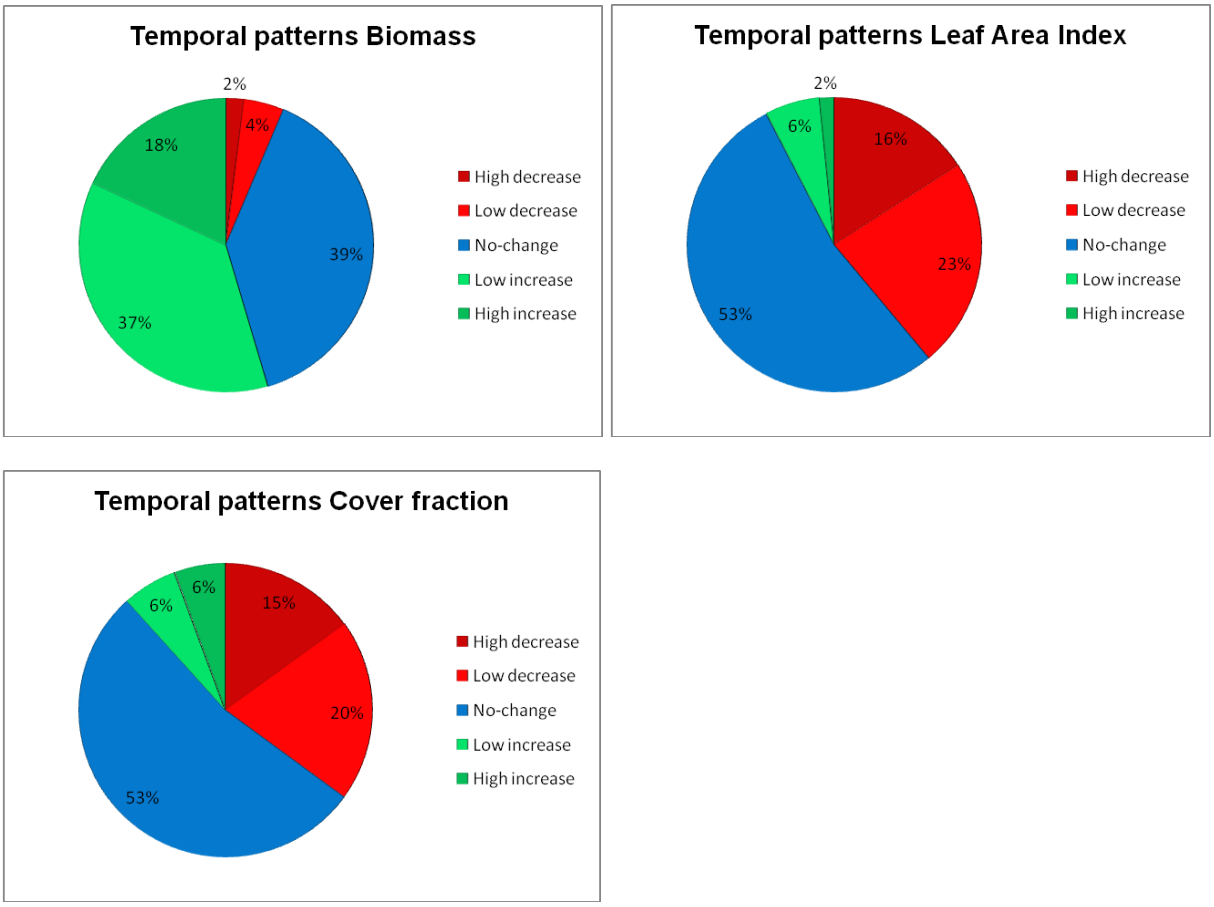

Figure 34: Temporal patterns for vegetation variables

Change patterns expressed in relative amounts are shown in figure 34. In more than half of the natural vegetation areas biomass is increased. This is probably the results of the yearly net growth of vegetation which results in increasing biomass values. The classification in no-change, low or high increase depends on environmental circumstances and the vegetation species under consideration. The decreasing biomass amount is low, because these are only the result of logging or vegetation species that do not survive in the ecosystem and die.

39% of the LAI areas show a decreasing trend. This amount is more or less equally distributed over the low and high decreasing part. Areas with decreasing LAI values are located in les landes vegetation areas. This is probably the result of difficult LAI determination at these locations, because of low vegetation species, as earlier explained in paragraph: 3.4.3 Calibration of regression data.

The increasing pattern is low (8%) and is situated at locations where probably logging has taken place in the past. This means that logging has taken place in or before 2003 and that development of vegetation results in an increase in LAI values where the change magnitude is larger than the threshold.

The relative cover fraction amounts are similar to LAI, but are situated at other locations as is shown in figure 32 and 33. The change of cover fraction depends on the growth and development of vegetation. An increase in biomass does not immediately mean an increase in cover fraction. Trees prevent the penetration of light through the crown of the tree and less vegetation undergrowth is possible. This is probably an explanation for large decreasing cover fraction amounts (35%). The amount of increase is low (12%) and these areas are distributed over the entire area as shown in figure 33.

The relation in change patterns between vegetation variables is shown in figure 35. All bar charts show that there is not a certain relation present between biomass – LAI, biomass – cover fraction and LAI – cover fraction in terms of change patterns. This means that patterns shown in figure 31, 32 and 33 are not similar to each other.

An increase in biomass (55% of the area) results in 55% no-change areas and 38.3% decrease areas for LAI. This is proportional to the distribution of no-change biomass areas (39%) over LAI with 56.5% no-change and 33.6% decrease. A striking characteristic of the relation between biomass and LAI is that biomass increase or no-change areas for LAI mostly results in no-change or decreasing values. 76.4% of the decreasing change category of biomass (6%) results also in decreasing values for LAI.

The relation of biomass with cover fraction is similar to LAI except for biomass decrease. Biomass increase, no-change or decrease, results in no-change or decreasing value areas for cover fraction.

A change pattern relation between LAI and cover fraction is also not clearly identifiable. The only striking characteristic between these variables is that if the LAI area consists of an increasing pattern that there is 71% chance, and for LAI no-change 59% change that this also results in a no-change area for cover fraction.

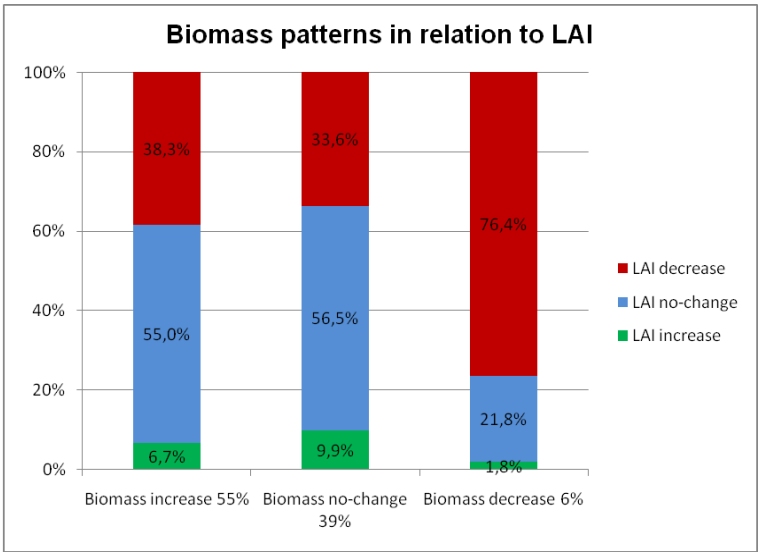

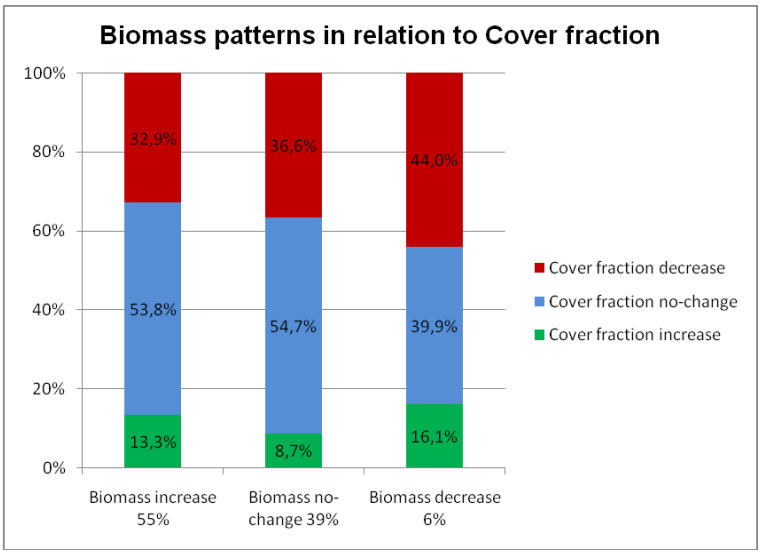

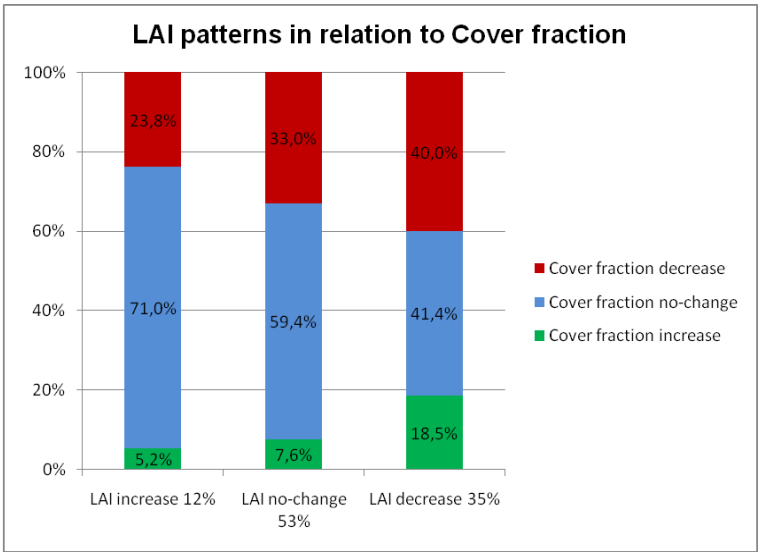

Figure 35: Change patterns between vegetation variables

4.5 Vegetation patterns in relation to environmental factors

Temporal patterns in vegetation are closely related to the ecosystem. The ecosystem consists of biotic and abiotic components that influence the growth and development of vegetation. The ecosystem is influenced by static and dynamic environmental factors as earlier explained in paragraph 3.6.

The change areas of biomass, Leaf Area Index and cover fraction are related to static environmental factors (geology, elevation, aspect and slope). Based on the environmental factor under consideration categories inside these factors are created. An overview of the distribution of change categories for the environmental factors is shown in figure 36 (aspect and geological unit) and 43 (elevation and slope). The resulting bar charts for each environmental factor are based on the amount of changed surface area (expressed in percentage) for each category. The relative surface area for each category inside an environmental factor is summarized in tables.

4.5.1 Geological unit

Figure 37, 38 and 39 show the relative temporal patterns in vegetation variables in relation to the geological unit. An overview of the distribution of geological units over the area is shown in figure 36. Table 17 shows that the area mainly consists of flysch (35%) and that other units are located between a relative cover amount of 2 till 16%.

Geological unit	Facies	Area
1	Dolomite	16%
2	Meltflows	12%
3	Flysch	35%
4	Schistes	8%
5	Sandy shale	2%
6	Argilites	6%
7	Sandstone	2%
8	Limestone	5%
9	White limestone	6%
10	Fluvial sediments	9%

Table 17: Geological units and covered area

Figure 36

Environmental factors: Aspect and geological unit

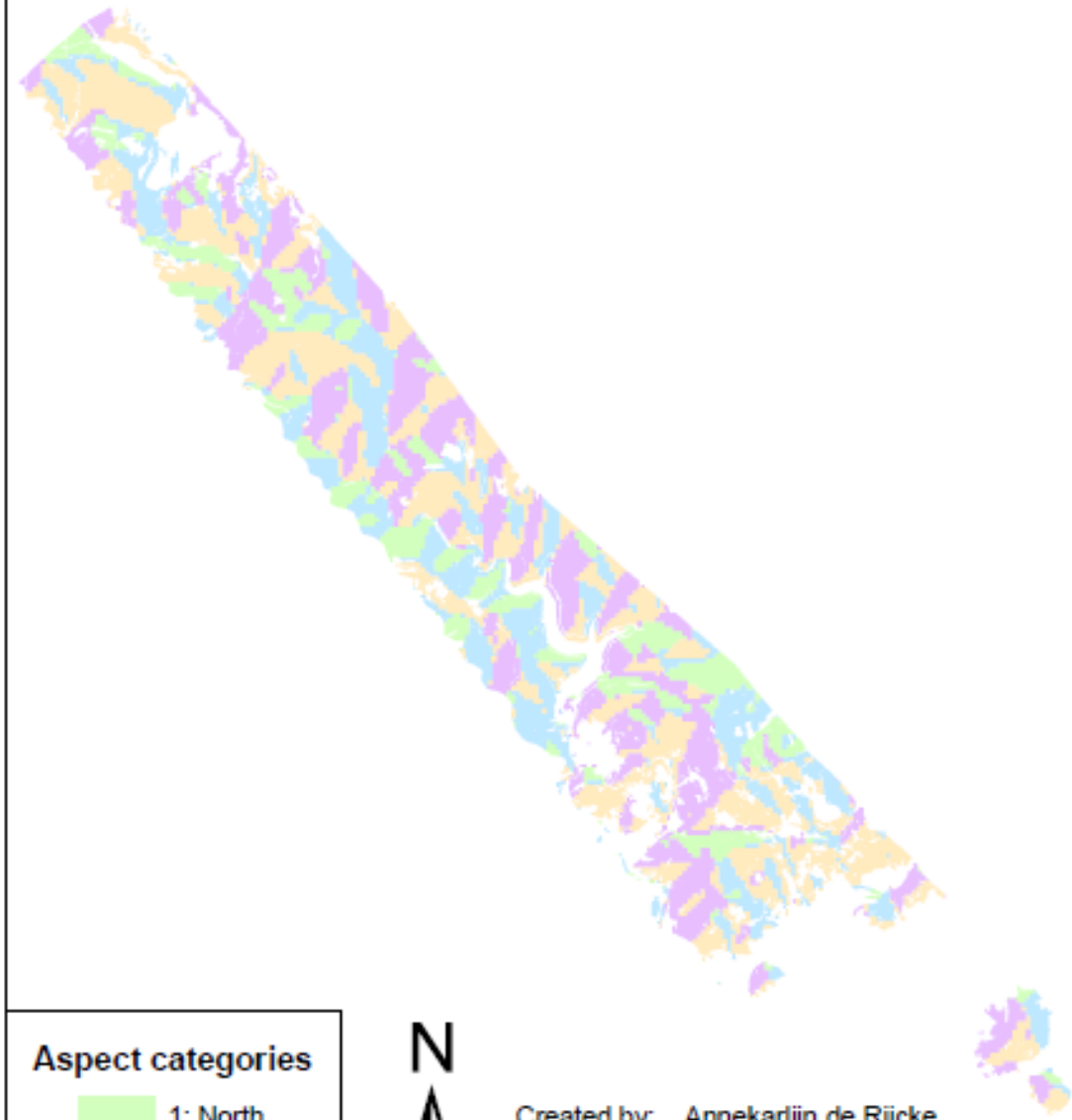

Aspect categories

- 1: North
- 2: East
- 3: South
- 4: West

N

Created by: Annekarlijn de Rijcke
Project: Temporal patterns in vegetation in the Mediterranean area
Date: 17-12-2010

1:85.000

0 1.000 2.000 4.000 Meters

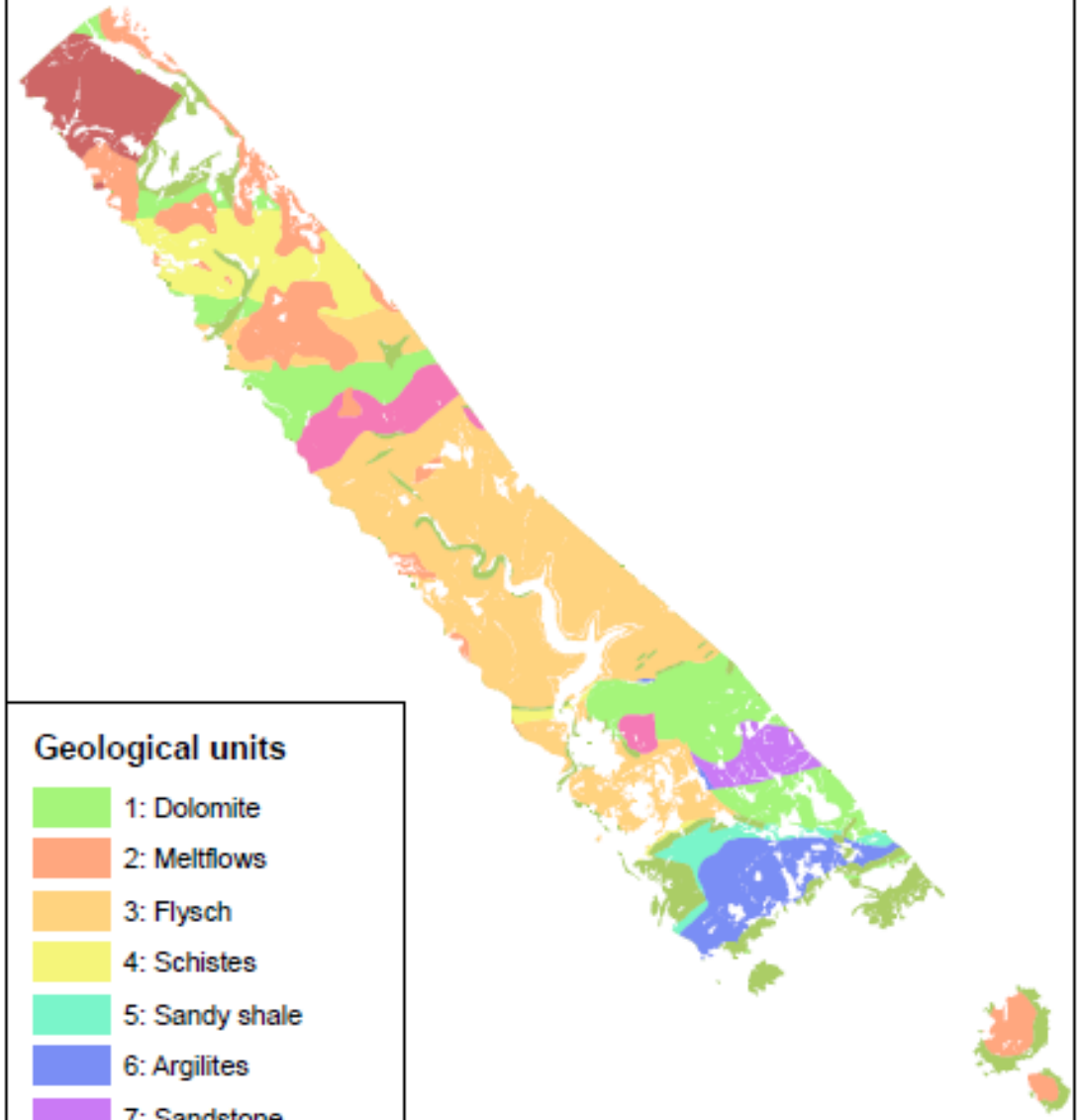

Geological units

- 1: Dolomite
- 2: Meltflows
- 3: Flysch
- 4: Schistes
- 5: Sandy shale
- 6: Argilites
- 7: Sandstone
- 8: Limestone
- 9: White limestone
- 10: Fluvial sediments

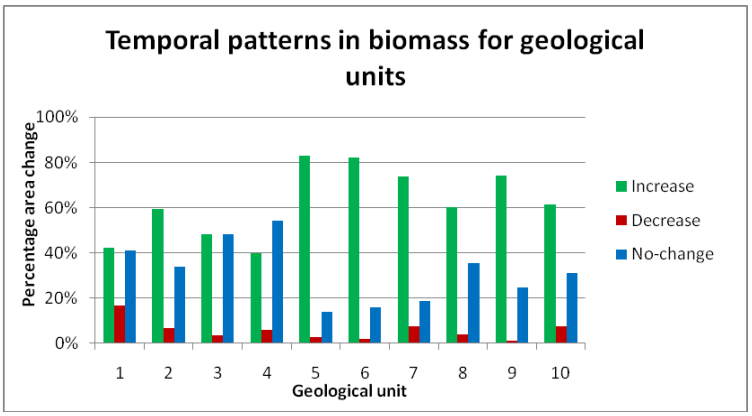

Figure 37: Temporal patterns in biomass in relation to geological unit

For biomass (figure 37) is not a fixed order present in the change categories of geology. The increasing bar is for most units the largest, except for unit 4 (schistes) where it is the bar of no-change areas. For unit 1 (dolomite) and 3 (Flysch) is the relative percentage of increase and no-change areas more or less equal. In all other units dominates the increasing part, especially for units 5 (sandy shale) and 6 (argilites) where more than 80% of the area has an increasing change pattern for biomass.

Decreasing biomass values are present in all units, but are minimal. Unit 1 (dolomite) shows the largest decrease with 17% of the total area of that unit. For the different geological units the relative amount of no-change areas vary a lot. It is minimal for unit 5 (sandy shale) and 6 (argilites) where the increasing bar dominates. Relative no-change amounts above 40% are reached for unit 1 (dolomite), 3 (flysch) and 4 (schistes).

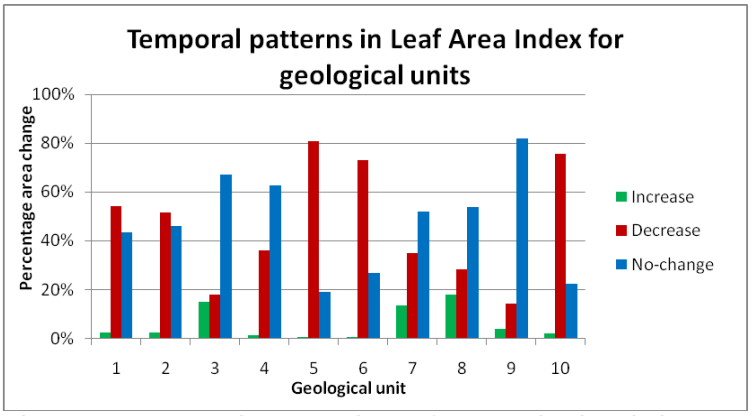

Figure 38: Temporal patterns in Leaf Area Index in relation to geological unit

For Leaf Area Index (figure 38) is not a general trend in the data present. In some units dominates the decreasing and for some units the no-change pattern. The relative change amount for unit 1 (dolomite) and 2 (meltflows) are similar to each other. The decrease is a little bit higher than the percentage no-change, but both are located around 50%. In unit 3 (flysch), 4 (schistes) and 9 (white limestone) the high percentage no-change (above 60%) dominates over the rest of the change categories. The largest decreasing bars (above 70%)

are reached for unit 5 (sandy shale), 6 (argilites) and 10 (fluvial sediments). Unit 7 (sandstone) and 8 (limestone) show that the percentage increase is half of the percentage no-change areas. Also increasing areas (approximately 17%) are present. Areas with an increasing change are mostly located in unit 3 (flysch), 7 (sandstone) and 8 (limestone).

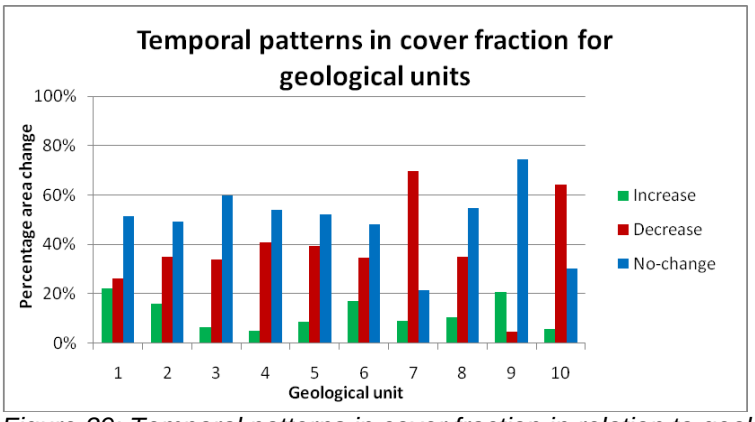

Figure 39: Temporal patterns in cover fraction in relation to geological unit

Cover fraction in relation to geology (figure 39) shows that most units, except unit 7 (sandstone) and 10 (fluvial sediments), the bar for no-change area is the largest, especially for unit 9 (white limestone) with 75% no-change areas. In unit 7 (sandstone) and 10 (fluvial sediments) the percentage decreasing areas dominate (above 64%). Increasing cover fraction areas are present in all units and are located above the 20% for unit 1 (dolomite) and 9 (white limestone).

Figure 37, 38 and 39 show that the high increase in biomass for unit 5 (sandy shale) and 6 (argilites) result in a high decrease in LAI. For cover fraction is the no-change bar for these units a little bit larger than the decreasing one. Change patterns for LAI (figure 38) and cover fraction (figure 39) are more or less equal for units 8 (limestone), 9 (white limestone) and 10 (fluvial sediments).

4.5.2 Aspect

Another environmental factor is aspect. This is used as environmental factor, because the aspect determines the influence of the sun on vegetation. The south and west located slopes receive more solar radiation than east and north located slopes. Vegetation on slopes that receive more solar radiation is dryer.

Aspect is divided in categories based on the main wind directions. Table 18 shows that most of the natural vegetation areas are located on south sloping hills. The smallest cover of natural vegetation areas (16%) is reached on north sloping hills.

Aspect category	Aspect direction	Area
1	North	16%
2	East	25%
3	South	33%
4	West	27%

Table 18: Aspect categories and covered area

There is a general trend in the change categories for aspect (figure 40, 41 and 42). For biomass the increasing bar is the largest followed by no-change and decreasing areas. The patterns between LAI and cover fraction are similar to each other in the sense that no-change areas are a little larger than the decreasing ones.

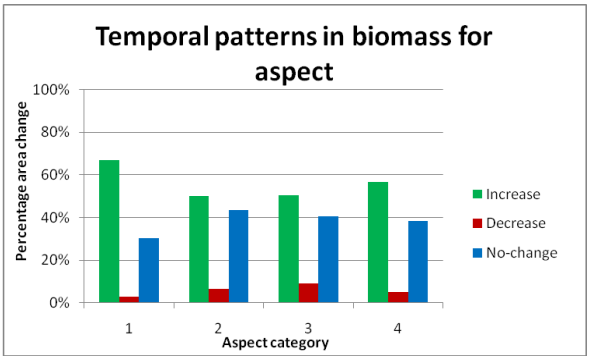

Figure 40: Temporal patterns in biomass in relation to aspect

A striking characteristic for biomass (figure 40) is that the highest increase is located in category 1 (aspect north). This is probable, because the sun has less influence on the north sloping hills, resulting that these hills can hold more water than hills with an aspect that receive more solar radiation. But there must also be taken into account that an increase in biomass is not necessary between years, because trees can reach the status of climax forest wherein the growth is minimal and changes between years are located around zero, resulting in no-change patterns. For category 2, 3 and 4 (east, south and west) the percentage increase and no-change are more or less equal. The decrease in biomass is for all categories low.

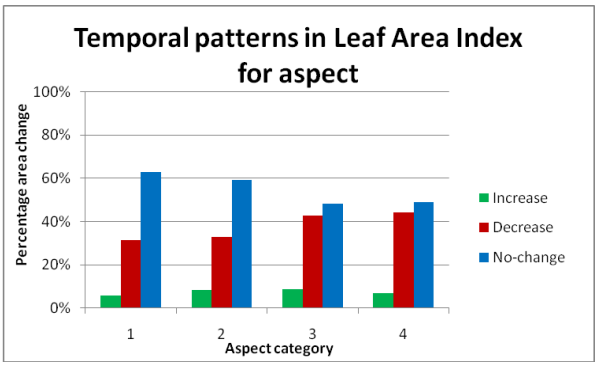

Figure 41: Temporal patterns in biomass in relation to aspect

The bar chart for LAI (figure 41) shows two different patterns. By aspect category 1 and 2 (north and east) is the percentage no-change two times the percentage decrease and for aspect category 3 and 4 (south and west) are the percentage no-change and decrease more or less equal. The percentage LAI increase is for all aspect categories similar and located around 7%.

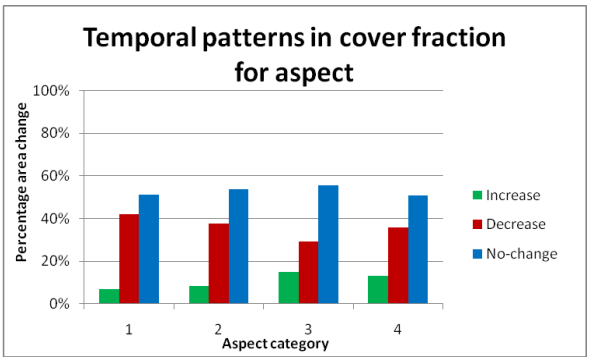

Figure 42: Temporal patterns in biomass in relation to aspect

Cover fraction changes does not show a clearly identifiable relation with the aspect categories (figure 42). For category 1 and 2 (north and east) are the decrease and no-change areas sufficient larger (29%) than the increasing areas. The largest increasing areas (around 14%) are reached for category 3 and 4 (south and west).

The sensitivity of change for aspect shows that category 1 and 2 (north and east) are different compared to category 3 and 4 (south and west) in terms of change patterns for LAI and cover fraction. This pattern is not visible for biomass where category 2, 3 and 4 are similar to each other and the striking characteristic is determined by the large increasing bar of category 1. The relative amounts do not show large different change patterns between the aspect categories.

Figure 43

Environmental factors: Elevation and slope

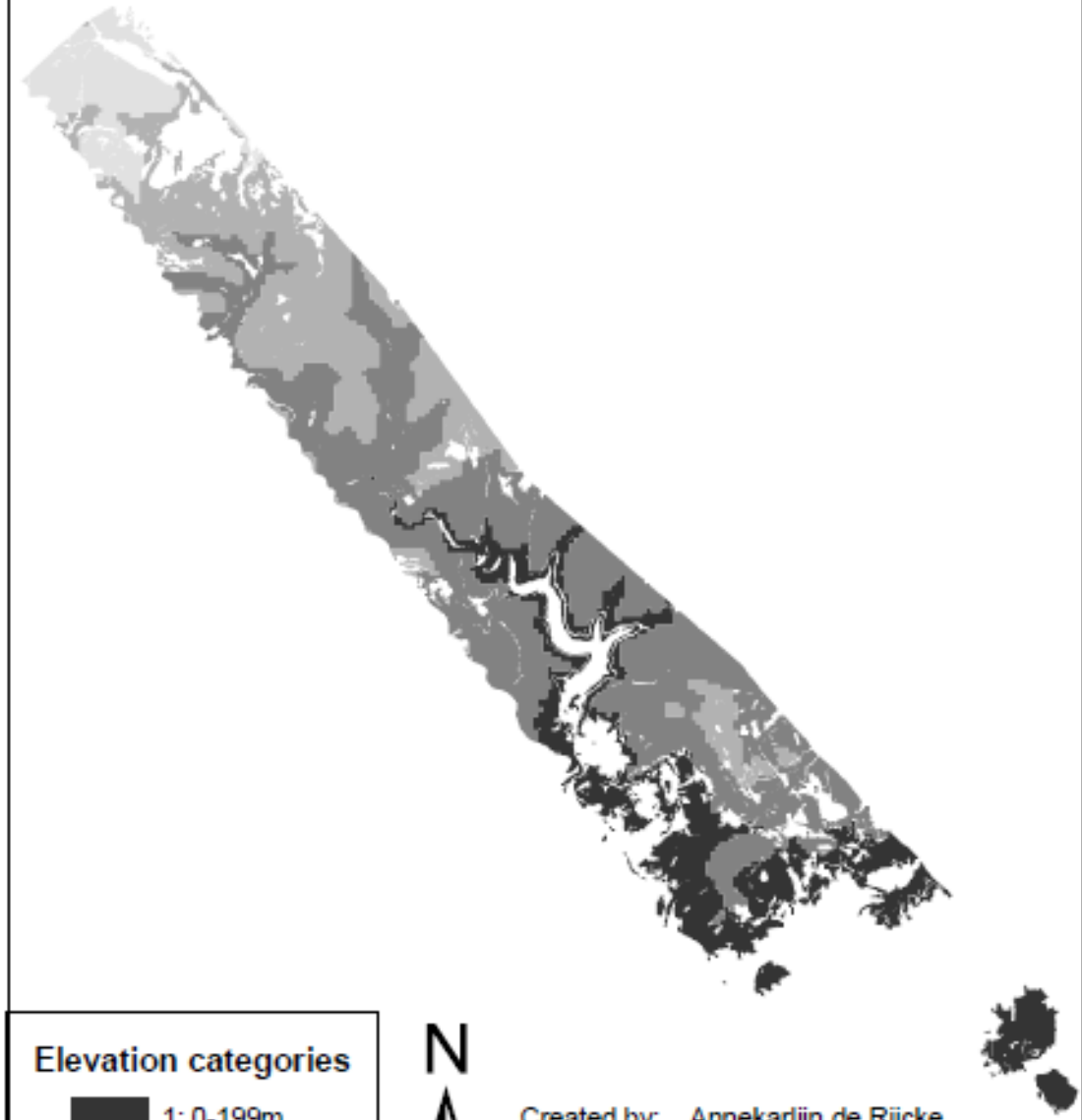

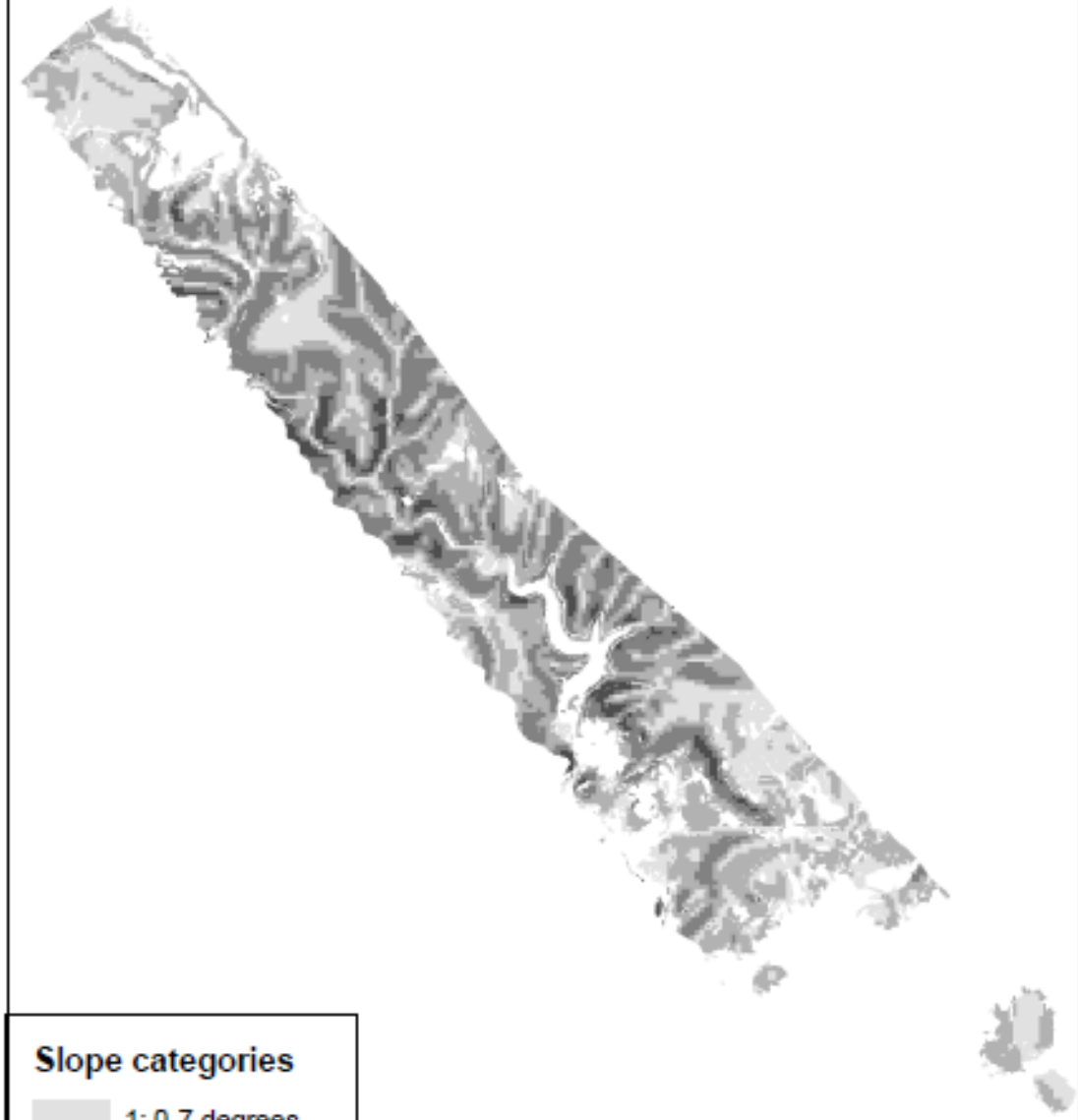

Elevation categories

- 1: 0-199m
- 2: 200-299m
- 3: 300-399m
- 4: 400-499m

N

1:85.000

0 1.000 2.000 4.000 Meters

Created by: Annekarlijn de Rijcke
Project: Temporal patterns in vegetation in the Mediterranean area
Date: 17-12-2010

Slope categories

- 1: 0-7 degrees
- 2: 8-15 degrees
- 3: 16-23 degrees
- 4: 24-33 degrees

4.5.3 Slope

The slope factor is divided into four categories based on the range of slope values (0 till 33 degrees) present in the natural vegetation areas. An overview of the distribution of slopes into categories is shown in table 18 and figure 43. The natural vegetation areas mainly consist of moderate slopes (8-15 degrees). Areas consisting of steep slopes are minimal 3.8%.

Slope category	Slope in degrees	Area
1	0-7	27.5%
2	8-15	41.7%
3	16-23	27.0%
4	24-33	3.8%

Table 19: Slope categories and covered area

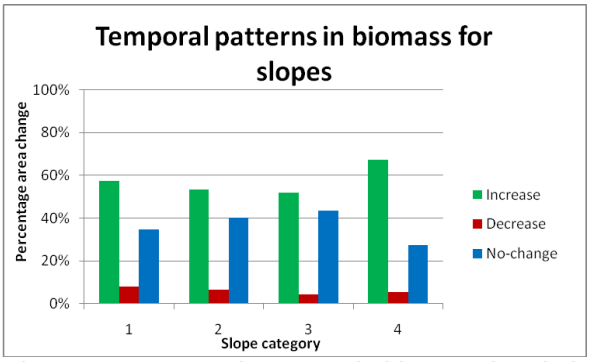

Figure 44: Temporal patterns in biomass in relation to slope

Biomass patterns in figure 44 show that the increasing bar is a little bit higher than areas with no-change, except for steep slopes (category 4). The steep slope category is dominated by increasing biomass, 67% compared with 27% for no-change areas. For all categories the decrease in biomass is low and located around 6%.

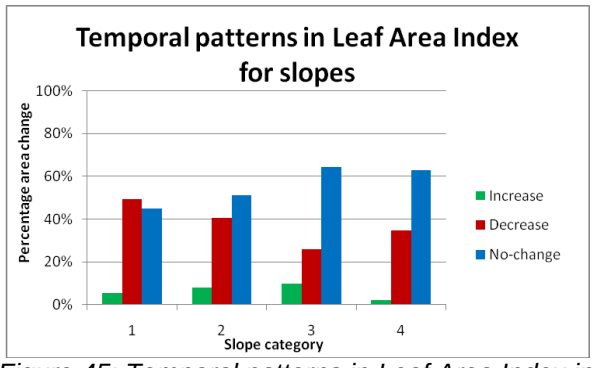

Figure 45: Temporal patterns in Leaf Area Index in relation to slope

In figure 45 is for LAI a clearly identifiable difference between categories 1 and 2 (0-15 degrees) and 3 and 4 (16-33 degrees). In the first two categories the percentage decrease

and no-change are more or less similar compared to the last two categories where the percentage decrease is half of the no-change areas. Increasing LAI values are present in all units, but are minimal in unit 4 (2%).

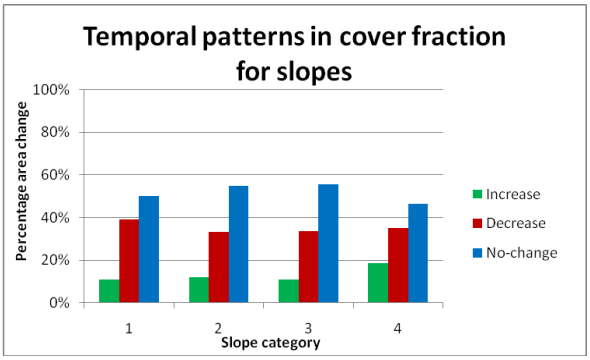

Figure 46: Temporal patterns in cover fraction in relation to slope

Temporal patterns in cover fraction for slopes show in general a no-change trend (figure 46). For categories 1 and 4 are the percentage no-change and decrease more or less equal. For category 2 and 3 is the difference in percentage between no-change and decrease larger. Increasing cover fraction areas are present in all categories. The increase is located around 11% for categories 1 till 3 and the largest increase (18%) is located on steep slopes (category 4).

LAI shows that the largest no-change areas are located in category 3 and 4. The largest increase in biomass is also reached in category 4. In this case the pattern in cover fraction does not give additional information and the distribution of changes is more or less equal distributed over the different slope categories. For biomass and LAI can the patterns probably be declared by the fact that vegetation is better developed on steep slopes. Vegetation on steep hills has to be strong to survive in terms of root strength and depth. As result of the vegetation strength is vegetation on these slopes less impressionable by environmental factors.

4.5.4 Elevation

The last environmental factor discussed is elevation. The elevation categories are based on the range of elevation values present in the study area. Figure 43 shows an increase from south-east to north-west. Most natural vegetation areas are located between 100m and 400m as is shown in table 20. Only 0.2% of the area was located between 0-99m. That is very small and a particular change pattern cannot be derived for this small category on its own, because it is not representative for a larger area. There is chosen to aggregate the 0-99m areas with the 10-199m areas in category 1.

Elevation category	Elevation	Area
1	0-199m	22.3%
2	200-299m	45.2%
3	300-399m	25.2%
4	400-499m	7.3%

Table 20: Elevation categories and covered area

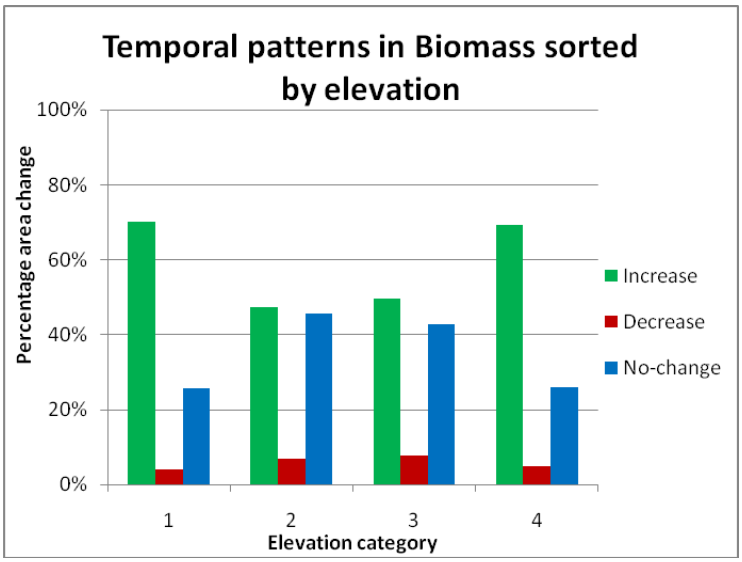

Figure 47: Temporal patterns in biomass in relation to elevation

Figure 47 shows the biomass patterns in relation to elevation. The increasing bar chart dominates for category 1 and 4 with 70% change. The percentage increase and no-change are similar for category 2 and 3 which are located around 46% change. The percentage decrease is low (6%) and is equally divided over the categories.

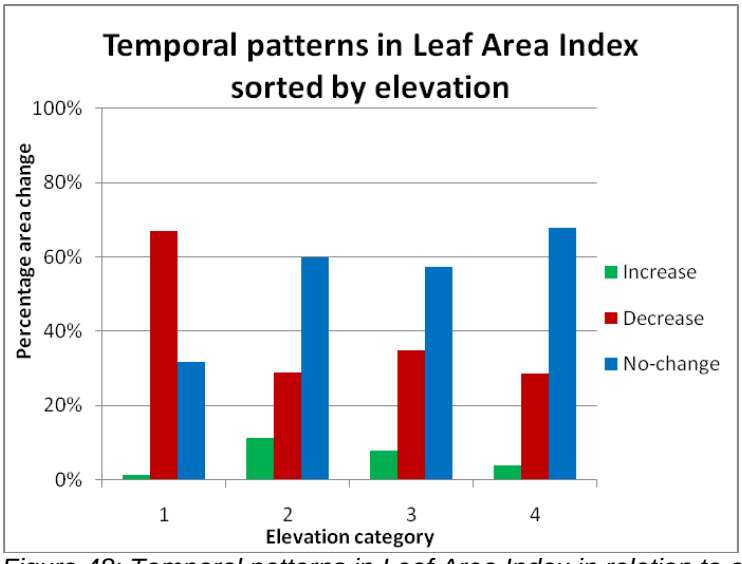

Figure 48: Temporal patterns in Leaf Area Index in relation to elevation

The patterns of biomass are not similar to the patterns for Leaf Area Index shown in figure 48. A striking characteristic is the large bar for decreasing areas in category 1 (0-199m)

compared with the large bars of no-change areas located in category 2, 3 and 4. In category one is the decrease two times the amount of no-change areas. It is probable that this is the result of that most les landes vegetation areas are located below 200m. These areas show large decreasing patterns as is mentioned in the explanation of figure 32. For the other categories are no-change areas much larger than the decreasing areas. Increasing patterns are mostly located in category 2 and 3 (around 10%) and are minimal in category 1 (1%).

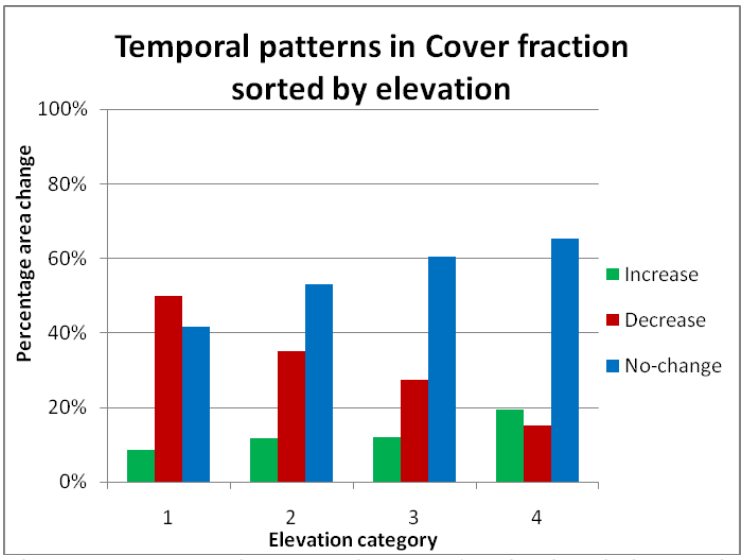

Figure 49: Temporal patterns in cover fraction in relation to elevation

The environmental factors geology, aspect and slope in relation with cover fraction do not show a clearly identifiable relation with the categories present inside a factor. This is not the case for the environmental factor elevation as shown in figure 49. The percentage decreasing areas is decreasing by an increase in elevation (from category 1 to 4). The reverse is true for the no-change areas. Also in increasing areas is a slightly increasing trend present. For category 1 is the percentage increase and no-change more or less similar. For category 2 till 4 becomes the difference between these two larger. A striking characteristic in category 4 is that the percentage increase is higher than the percentage decrease.

The explanation for these cover fraction patterns are difficult to made, but there can be concluded that cover fraction slightly increases from low to high elevations in the last five years. Besides that is there a decrease in decreasing change and increase in no-change by increasing elevations.

Discussion

This study investigated the mapping of temporal patterns in vegetation variables by use of object-based change detection on hyperspectral images of 2003 and 2008. The objective was to find an optimal segmentation method and scale for each vegetation variable. This is separately done for each vegetation variable to assess the spatial structure and variability on its own.

The vegetation variable values estimated in the field correspond with the results found in other Mediterranean studies. Leaf Area Index values estimated in the field, range from 0.78 to 5.5 with an average of 3.26. These results match well with a mean LAI value of 2.96 found by Caraux et al. (2003), LAI values ranging from 0.4 to 5.4 with an average of 3.2 found by Addink et al. (2007) and values ranging from 0 to 5.8 with an average of 2.93 found by Nijland et al. (2009).

Cover fraction values range from 6- 95% with an average of 69% and this corresponds with cover fraction values found by Nijland et al. (2009) ranging from 10 to 100% with an average of 74%.

For aboveground biomass values were found in a range from 1.9 to 680.8 ton/ha with an average value of 249.9 ton/ha. Biomass values in other studies range from 0.2 to 379.2 ton/ha with an average of 80.73 ton/ha (Nijland et al., 2009), and a mean biomass value of 270 ton/ha for a dense French evergreen oak forest (De Jong et al., 2003). The maximum biomass values in other studies are much lower than the results found during the fieldwork in 2009. This is probably the result that measurements were also done inside a reforestation area consisting of large Pine trees (*Pinus sylvestris*) trees.

Sources in field measurements that contribute to the uncertainty in model results are the locations of field plots, measurement inaccuracies in the way how vegetation measurements are done and uncertainty in the GPS device itself:

The locations of field plots were defined before the fieldwork. In some cases it was not possible to reach these points as result of steep slopes, to dense forest, private properties, etc. But sometimes we changed the location of sample points, because these were spread over a large area where it was difficult to reach the points. The samples are moved to locations where points lay closer together.

Vegetation measurements were done to obtain information about aboveground biomass, Leaf Area Index and cover fraction. Biomass estimation is done with three allometric formulas. The formulas used depend on the two main vegetation species present in the area and a shrub version. Other measured tree species were divided in two groups on basis of morphological similarity to the two main vegetation species. It would be satisfying to

have more formulas available, because not all vegetation species are morphological similar to the main vegetation species (*Arbutus unedo and Quercus ilex*), as example the deforestation area has a lot of Pine trees (*Pinus Sylvestris*).

Information obtained to estimate biomass are tree height (not used in these allometric formulas, but is estimated if other formulas are used), diameter of the tree and maximum projected area of shrubs. The height of the tree has to be visually estimated, because the device that can be used for it, did not work well in dense forest. The diameter of the tree has to be measured at 50 cm, but this is not constantly done, because of trees where stems are growing together at the same height. A consequence is that measurement has to be done above the location where stems are fusing by measuring each stem separately.

The coordinates of the plot were assessed by a GPS-device that has an accuracy of 5-10m. The geometric accuracy of a pixel in an image is 5m. Although coordinates will match, field observations are not necessarily linked to the correct pixel (geometrical mismatching). To reduce this problem field observations are linked to windows consisting of 3 by 3 pixels. These windows are centred on the plot location to obtain pixel values from.

In studies done before (Addink et al., 2006, Addink et al., 2007, Nijland et al., 2009) images were first segmented before ridge regression was applied. I decided to apply ridge regression on hyperspectral images first before segmentation took place, because I want to obtain vegetation patterns based on the spatial variability present inside the predictive map of a vegetation variable (biomass, Leaf Area Index and cover fraction).

For the application of regression analyses ridge regression is used, because it reduces the multi-collinearity present between the bands of hyperspectral images. The optimal regression function is obtained by using the lowest Generalized Cross Validation (GCV), representing the function with the lowest error variance.

The accuracy of ridge regression is assessed by a validation data set, meaning that a small part of the data (validation data set) is left out of regression analyses, so that it can be used to obtain the accuracy. On basis of R^2 information can be concluded that biomass (correlation 2003: 0.58 and 2008: 0.55) is the best predicted variable. Leaf Area Index (correlation 2003: 0.40 and 2008: 0.44) and cover fraction (correlation 2003: 0.35 and 2008: 0.27) are less accurate.

The accuracy of cover fraction is disappointing and I was in doubt if the final change pattern result for this vegetation variable is reliable, because of the low R^2 after the application of ridge regression.

Temporal patterns in vegetation are assessed by objects instead of pixels. Other studies (Addink et al., 2007 and Nijland et al., 2009) have shown that segmentation does provide better estimates for object-oriented parameters than for per-pixel estimations. Pixels use the spectral information of input images, but do not accurately represent the true nature of features on the Earth surface. Features are varied in size, shape, colour, etc. (Ouma et al., 2008). Besides that pixels are more sensitive to misregistration (Lunetta & Elvidge, 1998) and consists the resulting map of a “salt and pepper” effect (Desclee et al., 2005) if pixels instead of objects are used.

The optimal image segmentation method is obtained by using three segmentation methods with different object scales. In this study two methods are based on the principle of using the spatial structure and variability from both acquisition years and the third method only considers the spatial structure and variability of 2003.

As expected the highest R^2 and lowest RMSE are reached by the methods where the predictive vegetation variable maps from both acquisition years are used (R^2 biomass: 0.66, LAI: 0.42 and cover fraction: 0.41). This is probable, because the pattern depends on the spatial structure and variability present in both years. If only the characteristics of one year are taken into account, the prediction accuracy of the other year is much lower (R^2 biomass: 0.61, LAI: 0.40 and cover fraction: 0.39). The optimal segmentation method R^2 values for biomass and LAI compare well with the results of Addink et al. (2007a) with an R^2 of 0.46 for LAI and 0.4 for biomass.

In the validation of segmentation the R^2 value or cover fraction is much higher (0.41) than after regression analyses (2003: 0.35 and 2008: 0.27). An explanation for this is that field locations are linked to objects instead of a window (3 by 3 pixels) and that objects contain better results if they are compared to field data, because an object is a homogeneous segment and it is more confident that point correspond to objects instead to pixels.

As mentioned above two segmentation methods took the vegetation characteristics from both years into account. The first one considers the characteristics in vegetation variables simultaneously. The second one segments both images independently and the final boundary locations are based by merging the boundary locations of the objects of both images.

I expected that the first method delivers the best results, because the objects are then based on the spatial structure and variability present in both vegetation images simultaneously, but this is not the case for Leaf Area Index and biomass. Probably is this the result of that validation values are more similar when objects are firstly generated for the image years

separately. If segmentation for both years is done simultaneously the objects represent mainly the characteristics present in both image years. Spatial characteristics present in one of these images are not used for the final object boundary locations, because these are not present in both images.

The optimal segmentation scale varies between the vegetation variables used (biomass scale 4, LAI scale 8 and cover fraction scale 3). This is also found in other studies (Addink et al., 2007a and Nijland et al., 2009) where object-based vegetation patterns are estimated. These differences can be explained by the spatial structure and variability present inside the predictive vegetation variable map (heterogeneity in the data) and the segmentation methods used.

The determination of vegetation changes between 2003 and 2008 are based on image differencing, where images are subtracted from each other to determine change areas. Image differencing provides a powerful tool for the detection of changes (Lu et al., 2005).

An area is detected as change area if the change is larger than the threshold. This threshold is the absolute average residual of the validation data set of image segmentation. It can be concluded that it is probable that vegetation within the objects is changed if they exceed the threshold. Still an uncertainty around the value of this threshold has to be taken into account, because the residuals used to obtain this threshold contain uncertainty in the field (measurement errors) and the threshold varies if other points were used for the application of regression analyses and the accuracy control of regression and image segmentation.

Temporal patterns in vegetation are obtained for Leaf Area Index, biomass and cover fraction. For a large part of the natural vegetation areas an increase in biomass was present (55%). It is to be expected that biomass values increase between years as a result the accumulation of yearly net growth, but it is not necessary that this changes are large enough to exceed the threshold. Trees can reach the status of climax forest wherein the growth is minimal and changes are small. For the no-change areas for biomass does this not immediately mean that vegetation is not developing itself as result of environmental circumstances, but that the forest can also have reached the status of climax forest.

The change patterns for biomass are not similar to the change patterns for LAI and cover fraction. These mainly show a decrease (LAI 39% and cover fraction 35% decrease). This does not immediately mean that these temporal patterns are wrong, because an increase in biomass does not have to result in increasing values for cover fraction and/or LAI. For the LAI values are the previous two to four years dominant. The effect of environmental factors on this LAI value is large, as example: stormy weather can destroy leaves and result

in an underestimation of the LAI and cover fraction value if hyperspectral images are obtained before the leaves where destroyed and fieldwork is done after it.

It was expected that the change patterns for LAI and cover fraction were more or less similar, because by the analyses of fieldwork data an R^2 of 0.56 between these variables was found, but this is not shown in the change maps of these variables. Also the graph (figure 36) where the change patterns between the vegetation variables are compared does not show a certain relationship.

Temporal patterns in vegetation variables are compared with environmental factors. These factors are subdivided into categories to determine if a certain relation is present between change patterns and the categories inside an environmental factor. There are some patterns visible inside a specific category of an environmental factor (geology and elevation), but it is not certain that this is the case over longer period or that it only dominates in the change pattern between 2003 and 2008. Additional study over a longer period is required to describe more certain change patterns in relation to environmental factors.

Conclusion

This study investigated the determination of temporal patterns in vegetation with object-based change detection and to explain these changes with the use of static environmental factors. Patterns are obtained by the application of ridge regression and segmentation on hyperspectral images of 2003 and 2008. The three main questions of this study are: 1) Can aboveground biomass, Leaf Area Index and cover fraction be estimated from hyperspectral images? 2) Can changes in vegetation parameters be estimated with object-based change detection on hyperspectral images? 3) Can changes be explained on basis of environmental factors?

Vegetation variables can be assessed by hyperspectral images and the use of regression analyses. Ridge regression fits a function between field measurements and HyMap images. Field measurements for Leaf Area Index and cover fraction are done with hemispherical photos and biomass is obtained by using allometric formulas. Information derived from hyperspectral images are obtained by using the spectral signature of pixels covered by a 3 by 3 window. This window is necessary to reduce the problem of geometrical mismatch between the location in the field and the corresponding pixel location.

The resulting regression function is applied to hyperspectral images to obtain predictive vegetation maps. The aim is to assess the spatial structure and variability present in each variable separately. This cannot be done with pixels, because these do not accurately represent the true nature of vegetation patterns and pixels are fixed dimensions. Objects take the heterogeneity in the data into account and also reduce the problem of geometrical mismatching by the application of change detection.

Objects are generated by segmentation whereby homogeneous segments are formed. Segmentation took place for each vegetation variable separately, because biomass, Leaf Area Index and cover fraction have their own characteristic spatial patterns. Segmentation is done by using three methods and ten different object scales.

The optimal segmentation method, in the case of change detection, is reached when the spatial structure and variability of vegetation variables from both image years are taken into account. The optimal segmentation scale differs for the vegetation variable under consideration, but also for the image segmentation method used.

Changes in vegetation parameters between 2003 and 2008 are obtained by object-based image differencing. This takes place on basis of the homogeneous segments formed by segmentation. The result of image differencing is the change magnitude and an area is detected as change if the threshold (obtained by residual information of image segmentation) is exceeded.

Temporal patterns in vegetation variables are compared with environmental factors. There are some patterns visible inside a specific category of an environmental factor (geology and elevation), but it is not certain that this is the case over longer period or that it only dominates in the temporal patterns between 2003 and 2008.

Recommendations for further studies are:

- Assessing which method of obtaining temporal patterns performs the best. Patterns can also be obtained by first doing segmentation followed by regression analyses. During this study I only derive temporal patterns by first doing regression analyses followed by image segmentation, to take the spatial structure and variability of each vegetation variable into account.
- Additional studies over a longer period is required to describe whether changes occur at specific locations or that change patterns differ through time?
- This also applies for change patterns in relation to environmental factors. As can be seen in this study there is a certain relation present between the change patterns and geology and elevation, but it is not known whether this is by coincidence or a causal relation. To be more certain about these relations, field and image data over a longer timescale and compared between more years, are necessary.

References

Articles

- Addink E.A., Thonon I., De Jong S.M., Gorte B.G.H., Beck R., Van Persie M. & Kramer H., 2006. The Mutatis Mutandis project: Single detection, multiple users-Change detection using high spatial-resolution imagery in Dutch urban areas. Proc. EARSeL Workshop SIG Urban Remote Sensing, 8pp.
- Addink E.A., de Jong S.M. & Pebesma E.J., 2006. Spatial object definition for vegetation parameter estimation from HyMap data. ISPRS Commission VII Mid-term Symposium "Remote sensing" from pixels to processes", Enschede, the Netherlands.
- Addink E.A., de Jong S.M. & Pebesma E.J., 2007 a. Object definition for aboveground biomass and leaf area index estimation. Proceedings 5th EARSel Workshop on Imaging Spectroscopy. Bruges, Belgium.
- Addink E.A., de Jong S.M. & Pebesma E.J., 2007 b. The importance of scale in object-based mapping of vegetation parameters with hyperspectral imagery. Photogrammetric Engineering and Remote Rensing,73 iss.8 pp.905-912.
- Araujo T.M., Higuchi N. & Carvalho Jr. J.A., 1999. Comparison of formula for biomass content determination in a tropical rain forest in the state of para, Brazil. Forest Ecology and Management, 117, pp.43-52.
- Baudry J., 1991. Ecological consequences of grazing, extensification and land abandonment: Role of interactions between environment, society and techniques. Land abandonment and its role in conservation, pp.13-19.
- Bonet A., 2004. Secondary succession of semi-arid Mediterranean old-fields in south-eastern spain: Insights for conservation and restoration of degraded lands. Journal Arid Environments 56(2), pp.213-233.
- Caraux G.D. & Lacaze B, 2003. Monitoring leaf area index of Mediterranean oak woodlands: Comparison of remotely-sensed estimates with simulations from an ecological process-based model. International Journal of Remote Sensing, 24(17) pp.3441-3456.
- Cohen W.B. & Goward S.N., 2004. Landsat's role in ecological applications of remote sensing. Bioscience, 54, pp.535-545.
- Desclée B., Bogaert P. & Defourny P., 2005. Forest change detection by statistical object-based method. Remote Sensing of Environment, 102, iss.1-2, pp.1-11.
- Gao J., 2008. Mapping of land degradation from ASTER data: A comparison of object-based and pixel-based methods. GIScience & Remote Sensing, 45, iss.2, pp.149 -166.
- Gèze B., 1979. Languedoc Méditerranéen – Montagne Noire. Paris: Masson.
- Giorgi F., 2006. Climate change Hot-Spots. Geophys. Res. Lett. 33, iss.8.
- Giorgi F. & Lionello P., 2008. Climate change projections for the Mediterranean region. Global and Planetary Change, 63, iss.2-3, pp.90-104
- De Graaf G., 2006. Languedoc Roussillion. ANWB goud, 2nd edition.
    - General information about the Mediterranean area
- Hastie T., Tibshirani R. & Friedman J., 2009. The elements of statistical learning: Data mining, inference, and prediction. Stanford University, Springer Science, 2nd edition, 533pp.
- Hurrell, J.W., 1995. Decadal trends in the North Atlantic Oscillation: regional temperature and precipitation. Science, 269, pp.676–679.
- Jonckheere I., Fleck S., Nackaerts K., Muys B., Coppin P., Weiss M. & Baret F., 2004. Review of methods for in situ leaf area index determination Part I. Theories, sensors and hemispherical photography. Agricultural and forest meteorology, 121, iss.1-2, pp.19-35.
- De Jong S.M., Pebesma E.J. & Lacaze B., 2003. Above-ground biomass assessment of Mediterranean forests using airborne imaging spectrometry: The DAIS Peyne experiment. International Journal of Remote Sensing, 24, iss.7, pp.1505 -1520.
- Lillesand T.M., Kiefer R.W. & Chipman J.W., 2004. Remote sensing and image interpretation. 5th edition. New York: Wiley.
    - Image classification and change detection methods.
- Lu D.S., Mausel P., Brondízio E.S. & Moran E., 2004. Change detection techniques. International Journal of Remote Sensing, 25, pp.2365-2407.

- Lu D., 2006. The potential and challenge of remote sensing-based biomass estimation. International Journal of Remote Sensing, 27, pp.1297-1328.
- Lunetta R.S. & Elvidge C.D., 1998. Remote sensing change detection, environmental monitoring methods and applications. Chelsea, Michigan: Ann Arbor Press, 1st edition, 318pp.
    - Change detection methods and accuracy assessment.
- Luterbacher J., Lionello P., Malanotte-Rizzoli P. & Boscolo R, 2006. Mediterranean climate variability over the last centuries: A review. Mediterranean Climate Variability. Elsevier, Amsterdam, pp.27-148.
- Mather A.S., Fairbairn J. & Needle C.L., 1999. The course and drivers of the forest transition: the case of France. Journal of Rural Studies, 15, pp.65-90.
- Naveh Z. & Kutiel P., 1990. Changes in the Mediterranean vegetation of Israel in response to human habitation and land use. Woodwell GM The earth in transition: pattern and process of biotic impoverishment. Cambridge University Press, Cambridge, pp.259-299.
- Navulur K., 2007. Multispectral image analysis using the object-oriented paradigm. Boca Raton: CRC Press, 1st edition, 184pp.
    - Image segmentation and accuracy assessment.
- Nijland W., Addink E.A., De Jong S.M. & Van der Meer F.D., 2009. Optimizing spatial image support for quantitative mapping of natural vegetation. Remote sensing of environment, 113, iss.4, pp.771 -780.
- Ogaya R., Peñuelas J., Martinez-Vilalta J. & Mangiron M., 2003. Effect of drought on diameter increment of Quercus ilex, Phillyrea latifilia and Arbutus unedo in an holm oak forest of NE Spain. Forest Ecology and Management, 180, pp.175-184.
- Ouma Y.O., Josaphat S.S., Tateishi R., 2008. Multiscale remote sensing data segmentation and post-segmentation change detection based on logical modeling: Theoretical exposition and experimental results for forestland cover change analysis. Computers & Geosciences, 34, iss.7, pp.715 -737.
- Pereira J.M.C., Oliveira T.M. et al., 1994. Fuel mapping in Mediterranean shrubland using Landsat TM imagery. International Workshop on Satellite technology and GIS for Mediterranean forest mapping fire management, Luxembourg, Office for official publications of the European communities.
- Ross, J. 1981. The radiation regime and architecture of plant stands, Norwell, MA, p.392.
- Schläpfer D. & Richter R., 2002. Geo-atmospheric processing of airborne imaging spectrometry data. Part 1: Parametric orthorectification. International Journal of Remote Sensing, 23, iss.13, pp.2609 -2630.
- Schroeder L.D., Sjoquist D.L. & Stephan P.E., 1986. Understanding regression analysis: An introductory guide. Sage University Paper Series on Quantitative Applications in the Social Sciences, 07-057, Newbury Park, CA: Sage. 1st edition, 95pp.
- Sen A. & Srivastava M., 1990. Regression analysis: Theory, Methods, and Applications. Springer texts in Statistics. 1st edition, 347pp.
- Singh A., 1989. Digital change detection techniques using remotely sensed data. International Journal of Remote Sensing, 10, pp.989-1003.
- Sluiter R., 2005. Mediterranean land cover change, modelling and monitoring natural vegetation using GIS and remote sensing. NGS 333. Utrecht: Koninklijk Nederlands Aardrijkskundig Genootschap. 1st edition, 145pp.
- General information about the Mediterranean area, sensors and land abandonment.
- Sluiter R., De Jong S.M., 2007. Spatial patterns of Mediterranean land abandonment and related land cover transitions. Landscape Ecology, 22, iss.4, pp.559 -576.
- Snyder M., 2006. What is a climax forest? Northern Woodlands, Magazine, Autumn 2006 Issue.
- Tomaselli R., 1981. Main physiognomic types and geographic distribution of shrub systems related to Mediterranean climates. Ecosystems of the World, 11. Mediterranean-type shrublands, pp.95-106.
- Trigo R.M., Xoplaki E., Lüterbacher J., Krichak S.O., Alpert P., Jacobeit J., Sáenz J., Fernández J., González-Rouco J.F., 2006. Relations between variability in the Mediterranean region and mid-latitude variability. In: Lionello, P., Malanotte-Rizzoli, P., Boscolo, R. (Eds.), Mediterranean Climate Variability. Elsevier, Amsterdam, pp.179–226.
- Van der Windt H., Keulartz J., Swart S., 1995. Natuurbeelden en natuurbeleid, NWO, Den Haag, 2000, p.185.

- Weiss M., Baret F., Smith G.J., Jonckheere I. Coppin P., 2004. Review of methods for in situ leaf area index (LAI) determination Part II. Estimation of LAI, errors and sampling. Agricultural and Forest Meteorology, 121, iss.1-2, pp.37-53.
- Welles J.M., 1990. Some indirect methods of estimating canopy structure. Remote Sensing Rev., 5, pp.31-43.
- Wonnacott T.H.& Wonnacott R.J., 1990. Introductory statistics. University of western Ontario. Wiley. 5th edition, 416pp.

Websites

- Can-EYE output variables description. Information about the application Can-eye for the estimation of Leaf Area Index with hemispherical photos. www.avignon.inra.fr/can_eye
- Definiens eCognition Developer, http://www.definiens.com, Definiens Ecognition 8 – Reference book 2009.
- © Ecopedia.be 2009 http://ecopedia.be/faq#q1 Information about cover fraction.
- German Aerospace Center, Dais. http://www.op.dlr.de/dais/dais-scr.htm Information about the Digital Airborne Imaging Spectrometer DAIS 7915.
- German Aerospace Center, HyMap. http://www.op.dlr.de/dais/hymap/hymap_info.htm Information about the HyMap sensor
- GNU project. http://www.r-project.org/ Information about R
- NOAA Climate Prediction Center, Information about the East Atlantic (http://www.cpc.noaa.gov/data/teledoc/ea.shtml)
- www.sluitertijd.org Pictures of the dominant tree species in the Peyne area.
- Meteo-France (2006). Meteo-France – Previsions-Observation-Climatologie-Vulgarisation. http://www.meteo.fr
- R project for statistical computing. http://www.r-project.org

Appendix

1. Plot locations

Sample point locations

Appendix 1

Legend

Geological entities of sample points

- Dolomite
- Meltflows, Basaltes, tuffs
- Flysch with Conglomerates
- Schistes and Quartzite
- Sandy Shale, Schistes, Coals and Limestone
- Red slate/mudstone with some conglomerates
- Sandstone, Sandy Limestone
- Limestone, Limestones with chert
- White limestone, sandstone, marls

Explanation

The locations of sample points are mainly based on the geological entities and on change patterns of natural vegetation (NDVI). The total amount of visited sample point locations in the field is 201.

N

1:50.000

Created by: Annekarlijn de Rijcke
Project: Temporal patterns in vegetation dynamics in a Mediterranean area
Date: 16-02-2009

0 500 1.000 2.000 3.000 4.000 5.000 Meters

2. Vegetation abbreviation list

Vegetation code	Latin name	Common name
Ace	*Acer monspessulanum*	Montpellier Maple
Aun	*Arbutus unedo*	Strawberry tree
Bus	*Buxus sempervirens*	Box
Cas	*Castanea sativa*	Sweet chestnut
Coa	*Colutea arborescens*	Bladder senna
Ear	*Erica arborea*	Tree heath
Jas	*Jasminum fruticans*	Bush jasmine
Jun	*Juniperus communis*	Juniper
Lig	*Ligustrum vulgare*	Privet
Pil	*Pistacia lentiscus*	Mastic tree
Prp	*Prunus padus*	Bird cherry
Psy	*Pinus sylvestris*	Pine tree
Qco	*Quercus coccifera*	Kermes oak
Qil	*Quercus ilex*	Holly oak
Qpu	*Quercus pubescens*	Downy oak
Rus	*Ruscus aculeatus*	Butcher’s broom
Spj	*Spartium junceum*	Spanish broom
ulx	*Ulex parviflorus*	Gorse

3. Ridge Regression script

```
#calling script functions that are necessary for ridge regression
library(MASS)
library(ipred)

#reading the text file with the data about the plot locations, the variables and band information
tabel <- read.table(file="C:\\data2008\\samples\\calBiomass2008.txt",head=TRUE);

#Creation of a l300 lambda files, consisting of 300 lambda values in a certain range
l300 = signif(exp(seq(log(0.00001), log(10000), length=300)),6)

#Ridge regression function script
"lm.ridge" <-
function (formula, data, subset, na.action, lambda = 0, model = FALSE,
   x = FALSE, y = FALSE, contrasts = NULL, ... )
{
   m <- match.call(expand = FALSE)
   m$model <- m$x <- m$y <- m$contrasts <- m$... <- m$lambda <- NULL
   m[[1]] <- as.name("model.frame")
   m <- eval.parent(m)
   Terms <- attr(m, "terms")
   Y <- model.response(m)
   X <- model.matrix(Terms, m, contrasts)
   n <- nrow(X)
   p <- ncol(X)
   offset <- model.offset(m)
   if (!is.null(offset))
      Y <- Y - offset
   if (Inter <- attr(Terms, "intercept")) {
      Xm <- colMeans(X[, -Inter])
      Ym <- mean(Y)
      p <- p - 1
      X <- X[, -Inter] - rep(Xm, rep(n, p))
      Y <- Y - Ym
   }
   else Ym <- Xm <- NA
   Xscale <- drop(rep(1/n, n) %*% X^2)^0.5
   X <- X/rep(Xscale, rep(n, p))
   Xs <- svd(X)
   rhs <- t(Xs$u) %*% Y
   d <- Xs$d
   lscoef <- Xs$v %*% (rhs/d)
   lsfit <- X %*% lscoef
   resid <- Y - lsfit
   s2 <- sum(resid^2)/(n - p - Inter)
   HKB <- (p - 2) * s2/sum(lscoef^2)
   LW <- (p - 2) * s2 * n/sum(lsfit^2)
   k <- length(lambda)
   div <- d^2 + rep(lambda, rep(p, k))
   a <- drop(d * rhs)/div
   dim(a) <- c(p, k)
   coef <- Xs$v %*% a
   dimnames(coef) <- list(names(Xscale), format(lambda))
   df = colSums(matrix(d^2/div, p))
   residuals <- colSums((Y - X %*% coef)^2)/(n - df)
   GCV <- sqrt(1/n * colSums((Y - X %*% coef)^2)/(1 - colSums(matrix(d^2/div,
      p))/n)^2)
   cv <- vector()
   #for(i in lambda){cv <- c(cv, (errorest(formula, data, model = lm.ridge, lambda = i)$error) ) }
   res <- list(coef = drop(coef), scales = Xscale, Inter = Inter,
      lambda = lambda, ym = Ym, xm = Xm, GCV = GCV, CV10 = cv ,
                        kHKB = HKB, kLW = LW, df = df, residuals = residuals)
```

```
   class(res) <- "ridgelm"
   res
}

"predict.ridgelm" <-
function(x, newdata) {
        obj = x
        X = newdata[,-1]
        X = as.matrix(X)
        n = nrow(X)
        p = ncol(X)
        Xm = colMeans(X)
        X = X - rep(Xm, rep(n, p))
        X = X/rep(obj$scales, rep(n, p))
        # print(dim(X))
        X %*% obj$coef + obj$ym
}
```

#Application of ridge regression on basis of the script for all defined lambda values. Defined information consist of vegetation variable under consideration and band numbers

```
var <- lm.ridge(LBIOMASS ~ (B2+B4+B6+B8+B10+B12+B14+B16+B18+B20+B22+B24+
B26+B28+B30+B32+B34+B36+B38+B40+B42+B44+B46+B48+B50+B52+B54+B56+B58+
B60+B62+B64+B66+B68+B70+B72+B74+B76+B78+B80+B82+B84+B86+B88+B90+B92+
B94+B96+B98+B100+B102+B104+B106+B108+B110+B112+B114+B116+B118+
B120+B122+B124), tabel, lambda=l300);
```

#Selecting optimal lambda value for model prediction

```
optimum<-(lamda == min(var$GCV))
```

#Application of ridge regression on basis of the script for the optimal lambda value. Defined information consist of vegetation variable under consideration and band numbers

```
a <- lm.ridge(LBIOMASS~ (B2+B4+B6+B8+B10+B12+B14+B16+B18+B20+B22+B24+
B26+B28+B30+B32+B34+B36+B38+B40+B42+B44+B46+B48+B50+B52+B54+B56+B58+
B60+B62+B64+B66+B68+B70+B72+B74+B76+B78+B80+B82+B84+B86+B88+B90+B92+
B94+B96+B98+B100+B102+B104+B106+B108+B110+B112+B114+B116+B118+
B120+B122+B124), data=tabel,lambda=optimum)
```

#extraction of the intercept and the coefficients associated to their band numbers

```
b<-coef(a)
b
```

#saving of model predictions

```
write.table(b,file="C:\\data2008\\samples\\coef-cal-biomass.txt",sep="\t")
c<-t(as.matrix(b))
write.table(c,file="C:\\data2008\\samples\\coef-cal-biomass-1.txt",sep="\t")
```

4. Predictive model equations

Predictive model Biomass 2003

(2.95068925068672) + b2*float(-0.00596342340313544) + b4*float(0.002952550711811)
+b6*float(0.00140995495396534)+b8*float(-0.00090553352811284) + b10*float(-0.00188517993604260)
+ b12*float(-0.00170103976400236) + b14*float(-0.00149721537573547) +b16*float(-0.000294620258523946)
+b18*float(0.00222341242075259)+ b20*float(0.000280533007056993) + b22*float(5.37906163283353e-05)
+ b24*float(1.19428672257231e-05)+b26*float(-3.02714830727246e-05)+b28*float(-7.80165988104192e-05)
+ b30*float(-5.50179429638469e-05)+b32*float(-6.38622182004785e-05)+b34*float(-5.29324989220346e-05)
+ b36*float(8.56505356731027e-06)+b38*float(4.63307476091344e-05)+b40*float(-7.02034552274082e-05)
+ b42*float(-0.000371074056195999) + b44*float(-0.000141476004558516) + b46*float(-0.000125619186707591)
+b48*float(-1.98346006160676e-05) + b50*float(0.000179922334924728) +b52*float(0.000302619467446933)
+b54*float(0.000252976566295748) +b56*float(0.000172525735434636)+b58*float(-0.000115697740219612)
+b60*float(-0.000179179773532144)+b62*float(-0.000655120930908515)+ b64*float(-0.000231038982641447)
+b66*float(-8.81067126109879e-05)+b68*float(5.49261792192903e-05)+b70*float(-6.05647887215058e-06)
+b72*float(-0.000289093752380596)+b74*float(-0.000404217757800240)+b76*float(-0.000478985452734562)
+b78*float(-0.000272147908321149)+b80*float(0.000327599543641784)+b82*float(0.000618994050129143)
+b84*float(0.000543997434108433)+b86*float(0.000542301320710534)+b88*float(0.000726567118531107)
+b90*float(0.000438839880356478)+b92*float(0.00046204166614966)+b94*float(0.000477553310308092)
+b96*float(0.000651660828115314)+b98*float(-0.00014771179600732)+b100*float(-0.000330514940161092)
+b102*float(-0.00108377457944429)+b104*float(-0.00107829203298774)+b106*float(-0.00108471042014730)
+b108*float(-0.000772569978126291)+b110*float(-0.000501000530749255)+b112*float(-0.000492567406769459)
+b114*float(1.87923993209947e-05)+b116*float(0.000219457040371807)+b118*float(0.00108491433259059)
+b120*float(0.00109024294261197)+b122*float(0.000746384364178907)+b124*float(0.000459365815376402)

Predictive model LAI 2003

(2.11820219577002)+b2*float(0.00148375490630008)+b4*float(0.000268113287537447)+b6*float(0.000324176925447216)
+b8*float(-0.00106494935561051)+b10*float(-0.00049273716121569)+b12*float(-0.000394293924030495)
+b14*float(-0.000365550549209787)+b16*float(-0.000647859340813742)+b18*float(-0.00090268579944346)
+b20*float(2.89187201797559e-05)+b22*float(1.65152835737805e-05)+b24*float(-3.83367760348542e-05)
+b26*float(-5.34488011797708e-05)+b28*float(-6.95820049005829e-05)+b30*float(-6.4614065632282e-05)
+b32*float(-6.56530916909863e-05)+b34*float(-3.75076391875886e-05)+b36*float(1.87237774147519e-05)
+b38*float(6.43089656940237e-05)+b40*float(9.65733431338973e-05)+b42*float(0.000111767339183434)
+b44*float(7.91089376882015e-05)+b46*float(4.91183680843185e-05)+b48*float(5.42628478819216e-05)
+b50*float(8.3366591057672e-05)+b52*float(0.000201377766770854)+b54*float(0.000221536112722774)
+b56*float(0.000153772407572380)+b58*float(6.11708545746774e-05)+b60*float(-0.000237725647818851)
+b62*float(-0.000330008089519329) + b64*float(-0.000300542962440993)+b66*float(-0.000296853056802769)
+b68*float(-0.000292871432303195)+b70*float(-0.000198763115925046)+b72*float(1.28936533398274e-05)
+b74*float(8.20128517283063e-05)+b76*float(0.000169140495266190)+b78*float(0.000121095001255048)
+b80*float(3.63679442432929e-05)+b82*float(9.79755048225894e-05)+b84*float(0.000102747901634526)
+b86*float(0.000138494680641812)+b88*float(0.000129655221906053)+b90*float(7.75572342826703e-05)
+b92*float(-1.79758541784708e-05)+b94*float(-8.15792895618227e-05)+b96*float(-0.000492186137482965)
+b98*float(-0.000154431748109313)+b100*float(-0.000100772430052313)+b102*float(0.000122934020085462)
+b104*float(0.000293894129305445)+b106*float(0.000318851349824371)+b108*float(0.000159715011249662)
+b110*float(0.000175767579898431)+b112*float(0.000478253154189473)+b114*float(0.00040157426993061)
+b116*float(0.000432593471655339)+b118*float(0.000274503254398651)+b120*float(-0.000100837226499595)
+b122*float(-0.000173532270466027)+b124*float(-0.000545110102835673)

Predictive model Cover fraction 2003

(0.730993839429128)+b2*float(-0.00213219740360284)+b4*float(-0.00179937318570062)+b6*float(0.00395936476175586)
+b8*float(-0.00332196318979493)+b10*float(0.00294822701822826)+b12*float(-0.000146597112593523)
+b14*float(-0.00222973223439262)+b16*float(-0.00289638284984311)+b18*float(0.00478548878100265)
+b20*float(0.00162511538040107)+b22*float(-0.000311990987438432)+b24*float(-0.000967780466052504)
+b26*float(-8.47445876691177e-05)+b28*float(0.000716616038645093)+b30*float(-0.000300022447755657)
+b32*float(-0.000895336165184534)+b34*float(-0.000502080768495691)+b36*float(-0.00101510063313894)
+b38*float(-0.000419700461733097)+b40*float(-0.000181510957957157)+b42*float(-0.000637936739728014)
+b44*float(0.000857211834889939)+b46*float(0.00142155675898388)+b48*float(-0.00016844346280022)
+b50*float(-0.00051177233430568)+b52*float(0.00162967455568693)+b54*float(0.00248431929753804)
+b56*float(-0.00102342291178583)+b58*float(0.000265252348899406)+b60*float(-0.00142893600759646)
+b62*float(-0.00128206898241467)+b64*float(-0.00110410853606143)+b66*float(-0.000107167076787793)
+b68*float(0.000912929785165614)+b70*float(0.00184449124267565)+b72*float(-0.000102988380191581)
+b74*float(0.000709485942093305)+b76*float(4.36331959595425e-05)+b78*float(-0.00117544102581482)
+b80*float(0.000544972207880214)+b82*float(0.00185465021966967)+b84*float(-0.000875801208362631)
+b86*float(0.00129601336502823)+b88*float(-0.000402909950641243)+b90*float(-0.000959229806308314)
+b92*float(-0.000300091852834494)+b94*float(-0.000191202936650590)+b96*float(-0.000810651323781406)
+b98*float(-0.000689560985270540)+b100*float(0.000196294570323666)+b102*float(0.000877423772734415)
+b104*float(0.00301132550087543)+b106*float(0.000187930472476805)+b108*float(-0.00402601568911785)
+b110*float(-0.000628137567997401)+b112*float(0.000255133489603209)+b114*float(-0.000409054520113996)
+b116*float(-0.000960442466872364)+b118*float(-3.90292663291163e-05)+b120*float(0.000775747228317528)

+b122*float(0.00114443297494968)+b124*float(-0.00102685597351650)

Predictive model Biomass 2008

(1.67141899517903)+b2*float(9.0104597286123e-05)+b4*float(0.00164101759243052)+b6*float(-0.000417948244747415)
+b8*float(0.0137243493941070)+b10*float(-0.0113084475644193)+b12*float(-0.0048730712516289)
+b14*float(-0.0115480050320832)+b16*float(0.0165394054433834)+b18*float(-0.00447736022045567)
+b20*float(0.00406145854799496)+b22*float(-0.000914088113824573)+b24*float(0.00125080751820089)
+b26*float(0.00214236530666951)+b28*float(-0.00188827461210232)+b30*float(-0.00213084540051714)
+b32*float(0.000294100452834092)+b34*float(0.00209667925837786)+b36*float(-0.00057003275568093)
+b38*float(-0.00570858496550294)+b40*float(-0.00453508923020159)+b42*float(0.000191988607534636)
+b44*float(0.00512661350541834)+b46*float(0.00103420285221167)+b48*float(-0.00390265906185569)
+b50*float(0.0140355694307827)+b52*float(0.00483235448015157)+b54*float(-0.00865081812332156)
+b56*float(-0.00706733380210559)+b58*float(-0.000651228588748356)+b60*float(0.00189401696296088)
+b62*float(0.00373519420557218)+b64*float(-9.1525864793304e-05)+b66*float(-0.00177487422929696)
+b68*float(0.00608362383531425)+b70*float(7.21545329549665e-05)+b72*float(0.00206933190775673)
+b74*float(0.00245336662131898)+b76*float(-0.00392524728473230)+b78*float(-0.00909788448599115)
+b80*float(-0.002447940076129)+b82*float(0.0179545101708517)+b84*float(0.00475619898623354)
+b86*float(-0.00549915339004735)+b88*float(0.00143811636664983)+b90*float(-0.0059745488296149)
+b92*float(-0.0105539647792529)+b94*float(7.58436955886907e-05)+b96*float(-8.53987633018239e-05)
+b98*float(0.00439685159503327)+b100*float(-0.00307238267501191)+b102*float(-0.0064144463191577)
+b104*float(-0.00228568440033121)+b106*float(0.00118852852813458)+b108*float(-0.00334250049729459)
+b110*float(-0.00378672625031596)+b112*float(0.00384814966222513)+b114*float(0.00941204440091797)
+b116*float(0.000789314550086755)+b118*float(0.00639185621722994)+b120*float(0.00241830686730065)
+b122*float(-0.00616910537479809)+b124*float(0.00124117581996387)

Predictive model LAI 2008

(2.84763067251959)+b2*float(-0.00196374798301153)+b4*float(0.000879362933208142)+b6*float(0.000950402662584752)
+b8*float(0.00363092126775782)+b10*float(-0.00354398837656229)+b12*float(-0.00330544396877107)
+b14*float(-0.00175122805984397)+b16*float(0.0078646001622336)+b18*float(-0.00508696335402356)
+b20*float(0.00387139014636775)+b22*float(0.000902398371291394)+b24*float(0.000487324174901096)
+b26*float(-0.00106586452334234)+b28*float(-0.000311712959470746)+b30*float(-9.7999754021881e-05)
+b32*float(-0.000104758038436001)+b34*float(0.000212982684662966)+b36*float(0.000467350869817495)
+b38*float(-0.000589408883085822)+b40*float(-0.000178416236440130)+b42*float(-0.000911786719115204)
+b44*float(-0.00155446425572373)+b46*float(-0.000829429859153245)+b48*float(0.000705750164858313)
+b50*float(0.00131096579637716)+b52*float(0.00202603705814823)+b54*float(0.00116017886167592)
+b56*float(0.000268784186209149)+b58*float(-0.00105315471354357)+b60*float(-0.00075392601971893)
+b62*float(0.00126259919514661)+b64*float(-5.60937538958138e-05)+b66*float(0.000246645517607460)
+b68*float(0.00310034062784506)+b70*float(5.46952029643188e-06)+b72*float(0.000332729713562173)
+b74*float(0.000902362299390928)+b76*float(0.00111058153358523)+b78*float(0.000145709448500418)
+b80*float(-0.000760104814125225)+b82*float(-0.00207063493997484)+b84*float(-0.00191190332551067)
+b86*float(-0.000736535147925112)+b88*float(-0.000135492117906229)+b90*float(-0.00111212600971773)
+b92*float(-0.00120010305797933)+b94*float(0.000937673589516678)+b96*float(0.000108697407854108)
+b98*float(-0.00107080054283980)+b100*float(-0.000644871133260231)+b102*float(-0.00093972018232419)
+b104*float(-0.00139803188288959)+b106*float(0.000140605272820946)+b108*float(-0.00168988019948168)
+b110*float(-0.00190471771293552)+b112*float(0.000119170413074394)+b114*float(0.00203708163537563)
+b116*float(2.59450252433306e-05)+b118*float(0.00531761789001187)+b120*float(0.00144077201364788)
+b122*float(0.0013786656914548)+b124*float(-0.00313252298456795)

Predictive model Cover fraction 2008

(0.574392151072987)+b2*float(0.000216430377764195)+b4*float(-1.72511489191765e-05)+b6*float(0.00013667976247706)
+b8*float(0.000425676487319637)+b10*float(-0.000418111767004286)+b12*float(-0.00058361895004398)
+b14*float(-0.000206619882179932)+b16*float(0.00023061350330779)+b18*float(-0.000775394454935236)
+b20*float(0.000389223458331606)+b22*float(0.000248177773200244)+b24*float(0.000228300353981706)
+b26*float(7.97912959136784e-05)+b28*float(-9.7893494290224e-06)+b30*float(-0.000148334863221670)
+b32*float(-8.45879879667496e-05)+b34*float(-3.42111476181546e-05)+b36*float(-2.97620859184818e-05)
+b38*float(3.88230372021680e-05)+b40*float(-9.67131705205703e-05)+b42*float(-0.000197877986598758)
+b44*float(-0.000233344058195361)+b46*float(-0.000154284129513910)+b48*float(-6.89146569070995e-05)
+b50*float(0.000209484343876097)+b52*float(0.000290301861344405)+b54*float(0.000153292530986630)
+b56*float(6.85528049783527e-05)+b58*float(2.66685396320693e-05)+b60*float(0.000158984639435616)
+b62*float(0.000205188064375383)+b64*float(-6.90144736343518e-07)+b66*float(-0.000144374843833871)
+b68*float(0.000330821513204182)+b70*float(0.000123674963158083)+b72*float(0.000110738659656708)
+b74*float(4.31269241763254e-05)+b76*float(-3.40730067276337e-05)+b78*float(-0.000135011767619954)
+b80*float(-0.000155508960603584)+b82*float(-0.000239728178056354)+b84*float(-0.000294429272937084)
+b86*float(-0.000198309885511309)+b88*float(-8.36843697622885e-05)+b90*float(-0.000147250047786348)
+b92*float(-0.000117250548200688)+b94*float(-9.34873257818223e-05)+b96*float(0.000227736424604035)
+b98*float(1.51282808955920e-05)+b100*float(0.000190179842128993)+b102*float(0.000146567656185135)
+b104*float(0.000126380328948422)+b106*float(-0.000155726602277875)+b108*float(-0.000366262169113012)
+b110*float(-0.000289681265800889)+b112*float(0.000104954939707824)+b114*float(0.000141784225142650)
+b116*float(0.00031544084479422)+b118*float(0.00028171886241207)+b120*float(0.000344189157333162)
+b122*float(-0.000101975015640244)+b124*float(0.000301500501538109)